Mathematical Modelling of Water Soil Erosion and Sediment Yield in Large Catchments

by

Ning Ma

Study leader: G.R. Basson

Thesis presented in partial fulfilment of the requirements for the degree of Master of Engineering (Civil) at the University of Stellenbosch

University of Stellenbosch

November 2006

DECLARATION

I, the undersigned hereby declare that the work contained in this thesis is my own original work, and has not previously, in its entirety or in part, been submitted at any university for a degree.

Signature:

Date:

Pectora roborant cultus recti

SUMMARY

In many part of the world, but especially in Africa, land degradation leads to severe soil erosion and high sediment yields. Mathematical models and empirical methods can be used to simulate the sediment yields. In many cases spatial and temporal data are however limited in the large catchments often found in Africa. A model should be able to simulate the long-term hydrology and sediment yields for sub-catchments and should be physically based as far as possible. In this thesis several models were evaluated and the agrohydrological model of the University of Kwa-Zulu-Natal (ACRU) was applied on two large catchments with limited data in Kenya.

The key aim of the thesis was to assess the applicability of the ACRU modelling system for sediment yield prediction in large catchments under conditions of limited data availability.

Two catchments in Kenya which drain into Lake Victoria were selected for this research: Nyando (3562 km^2) and Nzoia River (13692 km^2). Lake Victoria, with a surface area of 68000 km^2 and an adjoining catchment of around 184200 km^2, is the second largest fresh water lake in the world and the largest in the tropics. The Lake Victoria Basin area is increasingly being used for domestic, agricultural and industrial purposes by the three riparian countries Kenya, Tanzania and Uganda. About 21 million people (year 2000) rely primarily on subsistence agricultural and pastoral production for their livelihoods. But pervasive poverty has hindered sustainable use of the land resources and there has already been considerable land degradation. There has also been expansion of the increasing on-site erosion (overland flow) and reducing buffering capacity of the natural vegetation in wetlands and in the riparian zones (Hansen, Walsh, 2000).

A regional assessment identified the Nyando River Basin and Nzoia River Basin as major sources of sediment flow into Lake Victoria on the Kenyan side of the Lake. Accelerated run off sheet erosion over much of the Nyando catchment area has led to severe rill, gully and stream bank erosion in lower parts of the river basin (Swallow, 2000).

The ACRU model is a hydrological model using daily time steps with the Modified Universal Soil Loss Equation (MUSLE, Williams, 1975) module to simulate soil erosion. The MUSLE sediment yield module uses factors that characterize physical conditions on the surface of a catchment as input information. Data required for the model include: sub-catchment daily rainfall, historical flow records, general catchment topographical information, meteorological information, land use and cover, soil characteristics, sediment yield data, etc.

The model used daily time steps for a 55 years record for the period 1950 to 2004. During calibration it was found that the sediment yield is overestimated which was expected since the model is a soil erosion model (based on MUSLE). The model was calibrated in each catchment against observed sediment load data, but this data were limited. Verification of the model was carried out by using satellite images and independent sediment load data when available.

Scenario analysis was carried out by changing land use in the model to investigate how soil erosion could be reduced. Grassland to replace subsistence farming was found most effective, but irrigated sugarcane was also investigated. The model was found to be very effective in indicating which sub-catchments contribute most of the sediment yield.

Under limiting data conditions it was found that it is very important to calibrate the model against field data. The most sensitive parameters affecting the sediment yield were found to be:

a) **Hydrological:**
- Daily rainfall spatial distribution of rain gauge
- Time of concentration
- Mean annual precipitation
- Minimum and maximum temperature
- Monthly evaporation

b) Soil and catchment characteristics:

- Number of sub-catchments making up catchment in model
- Catchment slope and slope length, steepness factor
- Land cover
- Crop coefficient
- Soil texture class and depths
- Soil erodibility factor

Pectora roborant cultus recti

SAMEVATTING

In baie dele van die wêreld, maar veral in Afrika, lei oorbeweiding en oorbewerking van grond tot ernstige gronderosie met hoë sedimentlewerings. Wiskundige en empiriese modelle kan gebruik word om sedimentlewerings te voorspel, maar in baie gevalle is data egter beperk in groot opvanggebiede wat algemeen voorkom in Afrika. ‘n Model moet die langtermyn hidrologie en sedimentlewerings van subopvanggebiede kan voorspel en moet sover moontlik ‘n fisiese basis hê. In hierdie tesis is verskeie modelle ondersoek en daar is besluit om ‘n agro-hidrologiese model van die Universiteit van KwaZulu Natal (ACRU) te gebruik om sedimentlewerings in twee groot opvanggebiede in Kenia met beperkte data te ondersoek.

Die hoofdoel van die tesis was om die toepaslikheid van die ACRU modelleringstelsel te toets vir sedimentlewering voorspelling in groot opvanggebiede waar data beperk is.

Twee opvanggebiede in Kenia wat in die Victoriameer vloei is gekies vir die studie: Nyando- (3562 km^2) en Nzoiariviere (13692 km^2). Victoriameer met ’n oppervlak van 68000 km^2 en ‘n opvanggebied van 184200 km^2, is die tweede grootste varswater meer in die wêreld en die grootste in die trope.

Die Victoriameeropvanggebied word toenemend gebruik vir huishoudelike, landbou en industriële ontwikkeling deur die lande om die meer: Kenia, Tanzanië en Uganga. In 2000 het sowat 21 miljoen mense in die streek staat gemaak op bestaansboerdery. Voortdurende armoede het volhoubare gebruik van die grond beperk wat gelei het tot gronderosie. Die omvang van die erosie is besig om groter te word as gevolg van verminderde erosiebeperking deur plantegroei in vleilande en rivieroewerplantegroei (Hansen en Walsh, 2000).

‘n Streeksondersoek het Nyando- en Nzoiarivier opvanggebiede geidentifiseer as hoofbronne van

sedimentvloei na Victoriameer vanuit Kenia. Versnelde afloop erosie oor groot dele van die Nyando opvanggebied het gelei tot ernstige donga en rivieroewererosie in veral die stroomafdele van die opvanggebied (Swallow, 2000).

Die ACRU model is ‘n hidrologiese model wat daaglikse tydstappe gebruik met die gewysigde universele grondverlies vergelyking (MUSLE), (Williams, 1975), wat gronderosie simuleer. Die MUSLE module gebruik faktore wat die fisiese eienskappe van ‘n opvanggebied beskryf. Data benodig vir die module sluit in: subopvanggebied daaglikse reënval, historiese vloeirekords, algemene topografiese inligting, metereologiese data, grondgebruik en grondbedekking, grondeienskappe, sedimentlewering data, ens.

Die model is gekalibreer teen data van ‘n 55 jaar periode 1950 tot 2004. Tydens aanvanklike kalibrasie is gevind dat sedimentlewering oorskat is omdat die model eintlik ‘n gronderosiemodel is. Die model is gekalibreer in elke opvanggebied, maar sedimentdata was beperk. Verifikasie van die model is uitgevoer met satelietbeelde (Nyando) en onafhanklike sedimentdata wanneer beskikbaar.

‘n Sensitiwiteitsontleding is uitgevoer deur die grondgebruik te verander in die model om sodoende erosie te probeer beperk. Grasveld (wat die natuurlike plantegroei is), is gebruik om bestaansboerdery te vervang en is baie effektief gevind. Suikerriet met besproeiing as grondgebruik het ook ‘n afname in erosie teweeggebring. Die model kan gebruik word om te voorspel watter subopvanggebiede dra die meeste by tot die sedimentlewering.

Onder beperkte data toestande is gevind dat dit baie belangrik is om die model te kalibreer teen velddata. Die mees sensitiewe veranderlikes wat die sedimentlewering bepaal is soos volg:

a) Hidrologies:

- Daaglikse reënvalstasie verspreiding in opvanggebied
- Tyd van konsentrasie van vloei
- Gemiddelde jaarlikse reënval
- Minimum en maksimum temperature
- Maandelikse verdamping

b) Grond- en opvanggebied eienskappe:

- Aantal subopvanggebiede in opvanggebied
- Opvanggebiedhelling
- Grondbedekking
- Gewasfaktore
- Grondtekstuur en dieptes
- Gronderosiefaktore

Pectora roborant cultus recti

ACKNOWLEDGMENTS

I would like to thank the following people and organizations, without them this study would not have been possible:

- Prof. Gerrit Basson for his guidance, knowledge and motivation throughout the study.
- The Lake Victoria Environmental Management Project (LVEMP) for the opportunity and funding of this research.
- The colleagues from Ninham Shand for training on the ACRU model.
- Prof. A. Rooseboom for his kind support during the study.
- All the colleagues in the Institute of Water and Environmental Engineering.
- My wife Jane for her love and my family for believing in me and supporting me to achieve my goals.

TABLE OF CONTENTS

Pectora roborant cultus recti

Pectora roborant cultus recti

LIST OF FIGURES

Pectora roborant cultus recti

Pectora roborant cultus recti

LIST OF TABLES

LIST OF SYMBOLS

A	Average annual soil loss
C	Cover management factor
e	The kinetic energy of a moving object
E_s	Soil water evaporation
E_t	Plant transpiration
K	Soil erodibility factor
K_{max}	Maximum soil erodibility factor
K_{min}	Minimum soil erodibility factor
L	Longest watercourse in catchment
L	Slope length factor
m	The mass of a moving object
MAP_m	Mean annual precipitation measured at rainfall station
MAP_r	Mean annual precipitation collected from rainfall distributing map
N	Number of grid points
P	Supporting practice factor
Q_o	Sum of observed flows
Q_s	Sum of simulated stream flow
R	Daily rainfall data measured at rainfall station
R	Rainfall erosivity factor
R_i	Specific calibrated daily rainfall for certain sub-catchment
rk	Ratio of Kmax to Kmin
S	Slope steepness factor
v	The speed of a moving object
l_i	Distance along river between two consecutive contours
τ	Correction factor
C	Cover and management factor

L_1	Length of longest natural channel
S_i	Slope between two consecutive contours
K	Soil erodibility factor
P	Support practice factor
t_c	Time of concentration
S_A	Average catchment slope
Q_p	Peak discharge for the event
Y_{sd}	Sediment yield from an individual storm flow producing event
Q_v	Storm flow volume for the event.
S_L	Mean channel slope
P_m	Rainfall station monthly average precipitation
P_{S_i}	Rainfall station monthly precipitation
LS	Slope length and gradient factor
f_A	Sub-catchments monthly precipitation factors
ΔH	Contour interval
α_{sy}, β_{sy}	Location specific coefficients.

CHAPTER 1 INTRODUCTION

1.1 BACKGROUND

Lake Victoria, with a surface area of 68000 km^2 and an adjoining catchment of 184200 km^2, is the second largest fresh water lake in the world and the largest in the tropics. Lake Victoria is the source of the Victoria Nile, and as such the hydrological lifeline for much of Uganda, Sudan and Egypt. It also directly or indirectly supports 30 million people. Over the last 40-50 years the lake and its basin have undergone enormous ecological changes. In contrast, it takes about 73 years for a volume of water equivalent to the Lake's volume (~2760 km^3) to flow out of it (Piper *et al*., 1986).

Lake Victoria is of immense economic and environmental importance in the eastern and central African region. The lake basin supports one of the densest and poorest rural populations in the world, with population densities of up to 1200 persons per square kilometer. The Lake Victoria area is increasingly being used for domestic, agricultural and industrial purposes by the three riparian countries: Kenya, Tanzania and Uganda. About 21 million people (year 2000) rely primarily on subsistence agricultural and pastoral production for their livelihoods. Pervasive poverty has hindered sustainable use of the land resources and there has already been considerable land degradation. There has also been an expansion of these changes as increased on-site erosion (overland flow) and reduced buffering capacity of natural vegetation in wetlands and in riparian zones. The flow of nutrients from land to lake is causing a decrease in soil fertility on farmers' fields and contributes to the eutrophication of Lake Victoria. There is little doubt that sedimentation and nutrient runoff, urban and industrial point source pollution and biomass burning, have induced the rapid eutrophication of Lake Victoria over the last fifty years. Invasion of water hyacinth and loss of endemic biodiversity are interrelated and compound problems for the Lake Environment and welfare of its people (Swallow, 2000).

1.2 MOTIVATION

A regional assessment (Swallow, 2000) identified the Nyando River Basin and the Nzoia River Basin as major sources of sediment flow into Lake Victoria at Kenya side (see Table 1-1), and much of the initial work was concentrated on these river basins while methods were being refined. This study identified severe soil erosion and land degradation problems throughout the Nyando and Nzoia River basins. Especially accelerated run off sheet erosion over much of the Nyando catchment area has led to severe rill, gully and stream bank erosion in lower parts of the river basin. The principal causes of erosion include deforestation of headwaters and overuse of extensive areas of fragile lands on both hill slopes and plains, coupled with loss of watershed filtering functions through encroachment on wetlands and loss of riverine vegetation. Associated with soil erosion, there has been substantial depletion of soil quality over much of the basin. The people who live in the river basin are aware and concerned about water shortages and local land degradation but there is a low level awareness of the off-site effects. The lower parts of the river basin and the lake are particularly vulnerable to the return of large rainfall events, such as experienced in the early 1960's, which would cause catastrophic damage.

Table 1-1 Sediment yields at Nyando and Nzoia River mouths (Basson, 2005)

River	Catchment area (km^2)	Mean runoff (1950 to 2004) (m^3/s)	Sediment yield ($t/km^2.a$)	Sediment load (t/a)
Nyando	3652	21	142 (Probable) 346 (High Probable)	519969 1265309
Nzoia	12842	119	80 (Probable) 218 (High Probable)	1029820 2795892

* Notes: "Probable" and "high probable" values are given due to the limited suspended sediment data available, especially for medium to large floods. Sediment yield includes suspended and bed load.

Sediment and nutrient transport and mixing undoubtedly influence the water quality and ecology of Lake Victoria. In 2005, the three riparian countries around Lake Victoria (Kenya, Uganda and Tanzania) responded to these and other issues through the Lake Victoria Environmental Management Project (LVEMP) with the support of a large number of donors. The LVEMP's main objective is the management of the lake ecosystem through sustainable utilization to enhance socio-economic development of the riparian communities. A precursor to this goal is intensive limnological research of Lake Victoria to establish the present condition of the lake ecosystem and the potential impact of current and future human activities in the catchment.

The LVEMP project identified the need for this research to establish a methodology based on field studies and physically based numerical modeling to assess the sediment yields of two rivers: Nyando and Nzoia, and to evaluate possible catchment sediment yield management scenarios. The study area is shown in Figure 1-1 and Figure 1-2.

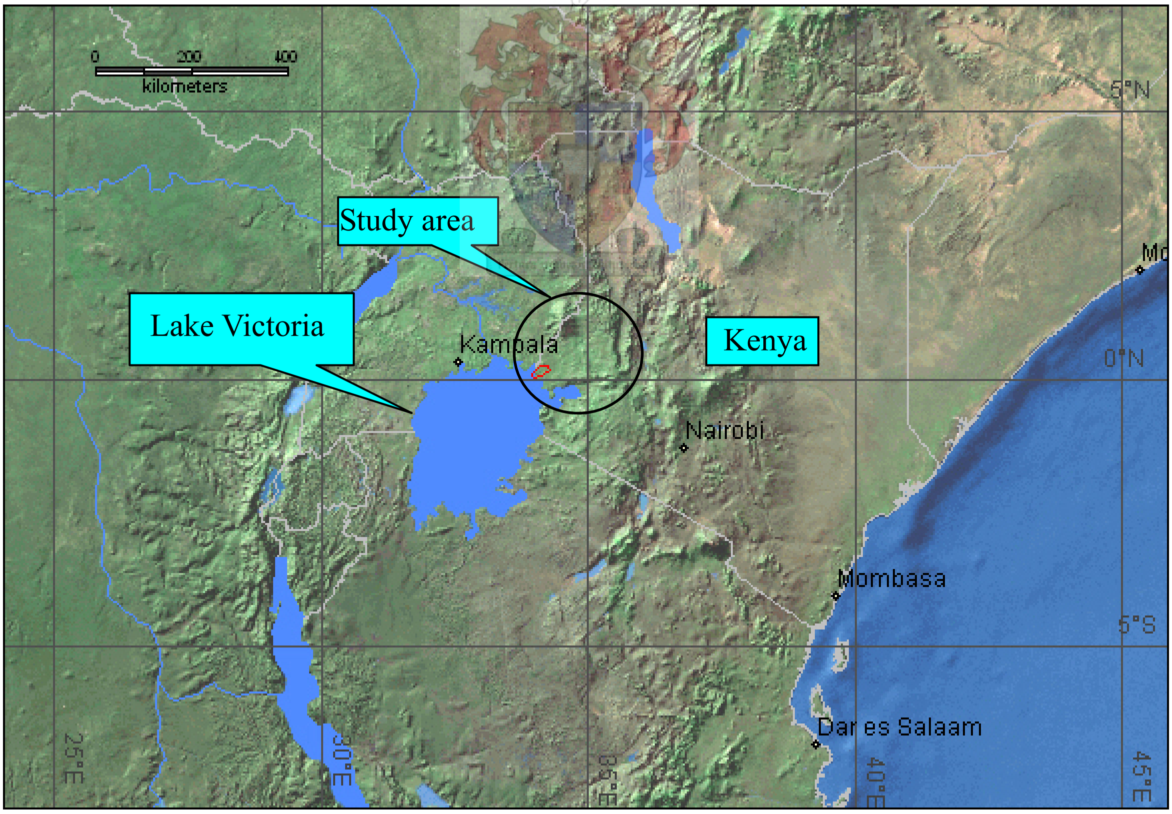

Figure 1-1 Overview of the study area

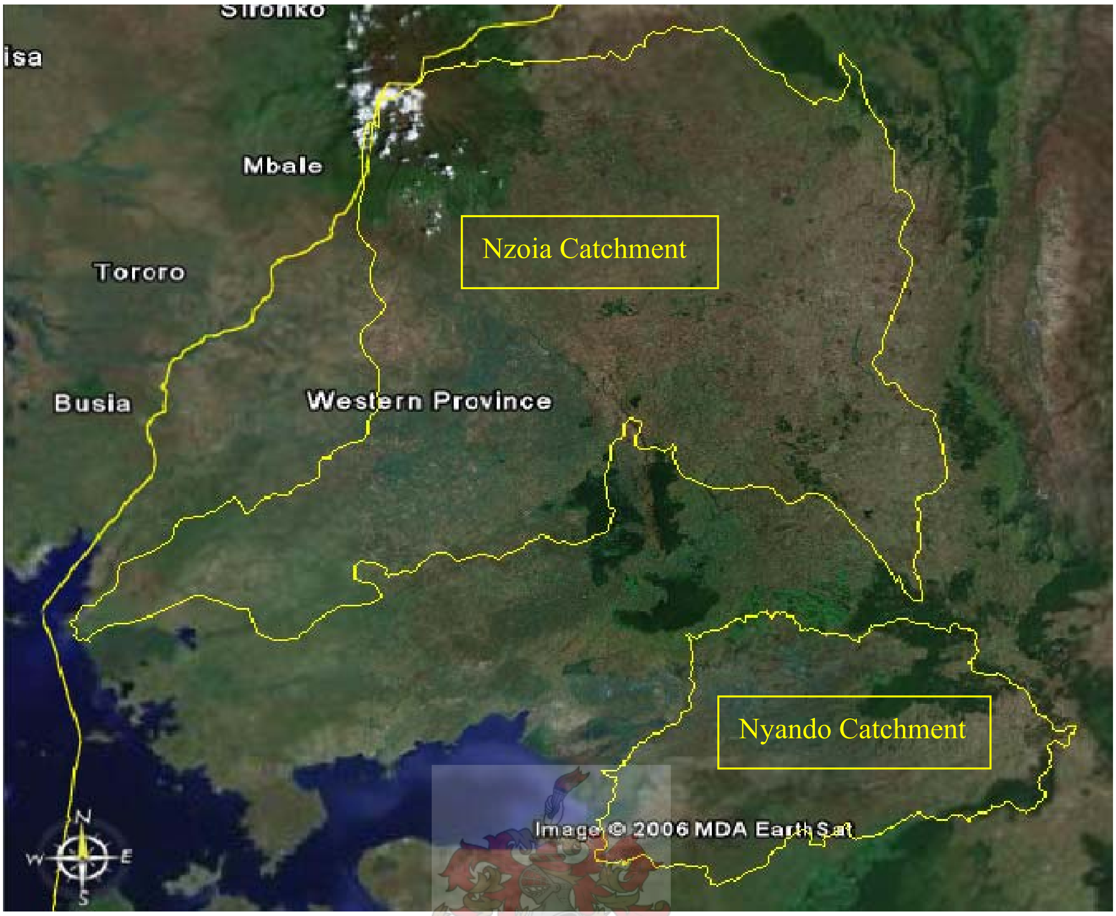

Figure 1-2 Study area with catchments

1.3 OBJECTIVES

The overall objective of this thesis is to evaluate a physically based soil erosion model and its accuracy to predict sediment yields in large catchments caused by water soil erosion. The specific applications are two river systems in the west of Kenya draining into Lake Victoria. Specific objectives are:

- Carry out literature review of mathematical modelling sediment yield prediction methodologies.
- Developing an understanding of the interrelationship between soil erosion and sediment yield in catchments.
- Set up and calibrate a hydrological, physically based model on two large catchments with limited data.

- Validate the selected sediment yield model against field data.
- Carry out parameter sensitivity analysis and the effect on predicted sediment yields by ACRU.
- Investigate possible land use management strategies for the specific case studies.

CHAPTER 2 METHODOLOGY

The methodology followed in this research is as follows:

a) A literature review was carried out of the causes of soil erosion and the model used to simulate or calculate soil erosion and sediment yields. Both regression type and physically based models were investigated.

b) Two catchments were selected for setting up of the physically based model (ACRU) that was used in this thesis and field data were obtained of land use and climate conditions.

c) The ACRU model was set up for each catchment for a year period of daily data and was calibrated against observed flows in the field. Thereafter sediment yields were simulated and calibrated with observed data.

d) Following calibration, more simulations were carried out to compare simulated against incremental catchment sediment yields observed in the field (not used during calibration).

e) Parameter sensitivity testing was carried out and evaluation done of the model simulation results given the limited data available and large catchments, a situation often found in Africa.

f) Possible land use change scenarios have been investigated to evaluate the influence on reducing sediment yields. Riparian vegetation and current subsistence farming in degraded area were investigated and alternatives such as irrigation and grassland (natural) were investigated.

Pectora roborant cultus recti

CHAPTER 3 REVIEW OF RESEARCH ON SOIL EROSION AND SEDIMENT YIELD MODELLING

3.1 INTRODUCTION

3.1.1 Background

Land resource is one of the three major geological resources (mineral resources, water resources, and land resources) as well as one of the most basic of human resources and labour production targets. Human land use reflects the degree of development of human civilization, but also results in direct damage of the land's resources, which are mainly manifested in soil erosion induced by alien invasive species, desertification, land salinization and soil pollution.

Soil erosion by water is one of the most serious crises the world faces today. It is estimated that the world farmland topsoil loses about 23 billion ton per year. The FAO (Food and Agriculture Organization, a branch of United Nations) estimates that the global loss of productive land through erosion is 5 to7 million hectares per year (Collins, 2001).

Soil erosion is the detachment and movement of soil particles by the erosive forces of wind or water. Soil detached and transported away from one location is often deposited at some other place. Although soil erosion can be controlled, it is almost impossible to stop completely (NSERL, USA, 2006).

Annual soil loss in South Africa is estimated at 300 to 400 million ton, nearly three ton for each hectare of land. Replacing the soil nutrients carried out to sea by South African rivers each year, with fertilizer, would cost R1000 million. For every ton of maize, wheat, sugar or other agricultural crop produced, South Africa loses on average of 20 ton of soil (Collins, 2001).

Soil erosion is a serious concern, occurring especially in semi-arid regions where the washing away of topsoil, which leads to the loss of crop production, occurs. It poses a threat to the sustainability of small scale and subsistence agricultural production. Many rural communities who are practicing subsistence agriculture and communal grazing, are the most affected by very severe soil erosion. Land degradation and soil erosion also leads to accelerated storage loss due to reservoir sedimentation.

3.1.2 Types of soil erosion

Soil erosion is a gradual process that occurs when the actions of water, wind, and other factors eat away and wear down the land, causing the soil to deteriorate or disappear completely. Soil deterioration and low quality of water due to erosion and runoff has often become a severe problem around the world. Soil erosion is a natural process, but becomes a problem when human activity causes it to occur at a much faster rate than under natural conditions. Soil erosion can be divided into two very general categories: *geological erosion* and *accelerated erosion*. Accelerated erosion is the type that will be covered in most depth in this study, dealing mostly with such problems as *wind erosion* and *water erosion.* Water erosion is caused by rain and poor drainage. Severe rains can be a major problem for farmers when they fall on bare soil. With an impact of up to 48 km/hour, rain washes out seed and splashes soil into the air. If the fields are on a slope, the soil is splashed downhill which causes deterioration of soil structure (Frankenberger, 1997). Soil that has been detached by raindrops is more easily moved than soil that has not been detached. *Sheet erosion* is caused by raindrops. Other types of erosion caused by rainfall include rill erosion and gullies:

- Sheet erosion can be defined as the uniform removal of soil in thin layers from sloping land. This, of course, is nearly impossible: in reality the loose soil merely runs off with the rain.
- Rill erosion is the most common form of erosion. Although its effects can be easily removed by tillage, it is the most often overlooked. It occurs when soil is removed by water from little

streamlets that run through land with poor surface draining. Rills can often be found between crop rows.

- Gullies are larger than rills and cannot be fixed by tillage. Gully erosion is an advanced stage of rill erosion, just as rills are often the results of sheet erosion.

Wind erosion cannot be divided into such distinct types. Occurring mostly in flat, dry areas and moist sandy soils along bodies of water, wind erosion removes soil and natural vegetation, and causes dryness and deterioration of soil structure. Surface texture is the best key to wind erosion hazard potential. All mucks, sands, and loamy sands can easily be detached and blown away by the wind, and thus are rated a severe hazard. Sandy loams are also vulnerable to wind, but are not as susceptible to severe wind erosion as the previously mentioned soils. Regular loams, silt loams, and clay loams, and clays are not damaged by the wind, but on wide level plains, there may be a loss of fine silts, clays, and some organic matter (Frankenberger, 1997).

3.1.3 Causes of soil erosion

As described in section 3.1.2, water is the main cause of soil erosion. According to Anthoni (2000) the factors affecting water erosion can be summarised as follows:

a) natural factors

- Heavy rains on weak soil: raindrops loosen soil particles and water transports them down hill.
- Vegetation depleted by drought: rain drops are free to hit the soil, causing erosion during rainfall.
- Steep slopes: gravity 'pulls harder': water flows faster; soil creeps, slips or slumps downhill.
- Sudden climate change: rainfall, erosion increases unexpectedly rapidly as rainstorms become more severe; drought, water dries up and soil biota die. A sudden rain may then cause enormous damage.

b) human-induced factors:

- Change of land (deforestation): the land loses its cover, then its soil biota, porosity and moisture.
- Intensive farming: use of the plough, excessive use of fertilizer and irrigation damages the land, often permanently.
- Housing development: soil is bared; massive earthworks; soil becomes loosened.
- Road construction: roads are cut; massive earthworks, leaving scars behind. Not enough attention paid to rainwater flow and maintenance of road sides.

Briefly, the causes of water soil erosion can be summed up in three parts: soil degradation, gravity, and rain. Most of the erosion and degradation are caused by human activities which become world-wide problems. Soil degradation can make soil lose nutrients and soil biota. It can get damaged by water logging and compaction. Erosion is the visible part of degradation, where soil particles are transported down-hill by the forces of gravity, water flow.

Gravity is not only the force that pushes both land and water down-hill, but also keeps soil in its place. The steeper the soil, the more it is pushed down-hill and the faster the water runs. Because of the enormous variability in field data, soil losses are difficult to quantify. Figure 3.1 shows how quickly erosion accelerates and also shows how crop land erosion increases with slope. According to Anthoni (2000), flat land is very stable (losing 2-5 times natural replenishment) but soil losses increase rapidly with land sloping at 2-5%. Land with a 10% slope has 8 times higher erosion potential, which makes it impossible to farm by ploughing, but perennial crops may be sustainable. At 15% slope, soil erosion has doubled again. But slopes over 20% appear to be less affected, and the reasons for this could be that they are higher uphill, less prone to receive the water from a field higher up, and the run from hillcrest to valley floor is shorter. The fields are shorter too. Although the lines (Figure 3-1) are rather confusing, the main message they bring is that soil slope has a significantly large effect on erosion.

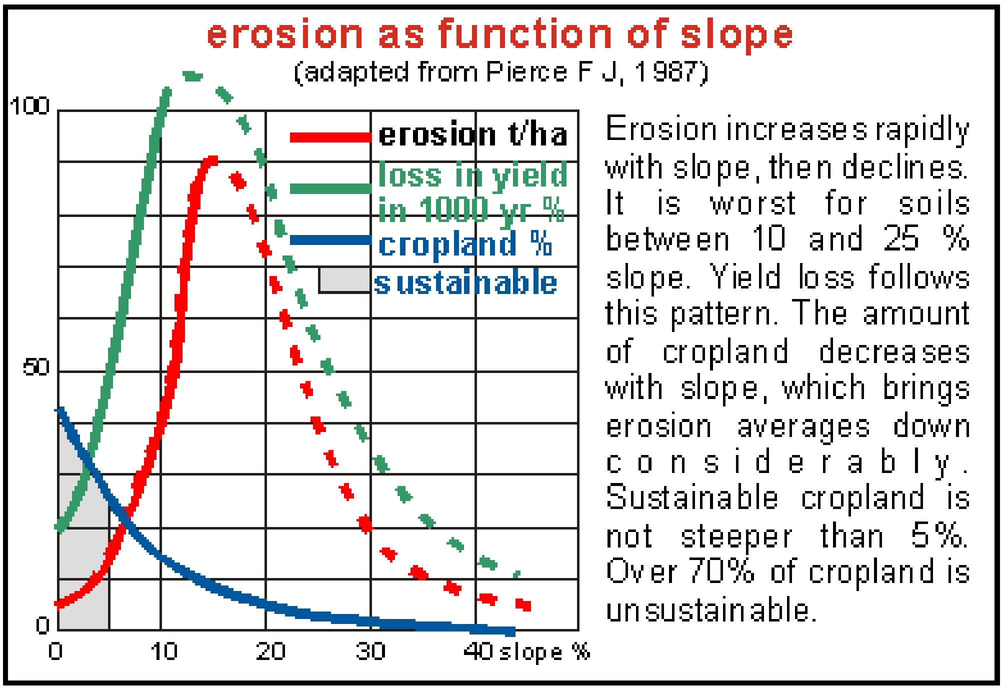

Figure 3-1 Erosion as a function of slope (Pierce, 1987)

Rain is undoubtedly the main cause of erosion. Water is about 800 times heavier than air, half to one third the weights of rock and about equal in weight to loose topsoil. When it flows, it can move loose substances with ease. Surprisingly, rain's most damaging moment is when a water drop hits the ground. Figure 3-2 shows the effect of raindrop impact. This was found recently, whereas before it was thought that sheet wash (the flow of water over the soil) was the most destructive. The kinetic energy (e) of a moving object is equal to half its mass (m) multiplied by its speed squared (v):

$$e = \frac{m \times v^2}{2} \qquad \text{Eq 3.1}$$

As water droplets grow in size, both their speed and mass increase. The mass of a 5 mm raindrop is 5x5x5=125 times that of a 1 mm drop and its 'terminal' speed doubles, resulting in a destructive energy 500 times larger. Thus the destructive power of rain increases dramatically as the rainstorm produces larger drops, which is relatively rare. But when it occurs, its effect is profoundly destructive. Since around 1987, rains have become heavier everywhere in the world, and with it, erosion from raindrop impact (Anthoni, 2000).

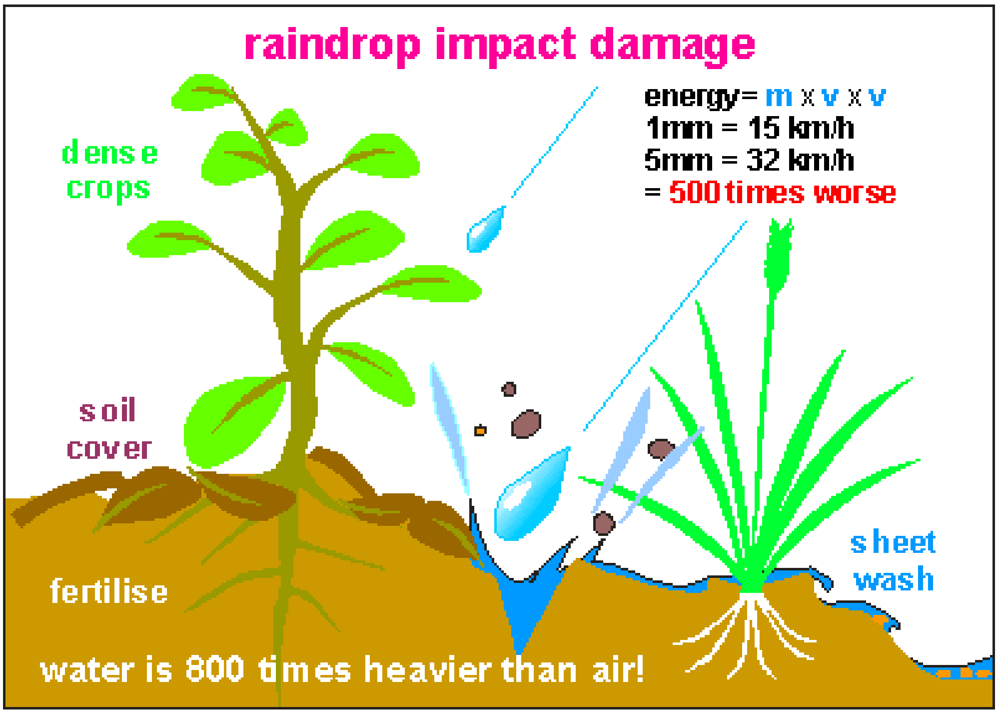

Figure 3-2 Raindrop impact damage (Anthoni, 2000)

As raindrops hit the soil, they loosen its structure, freeing up fine clay particles, which do not settle down easily, and which are transported down-hill in the sheet wash. Figure 3-3 shows how particles are transported and it applies to wind, dunes, beaches, coasts, rivers and estuaries. It illustrates the friction a particle experiences when moving through a medium (water and air). The scientist Stokes formulated this mathematically and it is shown in the three red curves. The left curve gives the flow velocity at which particles settle out, the rightmost curve the speed at which cohesive material is eroded and the central curve the current velocity to erode loose material (Anthoni, 2000).

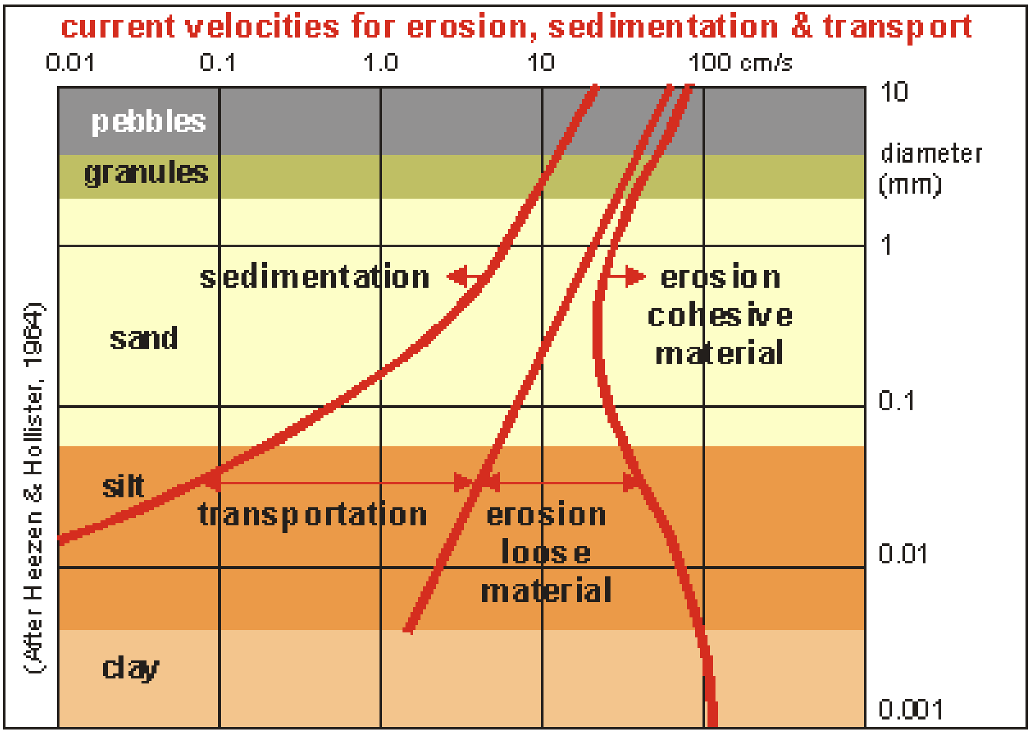

Figure 3-3 Current velocities for erosion, sedimentation & transport (Heezen, Hollister, 1964)

3.1.4 Soil erosion control

Soil erosion is caused by surface runoff on a slope. The basic principles of prevention and control measures are: reducing surface runoff, reducing runoff speed, capacity and enhancing soil absorbent surface counter capacity and its datum erosion, and by changing the land use. The only way to fight water erosion is to keep the soil covered, either by dense plants or by ground mulch. Hence the importance of growing a cover crop under horticulture (fruits and wine), keeping the soil covered after harvesting (stubble on the field), and not overgrazing pastures. On building sites, mulch should be spread on the soil or covered with plastic sheets. A temporary grass cover may also be used. Road sides should be vegetated and not mowed to expose the dirt. Fertilization helps to make foliage denser and to produce more leaf litter.

Another important factor which strongly affects the soil erosion is human activity, especially the daily increased farming action. The key of minimizing soil erosion and saving the farm lands is the farmer. Finally, farmers are the ones who must reduce the level at which erosion sediments are dislodged from their cropland.

3.2 THEORY OF THE SOIL EROSION ESTIMATION

The amount of erosion is not easy to measure directly, but can be estimated from a number of factors that have been measured for all climates, soil types, topography and kinds of land use. The factors are combined in the 'Universal Soil Loss Equation', which returns a single number, the tolerance factor, equivalent to predicted erosion in ton/ha. The Universal Soil Loss Equation (USLE) has been used for many years to predict erosion on any field. The USLE for estimating average annual soil loss is (Foster & Elliot, 1991):

$$A = RKLSCP \qquad \text{Eq 3.2}$$

Where,

A = Average annual soil loss: the predicted erosion or tolerance factor in ton/ha.

R = Rainfall erosivity factor: a factor dependent on climate and likelihood of extreme events.

K = Soil erodibility factor: an estimate made from soil properties. It depends on the particle sizes and proportions of sand, silt and clay, organic matter, granularity and profile permeability to water.

L = Slope length factor: the slope length is the length of the field in a down-slope direction. The longer the slope, the more water accumulates at the bottom of the field, increasing erosion. It also depends on the land's slope.

S = Slope steepness factor: calculated from the slope of the land in %.

C = Cover management factor: depends on crop growth rate in relation to the erosivity variation in the climate.

P = Supporting practice factor: reflects the use of contours, strip cropping and terracing.

The USLE is limited to determining soil losses caused by single storm events. Therefore, the Modified Universal Soil Loss Equation (MUSLE) was developed based on USLE by Williams and Berndt (1972). For prediction of sediment yield from the land surface on an annual basis rather than for a single storm event, MUSLE can also be used.

Sediment yields are modeled on a day-by-day basis by activating MUSLE (Williams, 1975). This version of the equation, overcomes the inability of the standard USLE equation to directly determine soil loss estimates for individual storm events, and finally eliminates the need to determine sediment delivery ratios which were used by the USLE to estimate the proportion of eroded soil which leaves the catchment (Basson, 2004). The MUSLE equation will be described in more detail in section 3.3.

According to Basson (2004), with the development of hydrological models to simulate rainfall-runoff processes in larger catchments, the USLE and later MUSLE methodology was incorporated directly ignoring, initially, to a large extent the completely different way in which a small catchment (plot scale) to farm scale to large catchment scale (> 2000 km^2) responds in terms of soil erosion and sediment yield. The sediment yield in large catchments is often overestimated, due to deposition of eroded sediment in the large catchment.

3.3 MODIFIED UNIVERSAL SOIL LOSS EQUATION (MUSLE)

3.3.1 Background of MUSLE

The USLE is the most widely used regression model for predicting soil erosion. It is an empirical formula for predicting soil loss due to sheet and rill erosion. The equation was developed from over 10000 plot-years of runoff and soil-loss data, collected on experimental plots of agricultural land in 23 states of USA since 1930 (Basson, 2004).

It was recognized that application of the USLE is limited to soil loss, therefore another procedure for computing the sediment yield from a catchment was developed (Williams and Berndt, 1972). The method determines a sediment yield based on single storm events. If the sediment yield from the land surface on an annual basis rather than on a single storm event required, MUSLE can be used. Long term integration of storm events and sediment transport can also be achieved by incorporating MUSLE in a hydrological model. MUSLE is a method which is generally applicable as predictor of wash load and it is more appropriate to use than the USLE method in semi-arid conditions (Basson, 2004).

3.3.2 Mathematical theory of MUSLE

The MUSLE sediment yield module uses factors that characterize physical conditions on the surface of a catchment as input information. Event-based sediment yield is calculated from:

$$Y_{sd} = \alpha_{sy} \left(Q_v q_p \right)^{\beta_{sy}} K.LS.C.P. \qquad \text{Eq 3.3}$$

where

Y_{sd} = sediment yield from an individual storm flow producing event (ton)

Q_v = storm flow volume for the event (m^3) from the area under study, i.e. the catchment, sub-catchment or land use class

q_p = peak discharge (m^3/s) for the event

K = soil erodibility factor

= rate of soil loss per rainfall erosion index unit (ton.h.N-1 ha-1)

= f (soil texture, organic matter, structure, permeability, antecedent soil moisture condition)

LS = slope length and gradient factor

= f (gradient)

C = cover and management factor

= f (vegetation height, canopy cover, litter/mulch, surface roughness)

P = support practice factor

= f (slope, conservation practices)

α_{sy}, β_{sy} = location specific coefficients.

According to Simons and Senturk (1992), the MUSLE coefficients α_{sy} and β_{sy} are location specific, they must be determined for specific catchments in specific climatic regions. Kienzle and Lorentz (1993) reported that very little research has been undertaken on calibrating these coefficients. Default values of 8.934 and 0.56 for α_{sy} and β_{sy} respectively, have been used in southern Africa (Basson, 2004). Having been originally calibrated for catchments in selected catchments in the USA by Williams (1975), these values for α_{sy} and β_{sy} have been adopted extensively with varying degrees of success (Williams and Berndt, 1977; Kienzle, 1997).

3.4 PHYSICALLY BASED EROSION AND SEDIMENT YIELD MODELS

3.4.1 General

Physically-based, spatially-distributed modeling systems have particular advantages for the study of basin change impacts and applications to basins with limited records. Their parameters have a physical meaning (e.g., soil conductivity and sediment size distribution) and can be measured in the field. Disadvantages of physically-based models include heavy computer requirements, the need of evaluating many parameters (with associated problems of representation at different spatial scales and uncertainty) and a complexity which implies a lengthy training period for new users.

Four state-of-the-art models are described here: the WEPP model (USA), SHETRAN (UK), EUROSEM and LISEM models.

3.4.2 WEPP Model

The Water Erosion Prediction Project (WEPP) (The National Soil Erosion Research Laboratory, US, 1995) model is a process-based, distributed parameter, continuous simulation, erosion prediction model. It is applicable to small watersheds (field-size) and can simulate small profiles

(USLE types) up to large fields (there are several other programs used to predict soil erosion). It mimics the natural processes that are important in soil erosion. When rainfall occurs, the plant and soil characteristics are used to determine if surface runoff will occur. If predicted, then the program will compute estimated sheet & rill detachment and deposition, and channel detachment and deposition. The WEPP model includes a number of conceptual components which are used to predict and calculate these estimates of soil detachment and deposition.

Peak runoff rate is a very important parameter which is used in calculations to estimate flow depth and finally flow shear stress. WEPP uses either a semi-analytical solution of the kinematic wave model or a rough calculation of the kinematic wave model to determine the peak runoff rate. Sediment transport capacity is computed using a simplified function of shear stress to the power 3/2, times a coefficient that is determined through application of the Yalin equation at the end of the slope profile. The WEPP model also uses a steady-state sediment continuity equation to calculate sediment load down a hill slope profile.

Rill erosion rate may be either positive in the case of erosion, or negative in the case of deposition. Rill erosion in WEPP is calculated when the flow sediment load is below transport capacity, and flow shear stress acting on the soil exceeds critical shear stress.

Other model components include a soil component to adjust roughness, infiltration, and erodibility parameters as affected by tillage and consolidation, a plant growth component to provide daily values of crop canopy, biomass, and plant water use, and a daily water balance to determine the impacts of soil evaporation, plant transpiration, infiltration, and percolation on soil water status. Crop residue levels are also updated daily, with adjustments for decomposition as well as the impacts of tillage or other management operations. WEPP contains components to estimate frost, thaw and snow depths, as well as snow melt runoff in regions that experience freezing temperatures. Additionally, the model can be used to determine the impact of channel and sprinkler irrigation on soil erosion.

In watershed applications, WEPP allows simulations of groups of hill slopes, channels, and impoundments. Daily water balance, plant growth, and soil and residue status for channels calculated identically to that on hill slopes. Channel peak runoff rates are calculated using either a modified Rational Equation or the CREAMS peak runoff equation. Channel erosion is estimated using a steady-state sediment continuity equation.

WEPP ignores soil saturation at the foot of a hill slope due to saturation excess overland flow, and may well fail to predict important erosion features in a catchment. The model also cannot simulate gully erosion which is an important component in semi-arid regions (The National Soil Erosion Research Laboratory, US, 1995).

3.4.3 SHETRAN

The River Basin Flow and Transport Modeling System (SHETRAN) (Even, Parkin, and O'Connell, 2000) was developed by the Water Resource Systems Research Laboratory (WRSRL), and is based on the Systeme Hydrologique Europeén (SHE) hydrological modelling system. SHETRAN is a 3D, coupled surface/subsurface, physically-based, spatially-distributed, finite-difference model for coupled water flow, multi-fraction sediment transport and multiple, reactive solute transport in river basins.

SHETRAN represents physical processes using physical laws applied on a 3D finite-difference mesh. The mesh follows the topography of the basin, and the parameters of the physical laws vary from point to point on the mesh, thus allowing the representation of the spatial heterogeneity of the physical properties of the rocks, soils, vegetation cover, etc. SHETRAN can be used for basins of less than 1km^2 to 2500km^2 in area, and typically uses a mesh with 20,000 finite-difference cells, stacked 50 deep, to model hourly flow and transport for periods of up to a few decades. Stream channels are simulated as a network of links, each link running along the edge of a finite-difference cell.

SHETRAN can be used to construct and run models of all or any part of the land phase of the hydrological cycle (including sediment and contaminant transport) for any geographical area. It is physically-based in the sense that the various flow and transport processes are modeled either by finite difference representations of the partial differential equations of mass, momentum and energy conservation, or by empirical equations derived from experimental research. The model parameters have a physical meaning and can be evaluated by measurement. Spatial distributions of basin properties, inputs and responses are represented on a three-dimensional, finite-difference mesh. The channel system is represented along the boundaries of the mesh grid squares as viewed in plan (Basson, 2004).

According to Basson (2004) the typical processes modeled by the SHETRAN hydrological component are:

- Interception of rainfall on vegetation canopy (Rutter storage model)
- Evaporation of intercepted rainfall, ground surface water and channel water; transpiration of water drawn from the root zone (Penman-Monteith equation or the ratio of actual to potential evapotranspiration as a function of soil moisture tension)
- Snow pack development and snowmelt (temperature-based of energy budget methods)
- One-dimensional flow in the unsaturated zone (Richards equation)
- Two-dimensional flow in the saturated zone (Boussinesq equation)
- Two-dimensional overland flow; one-dimensional channel flow (Saint Venant equations)
- Saturated zone/channel interaction, including an allowance for an unsaturated zone below the channel
- Saturated zone/surface water interaction

The basic erosion and sediment yield component consists of subcomponents accounting for soil erosion by raindrop impact, leaf drip impact and overland flow, channel bed and bank erosion by channel flow, and sediment transport by overland and channel flow.

The sediment processes modeled and the equations used to describe them are:

- Soil erosion by raindrop impact, leaf drip impact and overland flow

- Two-dimensional total load convection in overland flow by size fraction, including input to the channels; deposition and resuspension of sediments in overland flow (mass conservation equation incorporating Engelund-Hansen total load and Yalin load transport capacity equations)
- One-dimensional convection of cohesive and non-cohesive sediments in channel flow by size fraction; deposition and resuspension of non-cohesive sediments in channel flow; channel bed erosion by channel flow (mass conservation equation incorporating Ackers-White and Engelund-Hansen transport capacity equations)
- Landslide erosion and sediment yield component
- Gully erosion

3.4.4 EUROSEM

The European Soil Erosion Model (EUROSEM) (Morgan, et al 1990) is the result of European Commission funded research involving scientists from Europe and the USA. The model simulates erosion on an event basis for fields and small catchments. It is a single-event, process-based model for predicting soil erosion by water fields and small catchments. The model is based on physical description of the erosion processes and operates for short time steps of about one minute.

Pectora roborant cultus recti

EUROSEM has a modular structure with each process described by a series of mathematical expressions. The water and sediment generated and routed over the land surface characterized as a series of interlinked uniform slope planes and channel elements. Information on vegetation, soil and topographical features is entered into the model which then simulates erosion patterns for individual rainfall events.

3.4.5 LISEM

The Limburg Soil Erosion Model (LISEM) (De Roo, 1996) is one of the first examples of a physically based model that is completely incorporated in a faster Geographical Information System (GIS). Processes included in the model are rainfall, interception, surface storage in micro depressions, infiltration, vertical movement of water in the soil, overland flow, channel flow, detachment by rainfall and through fall, detachment by overland flow, and transport capacity of the flow. Also, the influence of tractor wheeling, small paved roads (smaller than the pixel size) and surface sealing on the hydrological and soil erosion processes is taken into account.

LISEM simulates hydrological and soil erosion processes during single rainfall events on a catchment scale. It is possible to calculate the effects of land use changes and to estimate soil conservation scenarios. Driven with hypothetical storms of known probability of return, LISEM is a valuable tool for planning cost-effective measures to help mitigate the effects of runoff and erosion. LISEM also produces detailed maps of soil erosion and overland flow (DeRoo, Wesseling, Ritsema, 1996).

3.5 REGRESSION-TYPE MODEL-ACRU

3.5.1 Background of ACRU

The ACRU model had its hydrological origins in a distributed catchment evapotranspiration based study carried out in the Natal Drakensberg in early 1970s (Schulze, 1975). The acronym ACRU is derived from the Agricultural Catchments Research Unit within the Department of Agricultural Engineering of the University of Natal in Pietermaritzburg, South Africa. The agro-hydrological component of ACRU first came to the fore during the research on an agro-hydrological and agro-climatology atlas for Natal (Schulze, 1983). Since then the model has developed to its current status. The model has been verified widely on data from southern Africa and the USA, used extensively in decision making in southern Africa and by 1995 the model had been applied internationally in hydrological design, the simulation of water resources and research in Botswana, Chile, Germany, Lesotho, Mozambique, Namibia, Swaziland, USA and Zimbabwe.

According to the ACRU User Manual (2002), the ACRU modelling system is centered on the following aims (Figures 3-4 and 3-5):

- ACRU is a physical conceptual model, and variables are estimated from physical catchments.
- ACRU is a multi-purpose model which integrates the various water budgeting and runoff producing components of the terrestrial hydrological system with risk analysis, and can be applied in design hydrology, crop yield modeling, sediment yield simulation, reservoir yield simulation, irrigation water demand/supply, water resources assessment, planning optimum water resource utilization and resolving conflicting demands on water resources.
- ACRU has been designed as a multi-level model, with either multiple options or alternative pathways available in many of its routines, depending on the level of input data or the detail of output required.
- ACRU can also be operated as a point model, as a lumped small catchments model or on large catchments. For large catchments or in areas of complex land use and soils, ACRU operates as a distributed cell-type model. In distributed model, individual sub-catchments are identified, flows can take place from "exterior" through "interior" cells according to a predetermined scheme, with each sub-catchment able to generate individually requested outputs which may be different to those of other sub-catchments or with different levels of input/information.
- The model uses daily time steps, but monthly data can be transformed internally in ACRU to daily values by Fourier analysis.
- ACRU operates in conjunction with the interactive ACRU Menubuilder and Outputbuilder and the associated ACRU input Utilities. These are suites of software programs to aid in the preparation of input data and information. The ACRU Menubuilder prompts the user with unambiguous questions leading the user into inputting. The Outputbuilder allows the user to select, from a predefined list, which variables are to be stored during a simulation for subsequent output and analysis.

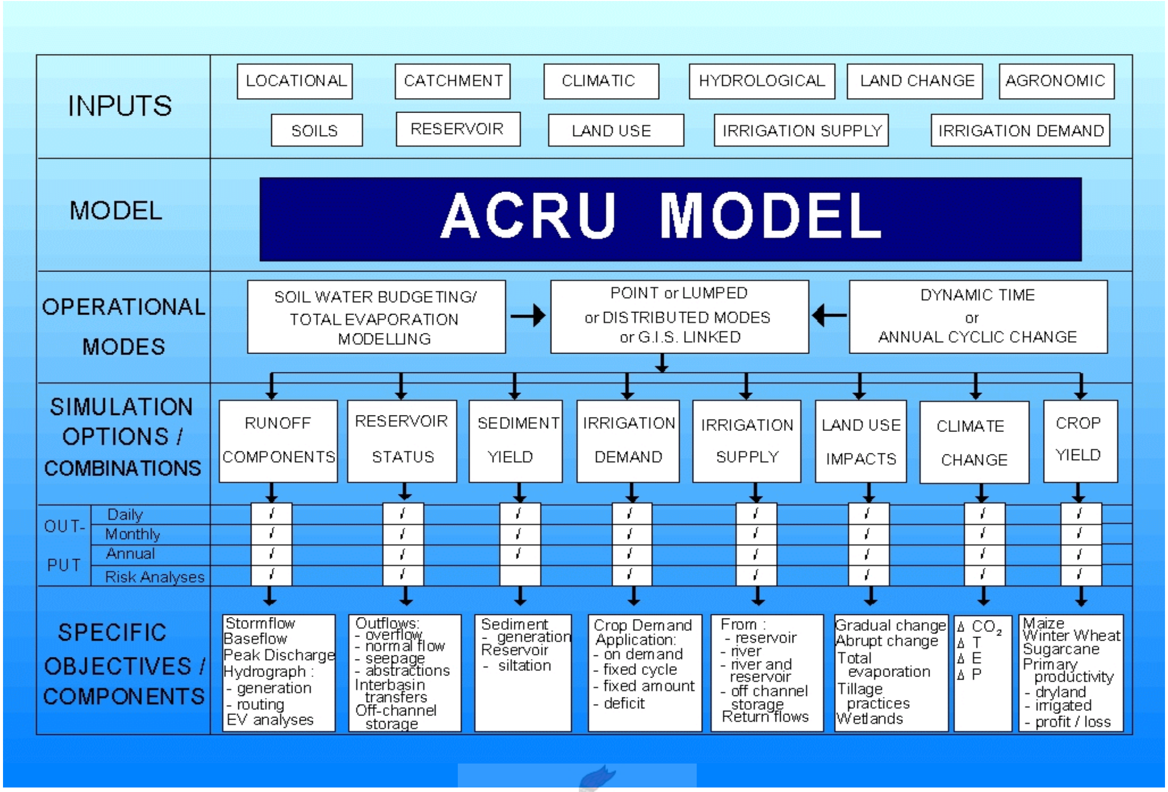

Figure 3-4 ACRU agrohydrological modeling system: Concepts (ACRU User manual)

Pectora roborant cultus recti

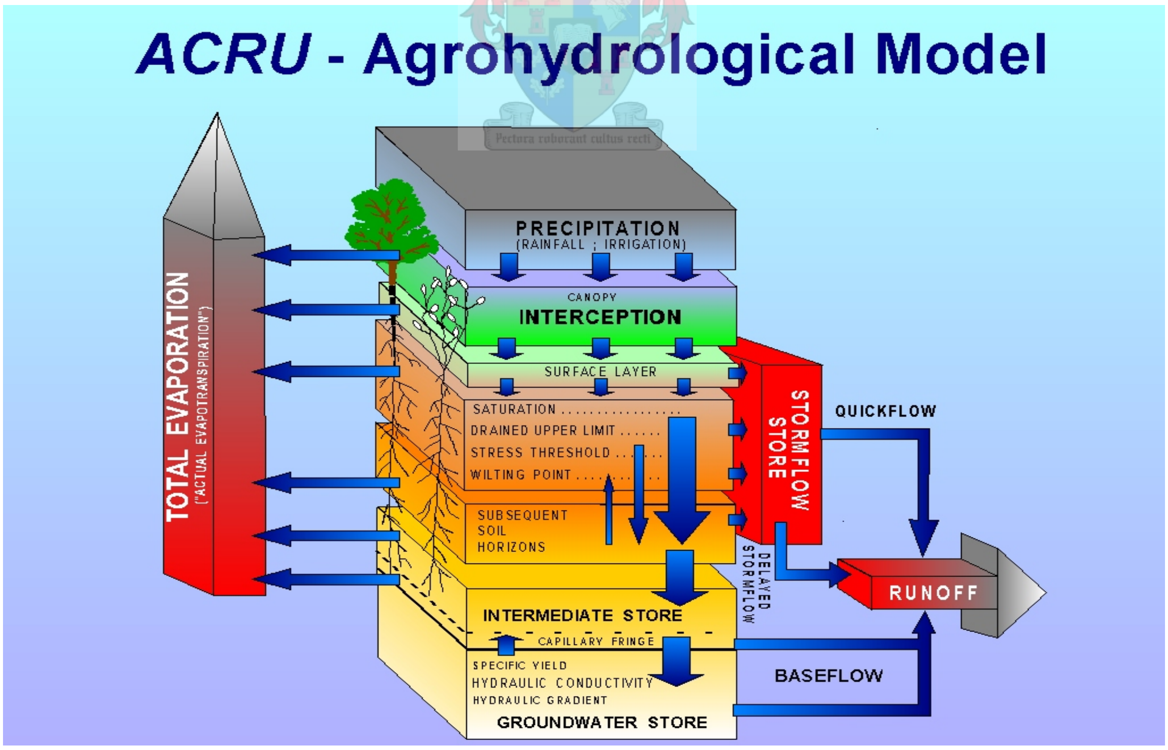

Figure 3-5 ACRU agrohydrological modeling system: General structure (ACRU User manual)

3.5.2 Typical applications of ACRU

Since 1986 the ACRU model has been used extensively to provide objective assessments for a range of water resource related problems. The "heart" of the ACRU model is "daily multi-layer soil water budget" (ACRU User Manual). A number of subhead modules were set up and proved for different objectives, such as:

- Water resources assessments, as: rainfall, evaporation, soil water, drainage from the various soil zones to next lower zones.
- Design flood estimation, as: storm flow, base flow, peak discharge
- Irrigation water demand and supply.
- Crop yield and primary production modeling.
- Assessments of impacts of land use changes on water resources.
- Assessments of hydrological impacts on wetlands.
- Groundwater modeling.
- Assessments of potential impacts of global climate change on crop production and hydrological responses.

3.5.3 Access to the ACRU modeling system

Historically ACRU was developed in a mainframe environment; hence the ACRU model is available for operation on a DOS based PC as well as on the Computing Centre for Water Research's (CCWR) UNIX based mainframe. For this study, ACRU3.00, PC-DOS version was chosen to simulate sediment yields in the Nyando and Nzoia River catchments in Kenya. The entire ACRU modeling system as depicted on Figure 3-6 is available in the PC-DOS version.

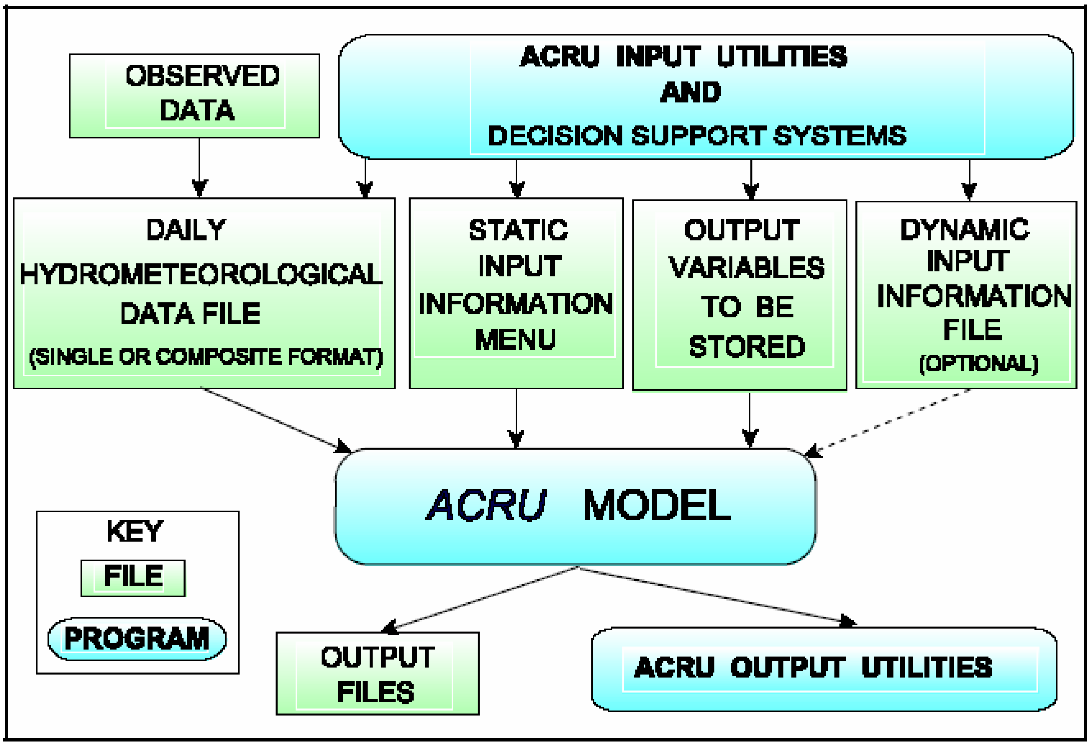

Figure 3-6 Components and linkages of ACRU modelling system (ACRU User manual)

3.5.4 Hydrological modelling incorporating MUSLE in ACRU

Sediment yields in ACRU system are modeled on a day-by-day basis by activating the MUSLE. The ACRU model applies the MUSLE routine in sub-catchments and a hydrological rainfall-runoff model routes the flow and sediment through the catchment. To achieve this objective, MUSLE option must be selected during the model construction. As equation 3.3 shows, there are several factors used to characterize the state of the catchment.

The ACRU model was used to simulate daily sediment yields for each of the 40 sub-catchments of the Mbuluzi catchment in Swaziland for the period of 1945-1995 (Basson, 2004). The total catchment area was about 2500 km^2, with the largest sub-catchment area about 200 km^2. One objective of this study was to assess the effects of land use management on sediment yields. The mean annual sediment yields were reduced in all the sub-catchments after replacing those areas of the present land cover which can be grazed with a grass cover in good hydrological conditions. In this example the simulated sediment yield seemed to be relatively high but the strong point of such a model is however to analyze the relative importance of different land uses and possible rehabilitation.

3.5.5 Conclusions

As a modelling system, ACRU is highly versatile with potential applications ranging from stream flow simulation to crop yield estimations, irrigation simulations, sediment yield, risk analyses and many more. The trade-off for this versatility is that the user needs to know some of the background of ACRU and must be able to prepare a certain amount of data and information before using/operating the modeling system.

Pectora roborant cultus recti

3.6 Model Comparison

A comparison of six physically-based erosion and sediment yield models is presented in Table 3-1.

Table 3-1 Comparison of six physically-based erosion and sediment yield models (Basson, 2004)

Model Feature	SHETRAN	ANSWERS	WEPP	EUROSEM	LISEM	ACRU
Simulation type:						
Continuous	Y	N	Y	N	N	Y
Single event	Y	Y	Y	Y	Y	Y
Basin size	<2000 km^2	<50 km^2	<2.6 km^2	small basin	small basin	*<2000 km^2
Spatial distribution	Grid	Grid or GIS raster	Grid	Uniform slope planes	GIS raster	GIS raster
Overland flow:						
Rainfall excess	Y	Y	Y	Y	Y	Y
Upward saturation	Y	N	N	N	Y	Y
Erosion process:						
Raindrop impact/ overland flow	Y	Y	Y	Y	Y	Y
Rilling	N	N	Y	Y	Y	Y
Crusting	N	Y	N	Y	Y	Y
Channel banks	Y	N	N	Y	N	N
Gullying	Y	N	N	N	N	N
Landsliding	Y	N	N	N	N	N
Output:						
Time-varying sedigraph	Y	Y	N	Y	Y	Y (daily)
Time-integrated yield	Y	Y	Y	Y	Y	Y
Erosion map	Y	Y	Y	Y	N	Y
Land use	Most vegetation covers	Mainly agricultural	Wide range of land use	Mainly agricultural	Mainly agricultural	Mainly agricultural

Y = yes, N = no

* Note: the catchment areas used in this study are 3652 km^2 and 12842 km^2.

Compared with regression-type models (e.g. ACRU), the physical process simulation models have many disadvantages. These disadvantages make the physical process models more complicated.

- Computationally "heavy" when large catchments are simulated.
- Data requirements are more extensive because of increased complexities.
- To complete a physical process model study, the operator must have wide knowledge of erosion, sedimentation and the watershed to ensure the accuracy of the simulated results.

However, in some ways data requirements are simplified for physical process models in that the necessary data are more easily measured and identified because of the physical process basis. Data requirements for regression models are often much more subjective and the parameters often harder to relate to observable and measurable quantities (Basson, 2004). Although regression models also require general knowledge of erosion and watershed, they require less input from the physical process models since the procedures for their applications are usually rigid. The application of regression models or physical process models can produce invalid results without proper training and understanding.

Pectora roborant cultus recti

For effective catchment managements and land care programs, it is critical to model catchment soil erosion processes. For these purposes the ACRU model was selected for use to simulate two catchments in Kenya: Nyando and Nzoia. These catchments' descriptions are provided in the next chapter.

CHAPTER 4 NYANDO RIVER AND NZOIA RIVER CATCHMENT DESCRIPTIONS

4.1 OVERVIEW OF STUDY AREAS

The Nyando River catchment and the Nzoia River catchment are two of the major catchments in Kisumu district, which is situated in Nyanza province in Kenya. These catchments are also two of the eleven catchments around Lake Victoria Basin and are a major source of livehoods of the growing population (Figure 4-1).

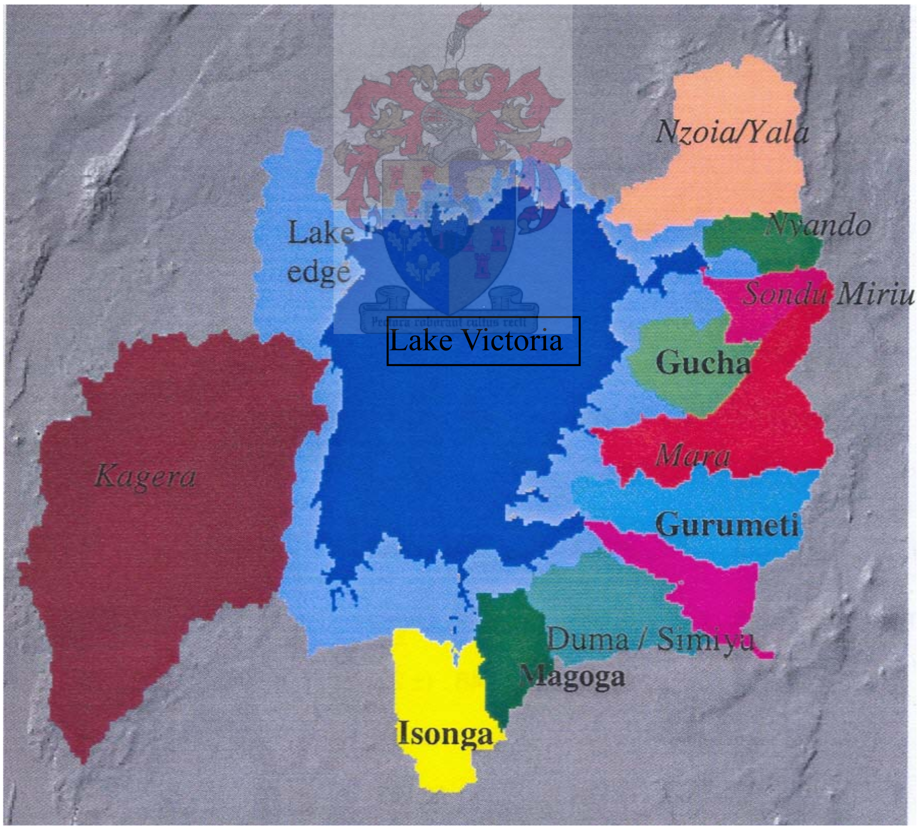

Figure 4-1 Location of Nyando and Nzoia catchments (Swallow, 2000)

A regional assessment (Swallow, 2000) identified the Nyando River and Basin as a major source of sediment and phosphorus flow into Lake Victoria, and many of the previous studies were concentrated on this river basin while methods were being refined. The study identified several soil erosion and land degradation problems throughout the Nyando river basin (Figure 4-2). Similarly, because of excessive usage of land as well as lack of scientific management, the Nzoia River Basin also faces the same problem as the Nyando River basin. It is expected that the delta (above water) at the Nzoia River mouth will reach the Uganda border in 115 years (Basson, 2005). At Winam Gulf the water depth near Kisumu could become less than 2m over a distance of 30 km if the water level drops below the current 1134 masl.

Figure 4-2 Nyando gully erosion

4.2 NYANDO RIVER CATCHMENT DESCRIPTION

The Nyando catchment study area covers an area of 3652km^2. The upland is very heterogeneous and there are huge spatial differences in the type and magnitude of erosion that different areas undergo. The altitude varies from 1070m at the lake shore in the south-western part of the watershed, up to 2700m in the north-eastern end of the watershed. Following the altitude gradient, the watershed can roughly be divided into 5 different land use zones. Small-scale subsistence maize and sorghum farming characterize the lower part of watershed, the lake plain, between 1100m-1300m. Large-scale sugar plantations and smaller sugar schemes are located between 1300m and 1700m. Gradually, the sugar plantations are being replaced by coffee in a zone ranging between 1600m-2000m. Small-scale tea farmers and large tea estates are located between 1900m-2100m. Relatively large-scale maize and horticulture (potatoes, cabbage, etc.) farming characterizes the areas above 2100 meters. The majority of the watershed is more or less continuously cropped. The few exceptions are two remaining forest areas-Tinderet and Mau forest- that are currently being heavily deforested (Hansen and Walsh, 2000).

The Nyando River has three major tributaries: Ainabngetuny, Kipchorian and Awach. Each of them drains a secondary water catchment. They are endowed with springs that feed into the streams which join the main river.

The annual rainfall ranges between 900mm and 2200mm. The evaporation does not vary much and almost equals the rainfall, except during the rainy seasons when the rainfall is much more than the evaporation. The mean maximum temperature occurs in March and the mean minimum temperature occurs in July. The annual average maximum temperatures range from 25-30 ^{0}C, while the annual minimum temperatures range from 10-12 ^{0}C. The satellite image of the Nyando basin with its longitudinal profiles is shown in Figure 4-3.

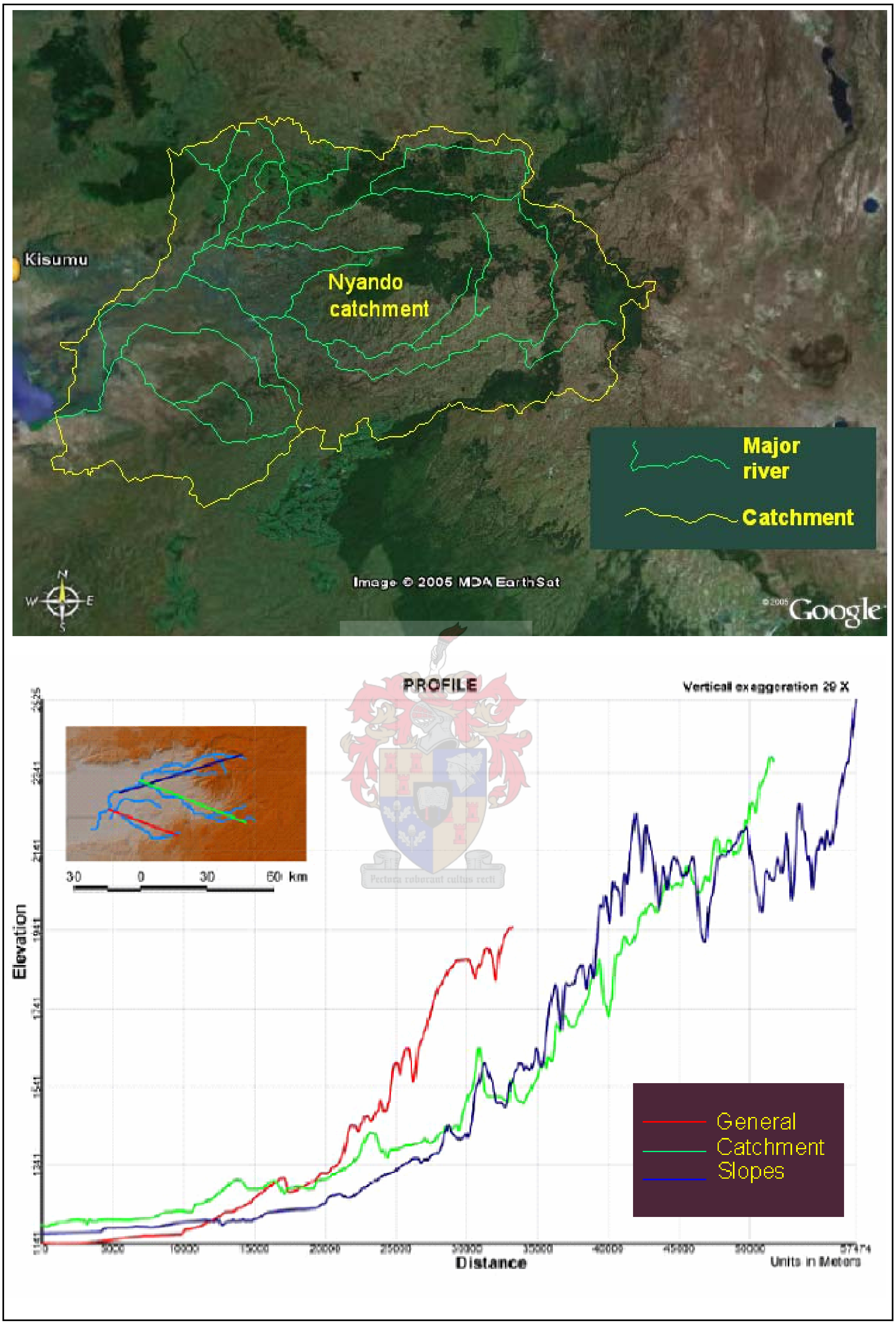

Figure 4-3 Nyando Catchment and longitudinal profiles (Onyango, Swallow & Meinzen-Dick, 2005)

4.3 NZOIA RIVER CATCHMENT DESCRIPTION

The Nzoia River catchment is located north of the Nyando River Catchment, and covers an area of 12842km^2. The Nzoia River is a 257 km long river, rising at Mount Elgon. It flows south and then west, eventually flowing into Lake Victoria near the town of Port Victoria. The altitude varies from 1100m at the lake shore in the south-western part of the watershed, up to 3000m in the northern end of the watershed at Mount Elgon. The river is important to Western Kenya, flowing through a region estimated to be populated by over 1.5 million people. It provides irrigation throughout the year, while the annual floods around the lowland area of Budalangi deposit sediment that contributes to the area's good agricultural production. Around the industrial region centred at Webuye, the river absorbs a lot of effluent from the paper and sugar factories in the area. The river has a number of spectacular waterfalls, and is thought to possess a good hydroelectricity generation potential.

The catchment's annual rainfall ranges between 1000 mm and 1800 mm. The evaporation and the temperature distribution are similar to Nyando Basin. The land use is similar to that of the Nyando Catchment. The satellite image of Nzoia Catchment is shown in Figure 4-4.

Pectora roborant cultus recti

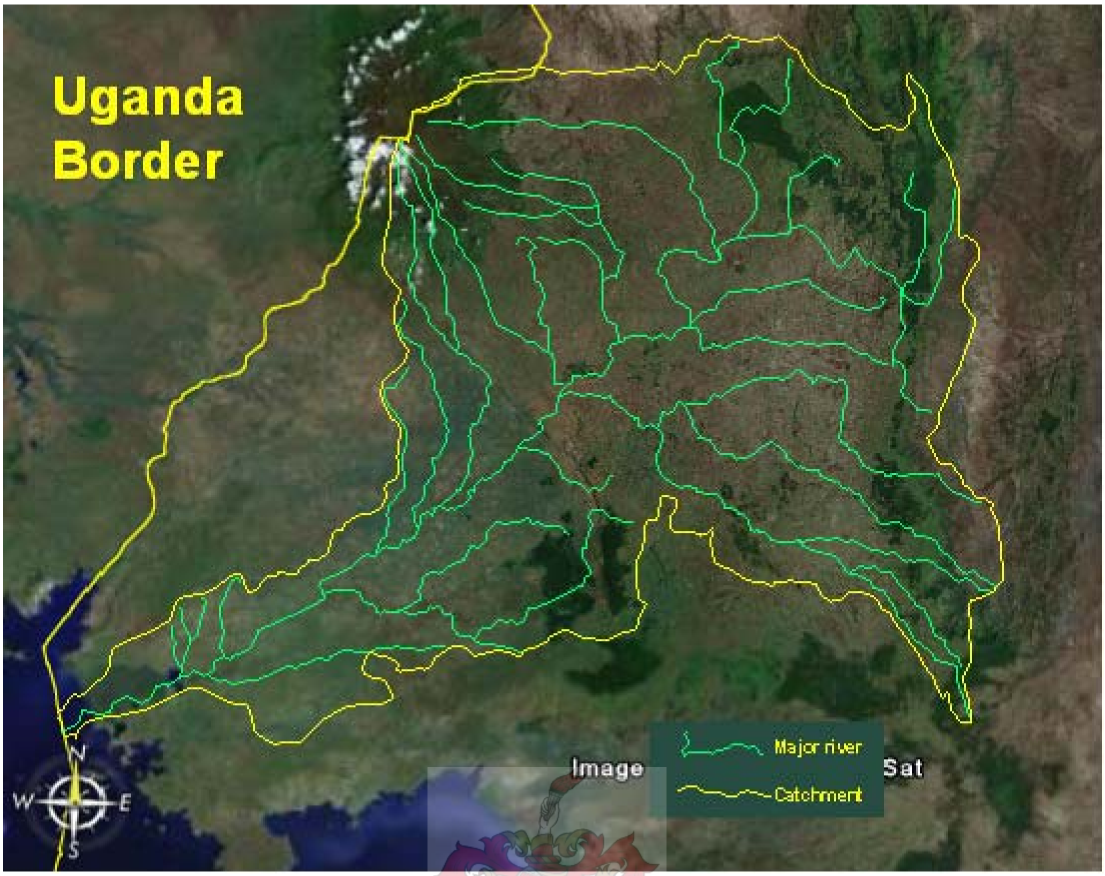

Figure 4-4 Nzoia catchment

Pectora roborant cultus recti

CHAPTER 5 DATA PREPARATION AND MODEL CONFIGURATION

5.1 INTRODUCTION

As the ARCU program manual describes, the ACRU is a multi-level model, with either multiple options or alternative pathways available in many of its routines, depending on the level of input data available or the detail required. The Nyando catchment and Nzoia catchment data preparation as well as model configuration are discussed in this chapter.

5.2 MINIMUM REQUIREMENTS OF MODEL CONFIGURATION

According to the ACRU User Manual minimum data and information required for running the model depends on the options chosen and on the availability of data/information to a particular user. Typical minimum data and information requirements which are compulsory inputs into the model and which are readily obtainable for southern Africa are summarized schematically in Figure 5-1. The optional inputs to the model are required to simulate specific processes (such as sediment yield), and typically required inputs are also included in Figure 5-1.

Pectora roborant cultus recti

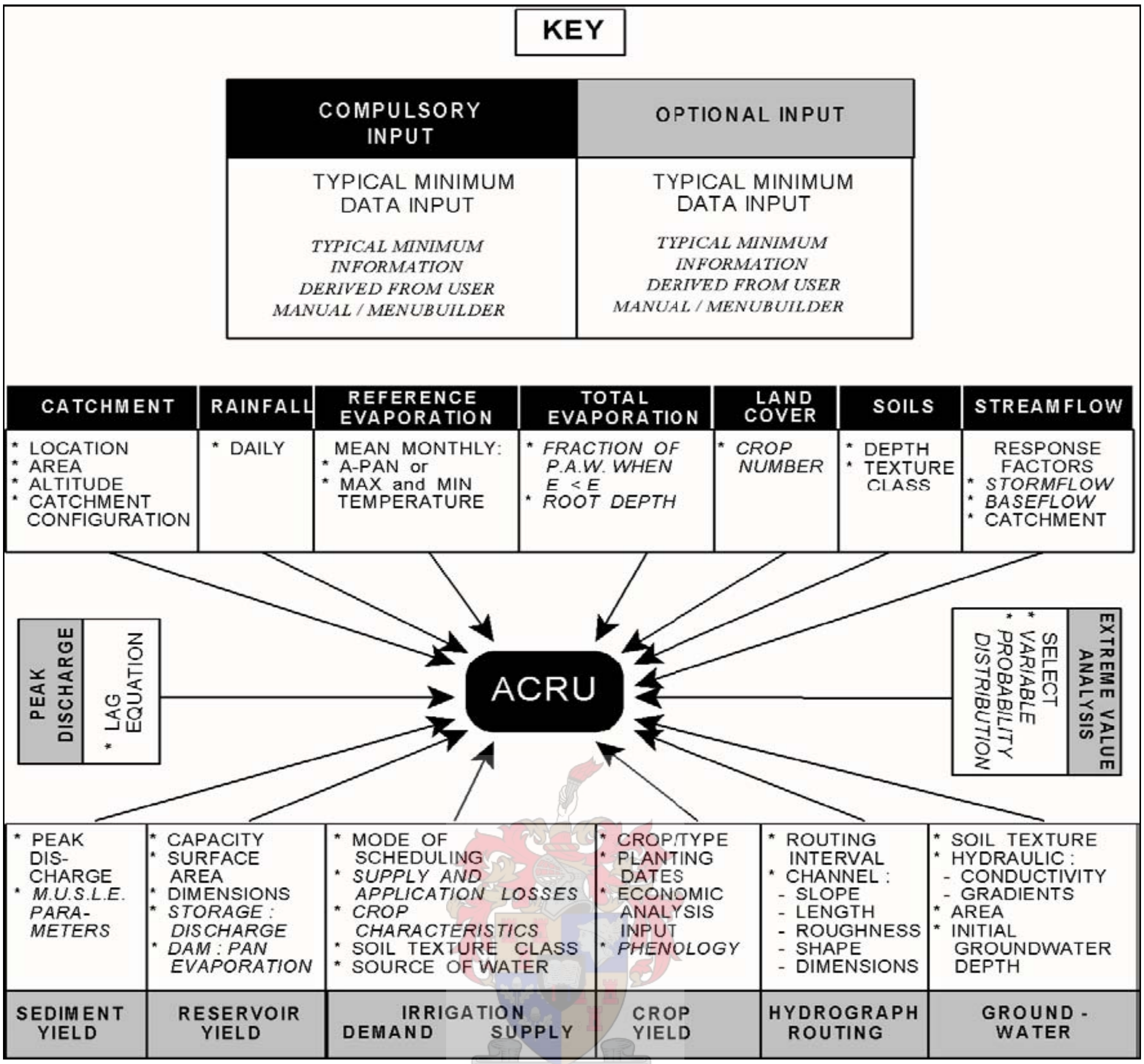

Figure 5-1 Typical minimum data and information required to run ACRU in southern Africa (ACRU User Manual)

In the context of the ACRU modelling system the MENU is an input file containing information which controls the execution of ACRU, as well as information describing relevant catchment characteristics. The information contained in the MENU includes:

- location information
- sub-catchment configuration
- input data file organization
- length of rainfall record
- other climate input, particularly with respect to reference potential evaporation

- soils information
- land cover and land use information
- total evaporation control variables (including options for enhanced CO_2 concentrations)
- runoff volume and peak discharge variables and parameters
- sediment yield options and input
- irrigation water demand and supply options and input
- reservoir yield analysis options and input
- crop yield options and input
- hydrograph routing options and input
- shallow groundwater modeling options and input
- wetland modeling and input
- extreme value analysis options

The total requirements for the menu input cover all aspects of ACRU applications, but many sections can be omitted if a particular simulation is not concerned with one or other aspect of the agrohydrological system or operation.

In this study, both Nyando River Catchment and Nzoia River Catchment models are aimed at performing sediment yield analysis. The typical data and information required to construct a sediment yield model are presented at Table 5-1.

Table 5-1 Sediment yield model minimum data requirement

General catchment information	Number of sub-catchments making up catchment			
	Area	km^2		Per sub-catchment
	Average Elevation	m		Per sub-catchment
	Latitude and Longitude of the centre of the catchments	degree and minutes		Per sub-catchment
	Indicator if catchment is to the north or south of hemisphere			Per sub-catchment
	indicator if catchment is to the east or west of Greenwich			Per sub-catchment
Meteorological	Rainfall	mm	Daily	Per sub-catchment
	MAP	mm		Per sub-catchment
	Min Temperature	^oC	Monthly mean of daily values	Per sub-catchment
	Max Temperature	^oC		Per sub-catchment
	Evaporation	mm	Monthly totals	Per sub-catchment
Land use and cover	Interception loss	mm/rainday	monthly	Can be estimated from similar land cover in ACRU manual CROP number system
	Average Crop Coefficient		monthly	
	Fraction of roots active in top soil		monthly	
	Effective rooting depth	mm	monthly	
Soils information	Texture Class			Binomial or Taxonomic Soil Classification
	Depths	m		
Peak Discharge	Average Catchment Slope	%		GIS or Topographies
	Time of Concentration	hr		Can be estimated from standard hydraulic equations
Sediment Yield	Maximum Soil Erodibility Factor			Can be estimated from Taxonomic or Binomial Soil Classification
	Minimum Soil Erodibility Factor			
	Slope Length & Steepness Factor			Topographies and Equations in ACRU manual
	Cover Factor		Monthly	Function of land use type
	Support Practice Factor			Function of land use type
	Fraction of event based sediment yield that reaches the outlet on the first day			

5.3 INPUT DATA PREPARATION AND CONFIGURATION

ACRU can be operated as a point model, but for large catchments of complex land use and soils, it could be divided into individual sub-catchments. Each sub-catchment requires individual daily rainfall and other input files.

All the data has to be modified into a format which is required by ACRU. Data for this research was supplied by the Water Department of Kenya. Unfortunately the Department only has very limited information, which could only used for a general model set up, such as 1:250 000 scale topographic maps, and daily rainfall data measurement from 1950 to 2004. The other necessary data had to be collected via other approaches, such as websites and previous research documentations. However, it was difficult to make the data found from different sources span the 1950 to 2004 period. It inevitably affected the precision of the simulated result. Many default values therefore had to be set in the ACRU software, when regional values could not be found.

5.3.1 Nyando River Catchment

Nyando River Catchment covers 3652 km^2. The altitude ranges from 1070 masl up to 2700 masl. There are three rainfall stations located in the catchment, namely Kericho, Koru, and Kano. Only a single gauging station measures discharge, near the downstream end of the main river at Ahero (Figure 5-2, 5-3, 5-4 & 5-5). Based on the number of rainfall stations, the land use, and tributaries, the entire catchment was divided into 10 sub-catchments (Figure 5-6).

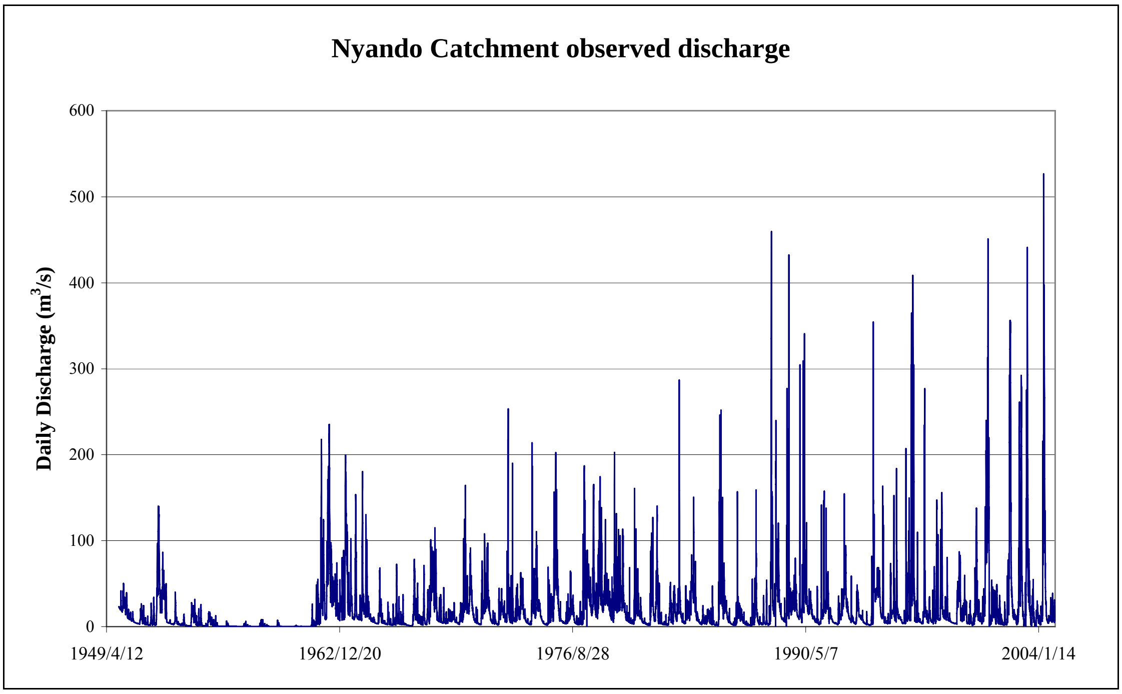

Figure 5-2 Nyando catchment observed daily flow at Ahero

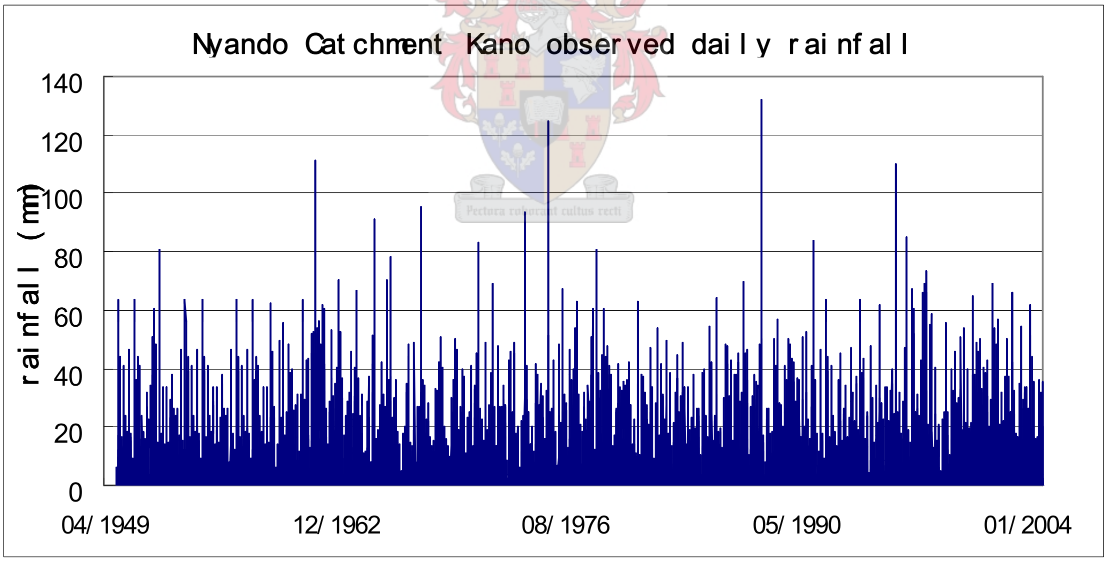

Figure 5-3 Nyando Catchment Kano observed daily rainfall

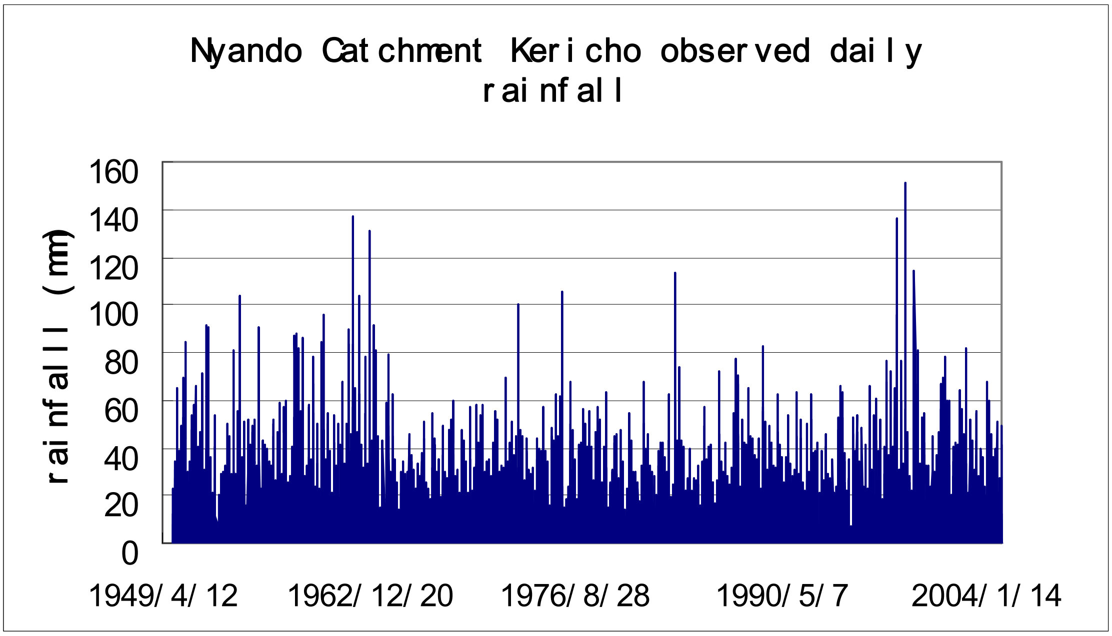

Figure 5-4 Nyando catchment Kericho observed daily rainfall

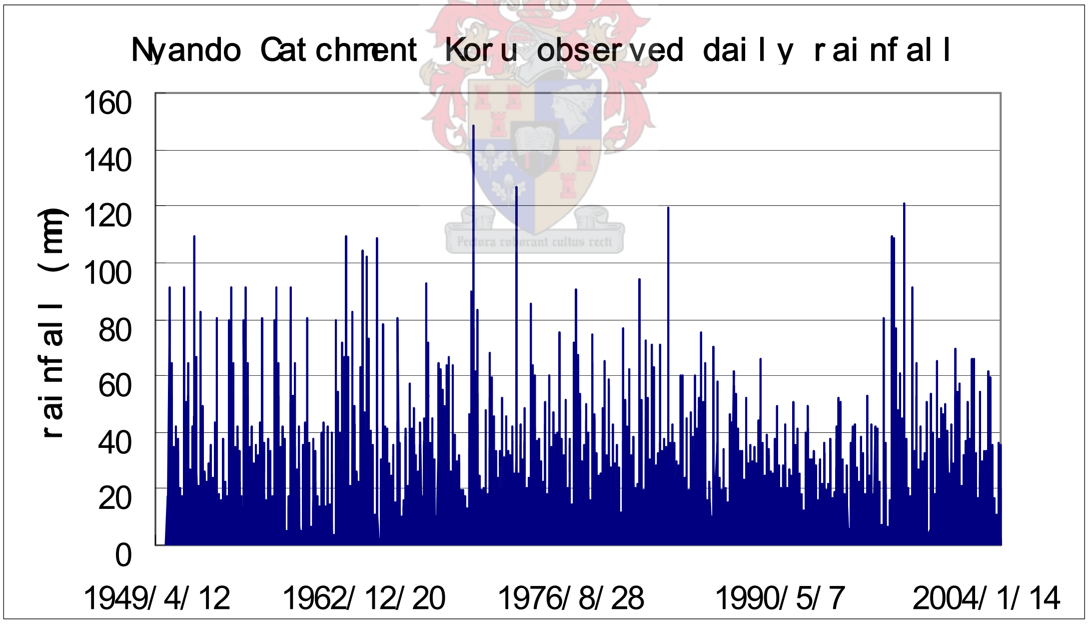

Figure 5-5 Nyando catchment Koru observed daily rainfall

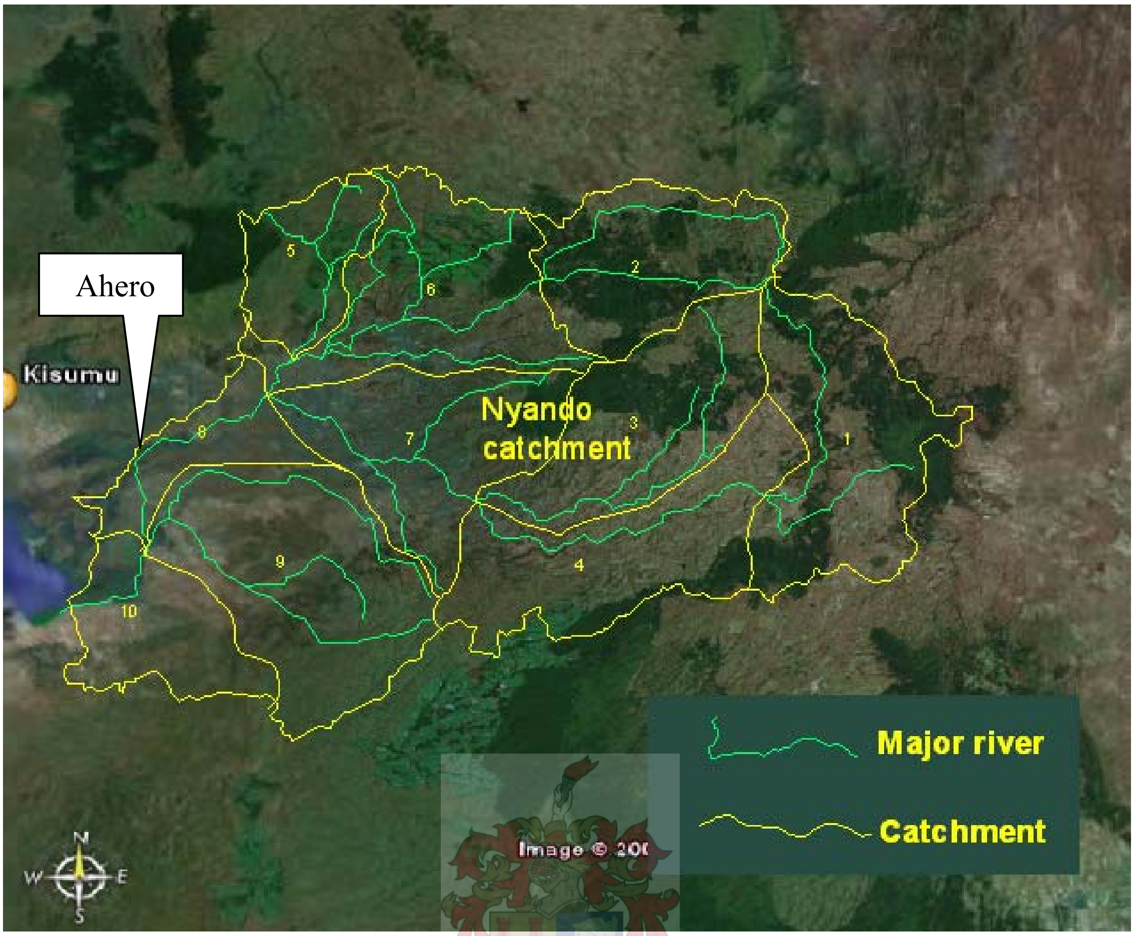

Figure 5-6 Nyando catchment with its 10 sub-catchments

a) Sub-catchments information

Sub-catchment data is provided in Table 5-2.

Table 5-2 Nyando River catchment model general sub-catchments information

Module	**General sub-catchments information**					
Subcatchment No.	**Area**	**Average Elevation**	**Latitude of the centre of the catchment**	**Longitude of the centre of the catchment**	**Indicator if catchment is in the northern or southern of hemisphere**	**Indicator if catchment is to the east or west of Greenwich**
Unit	km^2	masl	degree	degree		
1	460.4	2505	0.18	35.6	south	east
2	348.1	2360	0.00	35.33	south	east
3	394.6	2020	0.18	35.33	south	east
4	444	1973	0.27	35.33	south	east
5	193.8	1696	0.00	35.07	south	east
6	445.8	1723	0.00	35.15	south	east
7	406.1	1800	0.17	35.15	south	east
8	162.5	1230	0.13	34.98	south	east
9	557.8	1560	0.27	35.07	south	east
10	241.7	1140	0.3	34.88	south	east

b) Meteorological information

i. Daily rainfall and mean annual precipitation (mm) of sub-catchments

There are three rainfall stations with daily rainfall measurements from 1950-2004 available for Nyando Catchment, as well as a MAP (mean annual precipitation) contour profile map (Figure 5-7). Calculated rainfall stations' MAPs are: Kericho, 2175 mm; Koru, 1726 mm; and Kano, 1207 mm. The Kericho gauge covers sub-catchments 1 to 7; Koru is located in sub-catchment 8; while sub-catchments 9 and 10 are represented by the Kano gauge. The sub-catchments' MAPs were read from the rainfall contour map and given in Table 5.3:

Table 5-3 Nyando subcatchments MAP based on rainfall contour map

Subcatchment NO.	1	2	3	4	5	6	7	8	9	10
MAP (mm)	1100	1300	1300	1400	1600	1400	1300	1100	1100	1100

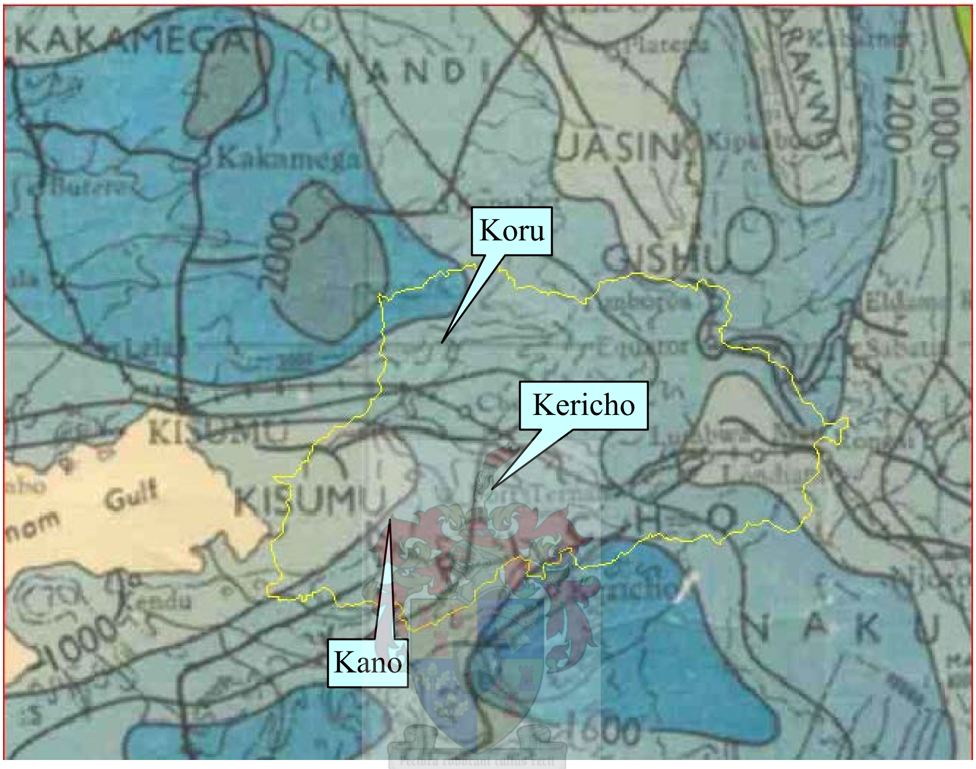

Figure 5-7 Nyando catchment MAP contour isolines

The rainfall station measured MAP values were much greater than the MAP values read from the rainfall contour distribution map; hence, the station measured daily rainfall of each sub-catchment had to be calibrated by using following the equation:

$$R_i = \frac{MAP_r}{MAP_m} \times R' \qquad \text{Eq 5.1}$$

Where:

R_i = specific calibrated daily rainfall for a certain sub-catchment (i = 1, 10)

MAP_r = mean annual precipitation collected from rainfall distributing map

MAP_m = mean annual precipitation measured at rainfall stations

R = daily rainfall data measured at rainfall stations

Different sub-catchment daily rainfall could be calibrated via Equation 5.1 by using relevant rainfall station records. Finally, the model used the scale MAP_s for the Nyando River sub-catchment catchments as shown in Figure 5-8.

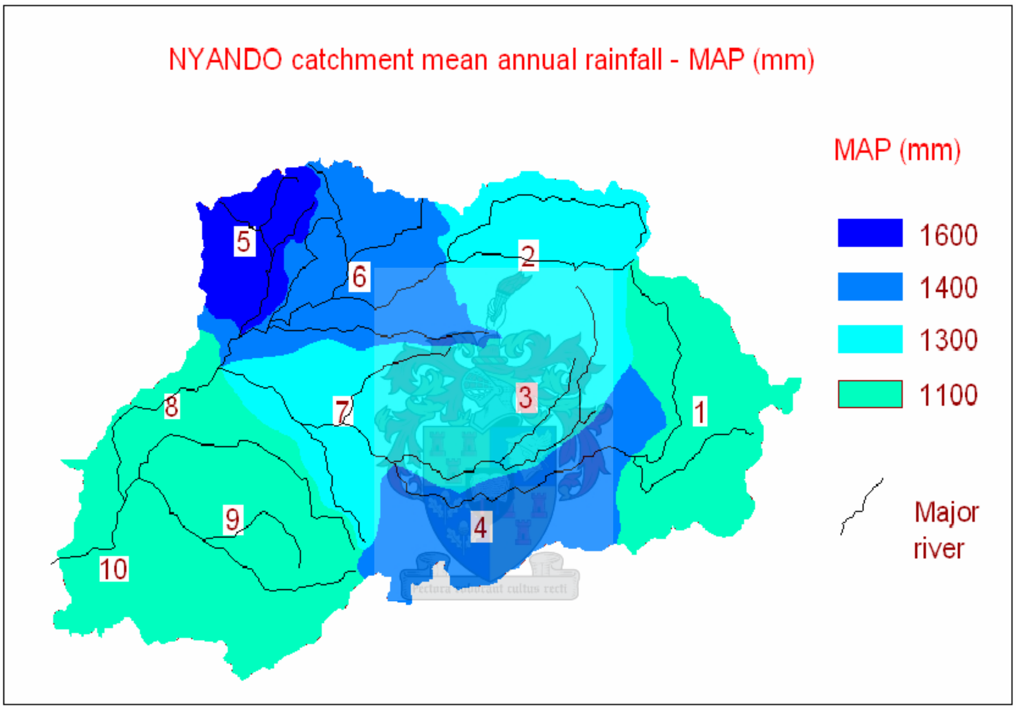

Figure 5-8 Adjusted Nyando catchment MAP as used in the ACRU model

ii. Minimum, maximum monthly mean of daily temperatures and monthly evaporation for sub-catchments

In the Nyando Catchment, generally, the mean maximum temperature occurs in February and the mean minimum temperature occurs in July. The evaporation does not vary much and almost equals the rainfall, except during the rainy seasons when the rainfall is more than the evaporation (Table 5-4). The graph (Figure 5-9) also clearly indicates the relationship between the monthly temperature and evaporation.

Table 5-4 Nyando catchment monthly temperatures and monthly evaporation

	Unit	JAN	FEB	MAR	APR	MAY	JUN	JUL	AUG	SEP	OCT	NOV	DEC
Max Temp.	**^{0}C**	27.5	28	28	27	26	25.5	25	26	27	26	26	26
Min Temp.	**^{0}C**	10.5	11	11	11.5	11	11	10	10.5	10	11	11	11
Monthly evaporation	**mm**	68	68	72.5	57.5	54	51	50	58	67.5	69	70	70

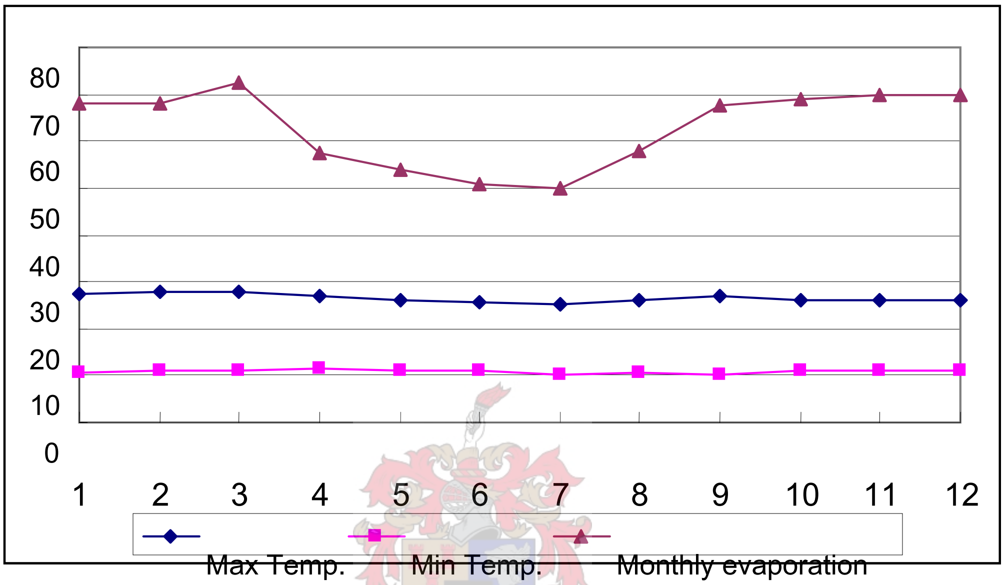

Figure 5-9 Monthly evaporation and temperatures of Nyando

c) Land use and cover information

According to the description in section 4.2, the different land covers are located at different altitude gradients. Each sub-catchment has its separate mean altitude, which differentiates land use. In addition, two extra factors had to be considered during the data preparation: one is that there is an area of wetland located at the Nyando River mouth, and the other factor is that the ACRU model does not include coffee and tea plantation factors. Consequently, it is impossible to simulate land use under the coffee and tea plantations conditions. For this model study, the land use properties of coffee and tea were assumed to be the same as sugar plantations.

The land use and cover of each sub-catchment is illustrated in Table 5-5, and Figure 5-10 also describes the layout of Nyando catchment & sub-catchment land use and cover. Forest cover is included in the model, but is not show in this Figure.

Four factors were used to describe land use and cover conditions. These were presented in Table 5-1 previously, and can easily be estimated from similar land covers in the ACRU manual CROP number system.

Table 5-5 Land cover of Nyando Catchment

Sub-catchment No.	1	2	3	4	5	6	7	8	9	10
Land cover	mixed crop	mixed crop	sugar cane	sugar cane	sugar cane	sugar cane	sugar cane	mixed crop	sugar cane	wetland

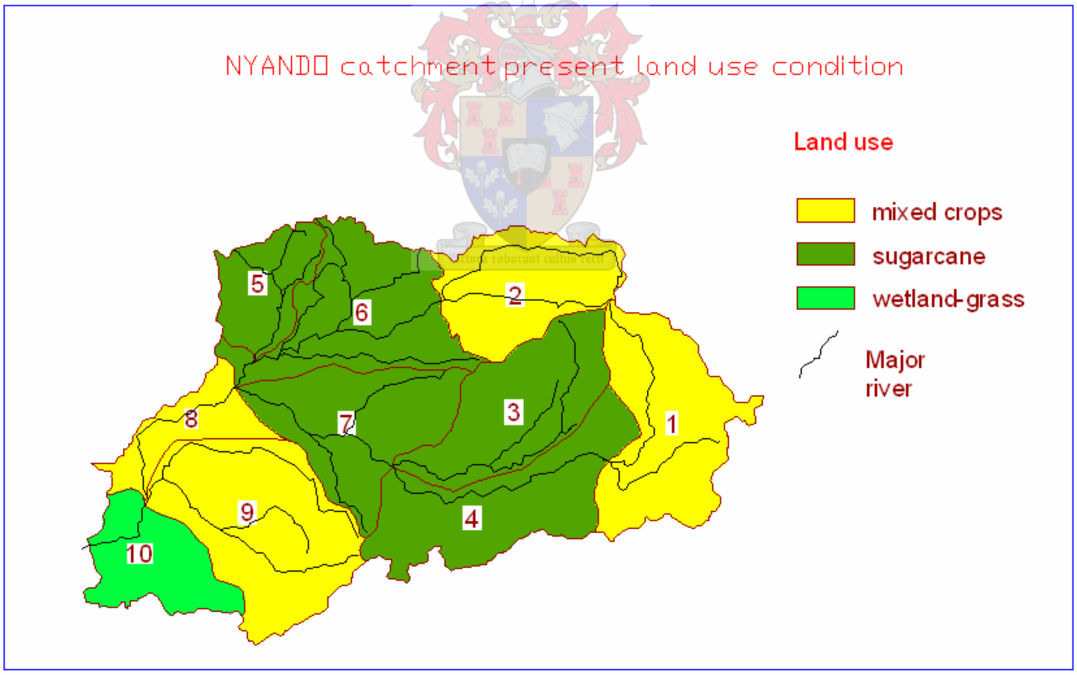

Figure 5-10 Nyando catchment's current land use (natural forests is not shown)

d) Soils information

Soils texture class, as well as depths were unknown during the model setup. A sand-loam-clay soil texture class was used as default value for the model configuration. Surface soil depth and second layered soil depth were also taken as default values. Soil type and depth were adjusted later as part of the variables changed during the model calibration to achieve current discharge and will be discussed in the following chapter.

e) Peak discharge information

The calculation of peak discharge information depends on two major factors:

i. **Average sub-catchments slope**; which is one of the important characteristics that determine the catchment response in the case of runoff (Shaw, 1988). The grid method was used to determine the average sub-catchments slope ($\bar{l}$), the equations used for the grid method were as follows:

$$\bar{l} = \sum_{i=1}^{N} \frac{l_i}{N} \quad \text{and} \quad S_A = \frac{\Delta H}{\bar{l}} \qquad \text{Eq 5.2}$$

Where,

S_A = average catchment slope

l_i = distance along river between two consecutive contours

N = number of grid points

ΔH = contour interval

Parameters l_i, N and ΔH were measured on 1: 250 000 topographic maps with the map contour intervals at 200m.

ii. **Time of concentration** is the time a water particle requires traveling from the furthest point in the catchment to the outlet. Time of concentration can consist of natural channel and overland flow components (Rademeyer, 2004).

Natural channel

The US Bureau of Reclamation Equation was used to calculate the time of concentration for channel flow.

$$t_c = \tau \left(\frac{0.87 L_1^2}{1000 S_L} \right)^{0.385} \qquad \text{Eq 5.3}$$

Where,

t_c = time of concentration (hour)

τ = correction factor

L_1 = length of longest natural channel (km)

S_L = mean channel slope (m/m)

According to Rademeyer (2004), experience has shown that the above equation results in too high values in some cases and too low in others. A set of correction factors (τ) has been developed by Kovacs (unpublished) to overcome this problem. See Table 5-6.

Table 5-6 Correction factors for t_c (Kovacs, unpublished)

A (km^2)	τ
< 1	2
1- 100	2 - 0.5 log A
100- 5 000	1
5 000- 10 000	2.42 – 0.385 log A
> 10 000	0.5

Mean channel slope (S_L) is defined difference from the average catchment slope. There are several methods used to estimate the mean channel slope. One of the methods Taylor-Schwarz (Flood Studies Report, 1975) was selected to estimate the mean channel slope in this study since it is scientifically more accurate than other methods.

$$S_L = \left(\frac{L}{\sum_{i=1}^{n} \frac{l_i}{\sqrt{S_i}}} \right)^2 \qquad \text{Eq 5.4}$$

Where,

L = longest watercourse in catchment (m)

l_i = distance along river between two consecutive contours (m)

S_i = slope between two consecutive contours (m/m)

Longest watercourse (L) is defined as the route that will be followed by a water particle taking the longest time to reach the catchment from a point on the catchment boundary. This distance consist of the natural channel (L_1) and overland flow (undefined channel, L_2). L was measured on 1: 250 000 topographic maps in this study.

<u>Overland flow</u>

The time of concentration of overland flow was not considered in the present study, because most of the sub-catchments do not have overland flow.

For the Nyando River with its tributaries as shown in Figure 5-11, the peak discharge calculation results are shown in Table 5-7.

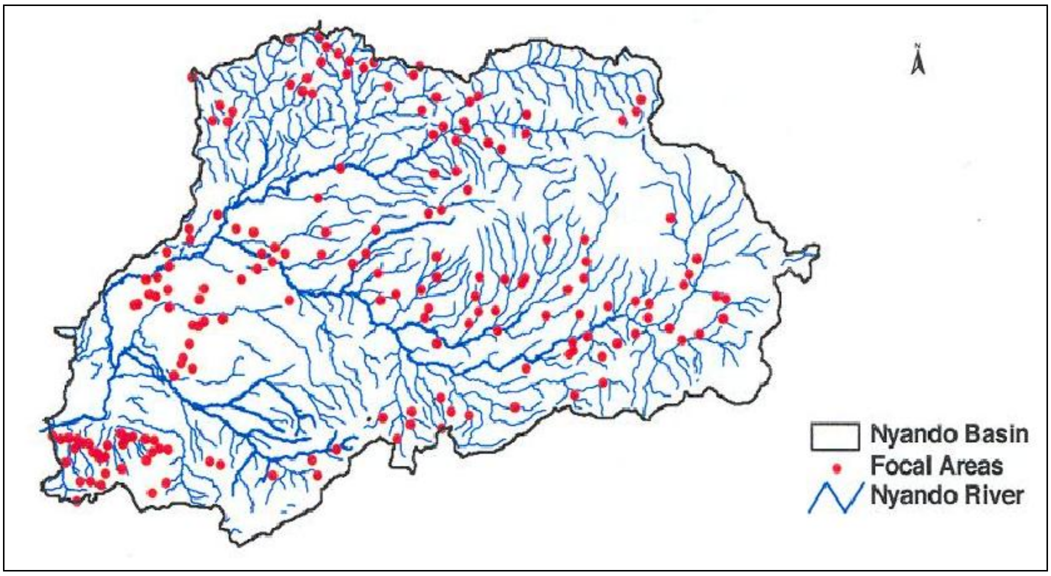

Figure 5-11 Nyando River with its tributaries (Hansen & Walsh, 2000)

(Note: Red dots are used in a separate study in the reference)

Table 5-7 Peak discharge variables of Nyando Catchment

Subcatchment No.	Unit	1	2	3	4	5	6	7	8	9	10
Mean catchment slope	**%**	1.4	2.9	2.5	1.6	2.3	1.1	0.3	0.3	1.4	0.3
Mean channel slope	**%**	1.4	2.9	2.5	1.6	2.3	1.1	0.3	0.3	1.4	0.3
Time of concentration	**hours**	5	3	4	5	3	5	12	6	5	5

f) Sediment yield information

The Modified Universal Soil Loss Equation (MUSLE) estimates the bulk delivery of sediment at a catchment outlet. Based on MUSLE, there are several factors used to characterize the state of sediment yield and soil erosion in ACRU systems, viz. the runoff erosivity constant, runoff erosivity exponent in terms of its runoff energy; the maximum and minimum soil erodibility in terms of the inherent soil loss potential, others such as slope length factor, the cover factor, and the support practice factor. All of these factors need to be considered to determine the sediment yield. Unfortunately, there is only very limited topographic data (viz. slope length and steepness) available at Nyando Catchment. Soil erodibility factors were not available for the model study. Accordingly, a number of default values had to be used to configure the first model set up. During the model sediment yield calibration, however, against observed data, the above mentioned soil erodibility data was adjusted by trial.

5.3.2 Nzoia River catchment

Nzoia River catchment covers 13691 km^2 which is a large catchment area. Its altitude ranges from 1070 m up to 3000 m. There are only three rainfall stations located in the catchment, named Eldoret, Bungoma and Kitale. A single flow gauging station measures discharge near the Nzoia River mouth (Figure 5-12, 5-13, 5-14, and 5-15). As the largest catchment around Victoria Lake in Kenya, the Nzoia River also has the highest average daily discharge at 118.7m^3/s (1950-2004). Twenty six sub-catchments were selected for the ACRU model (Figure 5-16). The information available for this catchment is even less than for the Nyando catchment, and therefore, the Nzoia catchment model had to use a large number of similar data from Nyando Catchment directly, and the accuracy of the simulation results would inevitably be affected.

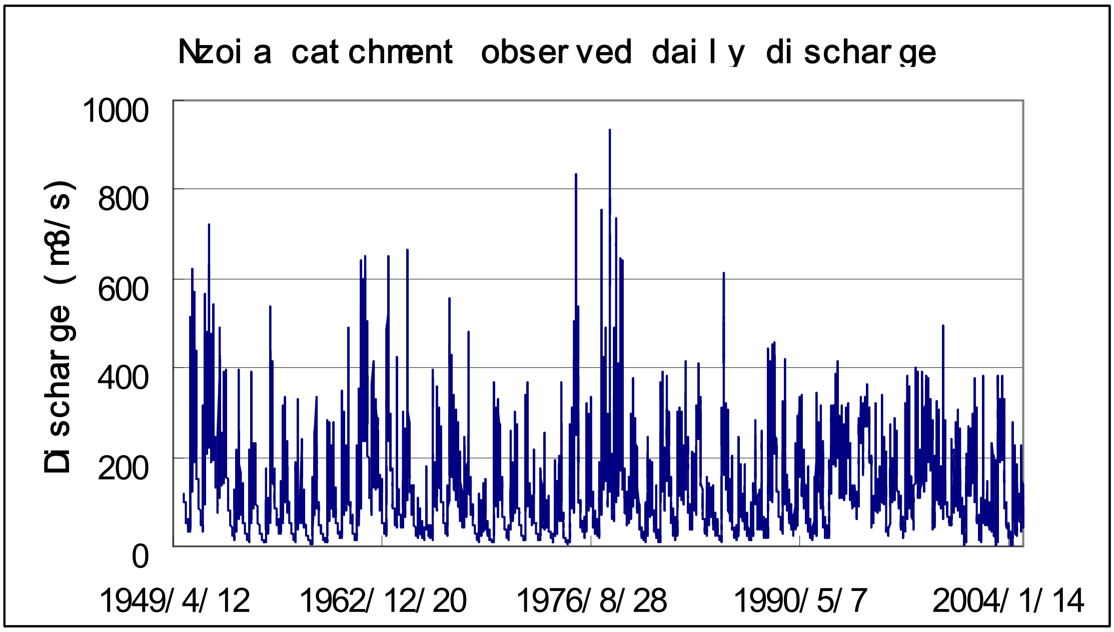

Figure 5-12 Nzoia catchment observed daily discharge

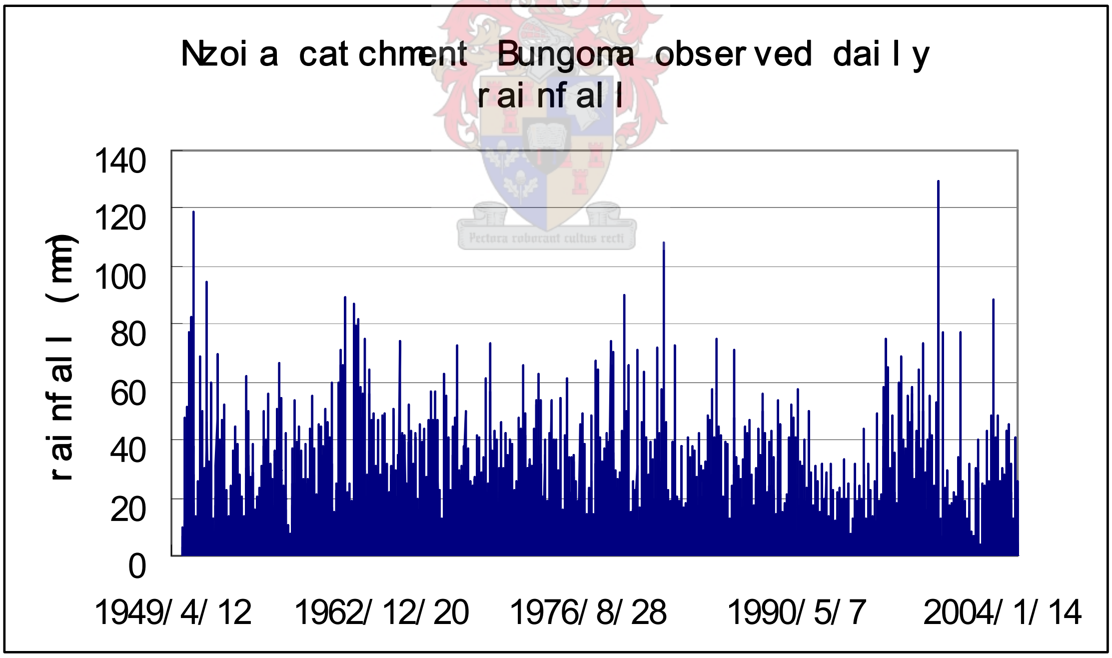

Figure 5-13 Nzoia catchment Bungoma observed daily rainfall

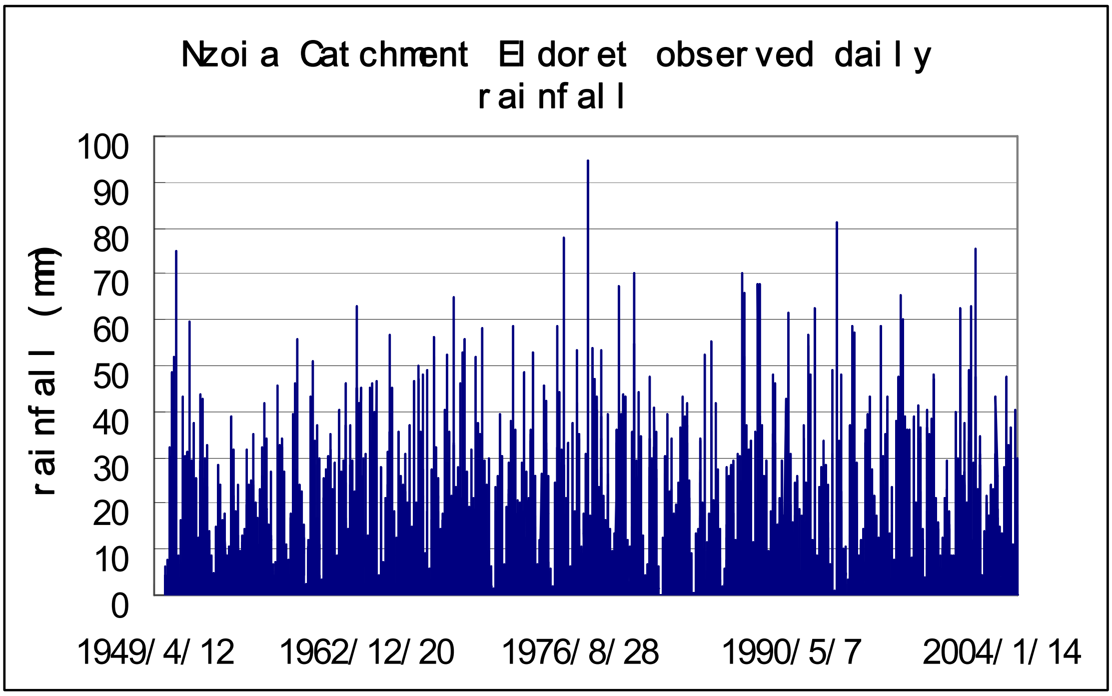

Figure 5-14 Nzoia catchment Eldoret observed daily rainfall

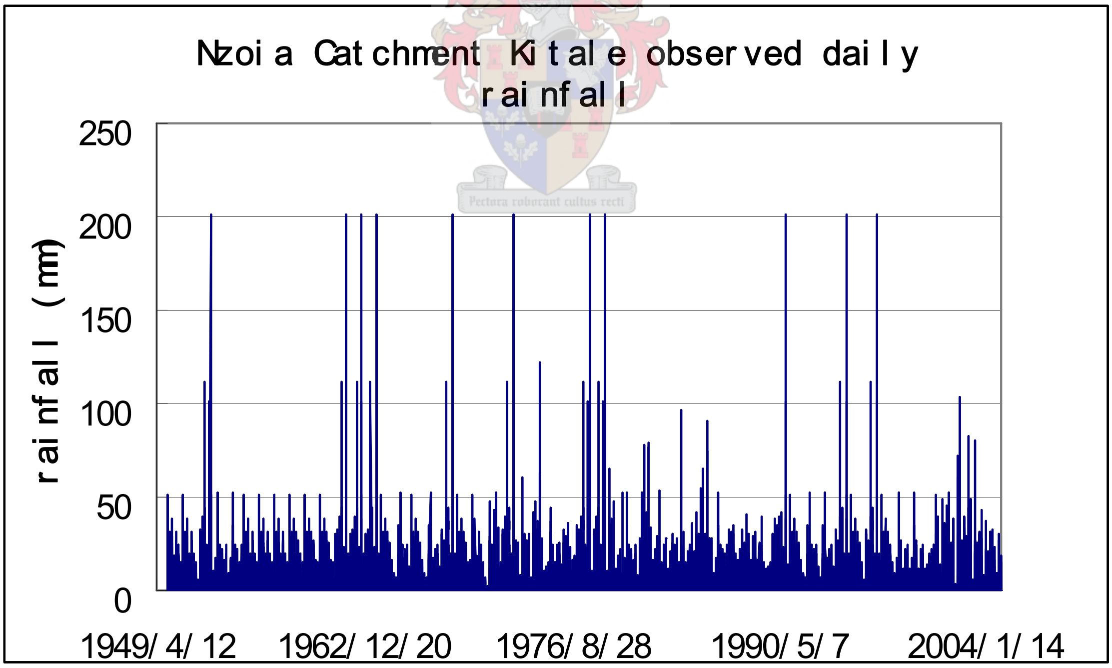

Figure 5-15 Nzoia catchment Kitale observed daily rainfall

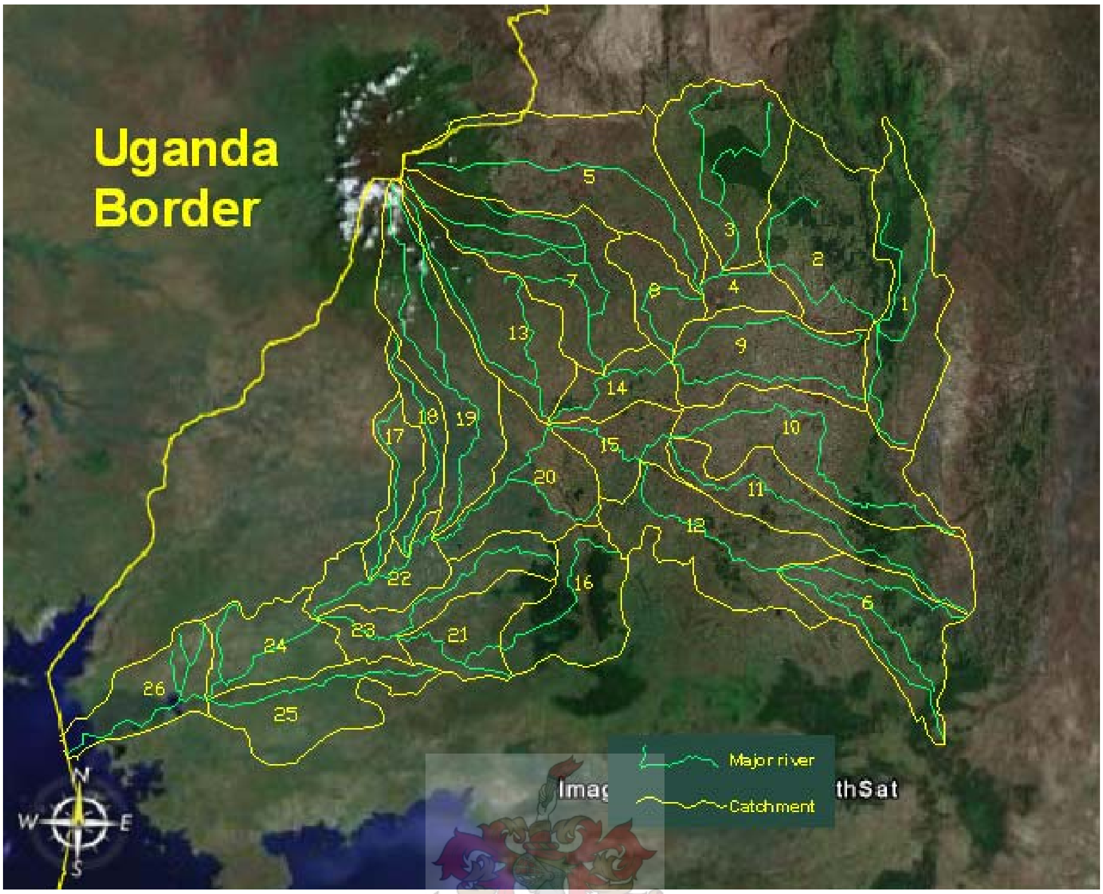

Figure 5-16 Nzoia catchment divided into 26 subcatchments

The model data configuration for Nzoia River Catchment followed the same procedure as for the Nyando River catchment.

a) General catchment/ sub-catchments information

General catchment & sub-catchments information is described as Table 5-8.

Table 5-8 Nzoia River catchment model general sub-catchments information

Module	General sub-catchments information					
Subcatchment NO.	**Area**	**Average Elevation**	**Latitude of the centre of the catchment**	**Longitude of the centre of the catchment**	**Indicator if catchment is in the northern or southern of hemisphere**	**Indicator if catchment is to the east or west of Greenwich**
Unit	km^2	masl	degree	degree		
1	710.61	2584	0.87	35.52	north	east
2	780.45	2280	1.35	35	north	east
3	727.4	2052	1.18	35.13	north	east
4	178.4	1900	1.22	34.92	north	east
5	1078.23	2781.6	0.9	35.15	north	east
6	569.93	2280	1.47	34.32	north	east
7	803.71	2888	0.88	34.97	north	east
8	266.84	1793.6	1.07	34.92	north	east
9	613.18	1976	1.25	34.3	north	east
10	820.11	2204	1.32	34.65	north	east
11	670.4	2280	1.33	34.5	north	east
12	713.89	1900	1.15	34.47	north	east
13	588.69	2796.8	0.77	34.87	north	east
14	258.19	1641.6	0.98	34.75	north	east
15	289.84	1641.6	0.98	34.63	north	east
16	504.89	1717.6	0.92	34.33	north	east
17	204.21	1398.4	0.58	34.55	north	east
18	222.04	1763.2	0.63	34.62	north	east
19	769.91	2766.4	0.67	34.78	north	east
20	556.19	1459.2	0.82	34.57	north	east
21	351.35	1368	0.7	34.28	north	east
22	311.42	1292	0.55	34.38	north	east
23	394.55	1368	0.63	34.35	north	east
24	402.47	1185.6	0.33	34.27	north	east
25	508.95	1276.8	0.4	34.15	north	east
26	397.02	1146.1	0.1	34.17	north	east

b) Meteorological information

i. Daily rainfall and Mean annual precipitation (mm) for sub-catchments

Three rainfall station MAP's based on measurements from 1950-2004 are available for the Nzoia Catchment, as well as a catchment MAP contour profile map (Figure 5-17). The rainfall station MAP_s are: Eldoret 1024mm; Bungoma 1527mm; Kitale 1233mm. The sub-catchment MAP_s read from the rainfall contour map are shown in Table 5-9:

Table 5-9 Nzoia River sub-catchment MAP values

Subcatchment NO.	MAP	Rainfall station stand in	Subcatchment NO.	MAP	Rainfall station location
1	1100	Eldoret	**14**	1100	Eldoret
2	1000	Kitale	**15**	1100	Eldoret
3	1100	Kitale	**16**	1700	Eldoret
4	1000	Kitale	**17**	1500	Kitale
5	1100	Kitale	**18**	1500	Kitale
6	1100	Eldoret	**19**	1500	Kitale
7	1100	Kitale	**20**	1700	Bungoma
8	1000	Kitale	**21**	1800	Bungoma
9	1000	Eldoret	**22**	1600	Bungoma
10	1100	Eldoret	**23**	1800	Bungoma
11	1100	Eldoret	**24**	1600	Bungoma
12	1100	Eldoret	**25**	1500	Bungoma
13	1200	Kitale	**26**	1300	Bungoma

Pectora roborant cultus recti

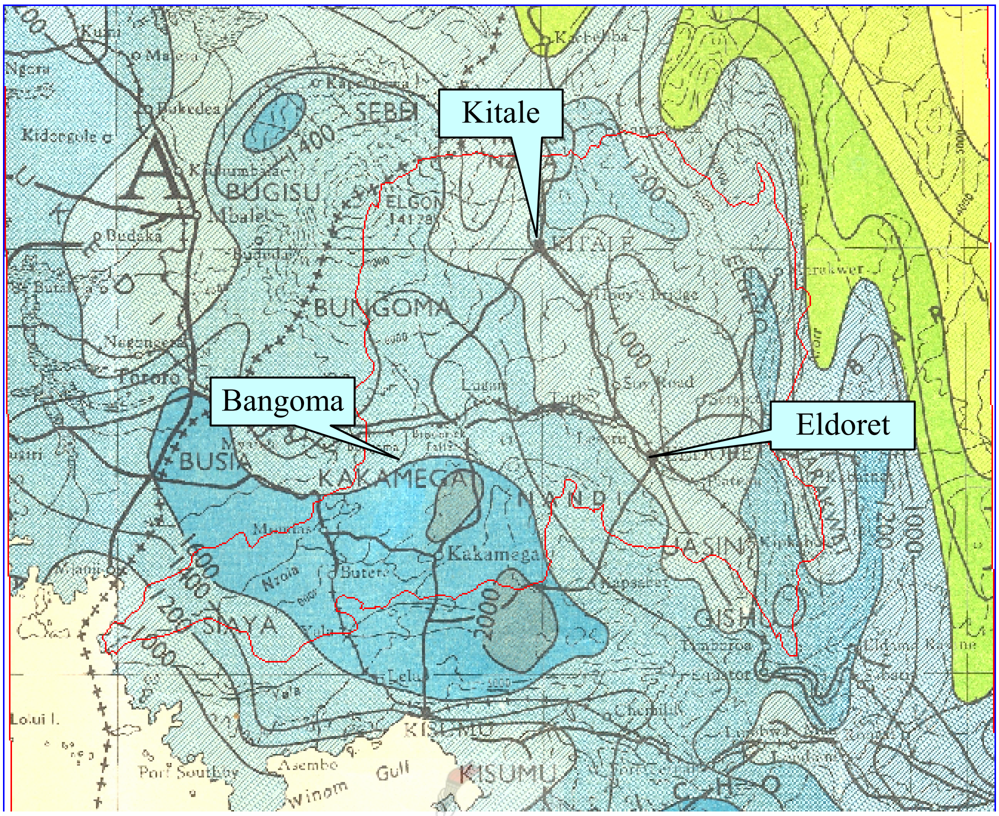

Figure 5-17 Nzoia catchment MAP isolines

The sub-catchments' MAP values used in the model of Nzoia River catchment are shown in Figure 5-18.

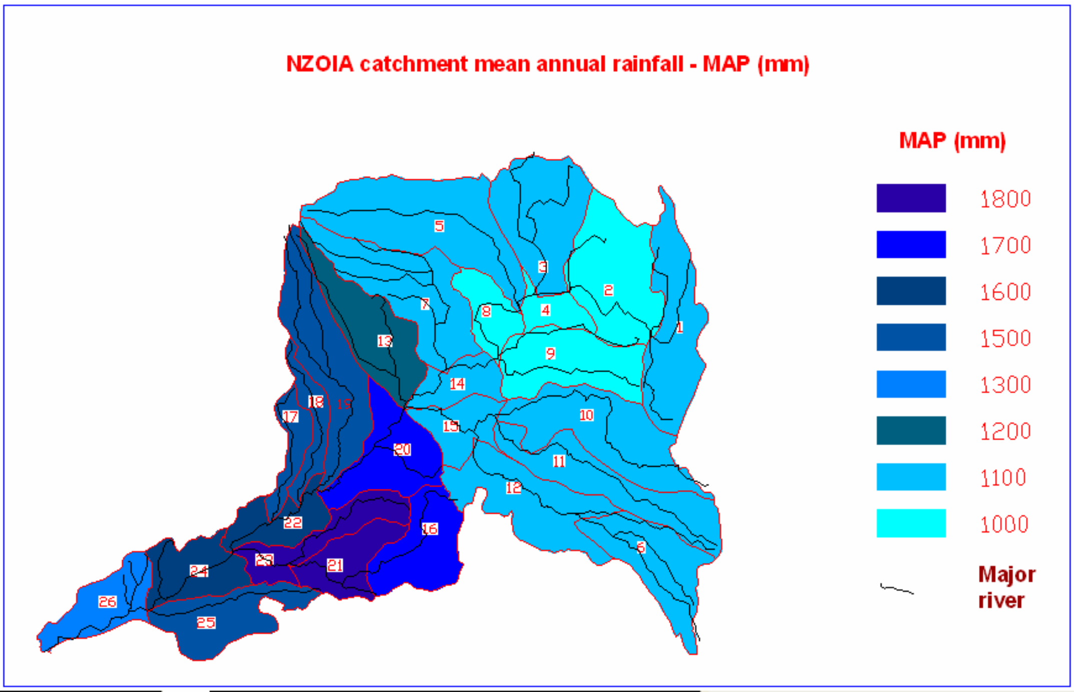

Figure 5-18 Adjusted MAP's of the Nzoia catchment as used by the ACRU model

ii. Minimum, maximum monthly mean of daily temperatures and monthly evaporation for sub-catchments

Temperature and evaporation data are not available for Nzoia River Catchment, and the Nyando River Catchment data had to be used to configure the Nzoia catchment model (according to Table 5-4).

c) Land use and cover information

The climatic conditions as well as topographic location of the Nzoia catchment are quite similar to those of the Nyando catchment. The Nzoia Catchment also has similar contour ranges to divide land use. These land use cover factors are roughly measured from topographic maps. In this case, combined land use and cover conditions were used in the Nzoia catchment model configuration. The different land uses and covers of each sub-catchment are presented in Table 5-10. Figure 5-19 shows the major vegetation layout of Nzoia catchment/ sub-catchments.

Table 5-10 Nzoia River catchment current land use distribution

Sub-catchment	Land use (%)						
	Mixed crops	Sugar cane	Village	Wetland	Forest	Bush	Swamp
1	45.0		6.0		28.0	21.0	
2	42.0		12.0		31.5	14.0	
3		54.0	18.0		28.0		
4		74.0	12.0	7.0		7.0	
5	47.0		18.0	14.0	21.0		
6	69.0		12.0	5.6	7.0	5.6	
7	60.0		12.0		28.0		
8		81.0	12.0	7.0			
9		52.0	6.0	28.0		14.0	
10	61.0		18.0	14.0	7.0		
11	56.0		18.0	4.0	18.0	4.0	
12		61.0	24.0	3.5	3.5	7.0	
13	63.0		12.0	3.5	21.0		
14		94.0	6.0				
15		62.0	24.0			14.0	
16		40.0	12.0		48.0		
17		90.0	6.0	3.5			
18		87.0	6.0	7.0			
19	66.0		6.0	7.0	21.0		
20		90.0	6.0		3.5		
21		69.0	24.0			7.0	
22	82.0		18.0				
23	82.0		18.0				
24	64.0		36.0				
25	64.0		36.0				
26	57.0		36.0				7.0

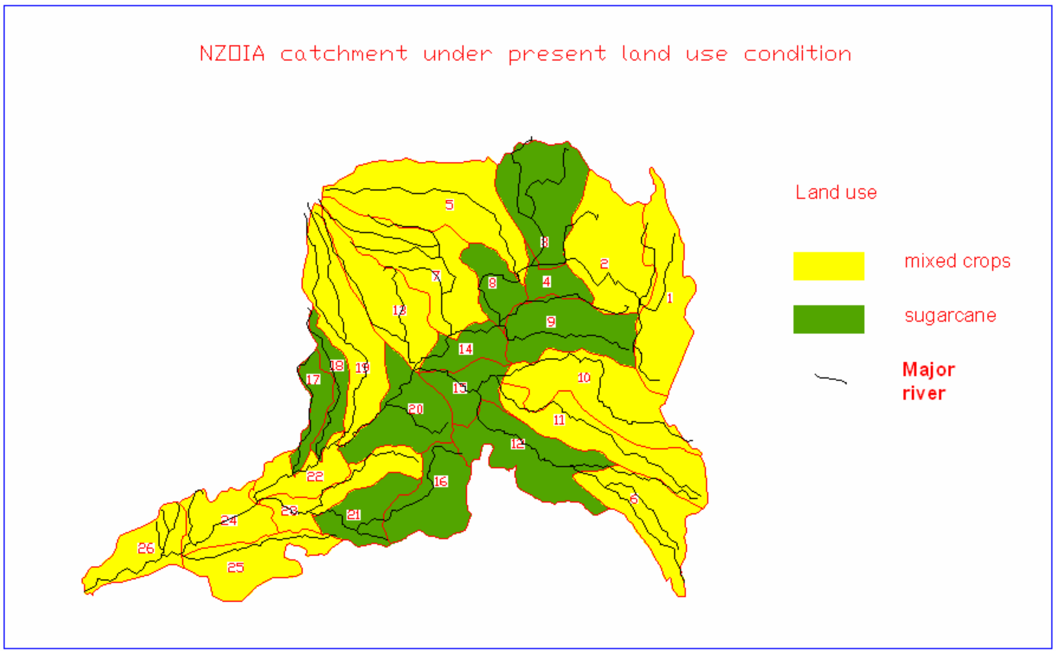

Figure 5-19 Nzoia catchment current land use used in the ACRU model

d) Soils information

Soil texture classes, and with it depths, were unknown during the model set up. Sand loam clay as default value has been used for model configuration. Surface soil depth and second surfaced soil depth were also taken as default values. Soil type and depth were however adjusted during the model calibration against observed flows.

e) Peak discharge information

The ACRU model calculates peak discharge data from rainfall. Average sub-catchments slopes were calculated by the grid method. The US Bureau of Reclamation Equation was used to calculate the time of concentration. 1: 250 000 topographic maps were used to collect contour interval, river length and some other essential topographical data.

For the Nzoia River catchment and sub-catchments the time of concentration calculation results are shown in Table 5-11.

Table 5-11 Nzoia catchment time of concentration

subcatchment	1	2	3	4	5	6	7	8	9	10	11	12	13
Main channel slope (%)	2.2	0.5	0.5	0.8	0.8	0.8	1.2	0.2	0.9	1.1	1.0	0.9	1.8
Main catchment steepness (%)	2.60	0.52	1.23	0.76	1.07	3.18	4.00	0.22	0.87	1.24	1.31	1.04	4.37
Time of concentration (hr)	5	7	8	5	12	10	9	9	6	9	10	7	7
subcatchment	**14**	**15**	**16**	**17**	**18**	**19**	**20**	**21**	**22**	**23**	**24**	**25**	**26**
Main channel slope (%)	0.7	0.8	1.1	0.5	0.7	1.1	0.6	1.3	0.5	0.6	0.2	0.5	0.1
Main catchment steepness (%)	0.82	0.86	1.98	0.60	1.76	3.68	0.76	1.27	0.52	0.64	0.23	0.52	0.06
Time of concentration (hr)	6	6	5	9	9	10	7	4	7	9	8	10	16

f) Sediment yield information

Soil erodibility factors can be estimated from Taxonomic or Binomial Soil Classification, and land cover factors were calculated by using ACRU land use types. Based on combined land use conditions, area weighting was performed for every sub-catchment cover factors. Default values were used for runoff erosivity constants.

Pectora roborant cultus recti

5.4 MODEL CONFIGURATION

5.4.1 Introduction

Once all the data was prepared to achieve the minimum sediment yield simulation model set up, the model could be built using the ACRU Menubuilder. All the variables have individually relevant names which the user can choose to build the model. The option/prompt appearing on the Menubuilder screen therefore has an equivalent numeric value in the menu. The following ACRU convention should be noted (ACRU User Manual):

Menubuilder Prompt	MENU Equivalent
YES (to a question)	1
NO (to a question)	0
LUMPED (catchment simulation)	0
DISTRIBUTED (catchment simulation)	1
NORTH (of equator)	1
SOUTH (of equator)	2
EAST (of Greenwich Meridian)	1
WEST (of Greenwich Meridian)	2
COMPOSITE (format for data input)	1
SINGLE (format for data input file)	2

5.4.2 Nyando River Catchment model configuration

The Nyando River catchment model configuration was set up as follows with the relevant variable name given at the end of each sub-item distribution.

A MENU file for the Nyando Catchment is prepared to enable the ACRU model to generate the stream flow from the distributed catchments -ICELL

The ten sub-catchments make up the Nyando catchment (Figure 5-6). Further sub-catchment

Pectora roborant cultus recti

information is given in Table 5-2 --ISUBNO, MINSUB, MAXSUB. The loopback mode will not be used at this stage –LOOPBK. No hydrograph routing is to be performed –IROUTE.

The sub-catchment configuration is depicted in Figure 5-20, from which the sub-catchment layout was determined –ICELLN, IDSTRM.

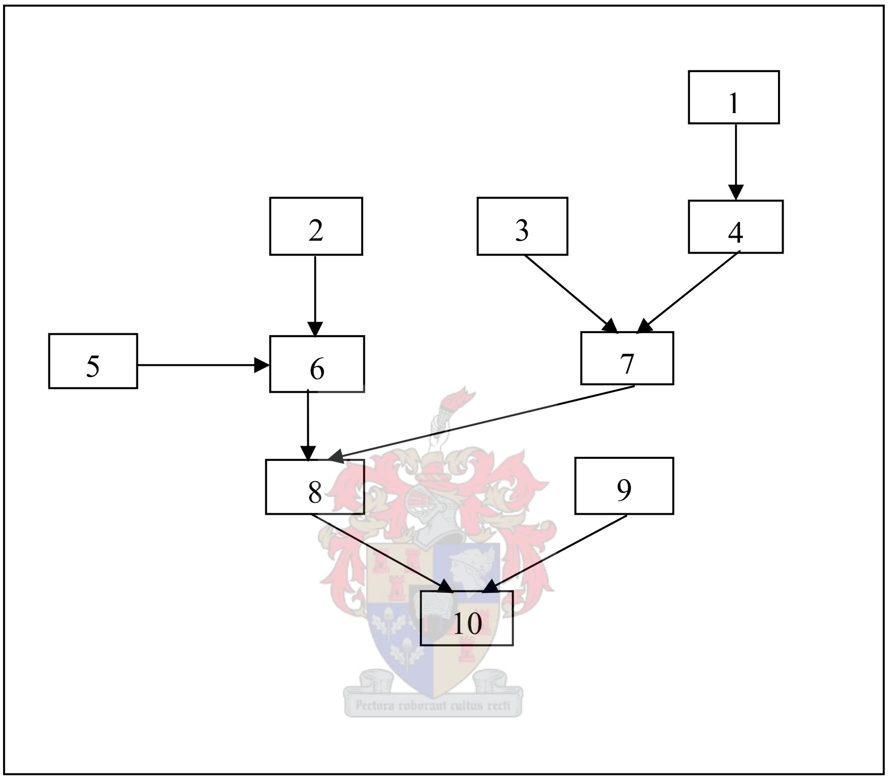

Figure 5-20 Nyando sub-catchment configuration

The climate data files containing daily rainfall are single format which is named as “A1.dat, A2.dat, etc.” – IRAINF.

Monthly precipitation factors were used to account for the spatial variability of the sub-catchments, and the rainfall data were prepared in the single ACRU format –PPTCOR, CORPPT (I), FORMAT.

There are two different MAP distributions available for catchments, viz. rainfall stations MAP and sub-catchment MAP measured from topographic maps. Monthly precipitation factors were estimated by using rainfall station records data. Rainfall station monthly precipitation could be estimated by using rainfall stations daily data (Table 5-12), rainfall station monthly average precipitation was obtained through rainfall station MAP, and the data was divided by 12 months. Monthly precipitation factors per sub-catchment were estimated using Equation 5.5.

$$f_A = \frac{P_{S_i}}{P_m} \qquad \text{Eq 5.5}$$

Where

f_A = sub-catchment monthly precipitation factor (A=1, 2…10)

P_{S_i} = rainfall station monthly average precipitation (i=1, 2…12)

P_m = rainfall station monthly precipitation

Calculated results of sub-catchments monthly precipitation factors also presented in Table 5-12.

Table 5-12 Monthly precipitation adjustment factors for different rainfall stations in the Nyando catchment

Rainfall Station:	Kericho		Koru		Kano	
P_{S_i} (mm)	181		144		101	
	P_m	f_A	P_m	f_A	P_m	f_A
Jan	97.3	0.54	104.7	0.73	84.8	0.84
Feb	110.2	0.61	109.7	0.76	94.1	0.94
Mar	177.2	0.98	171.8	1.19	127.5	1.27
Apr	282.3	1.56	243.2	1.69	196.1	1.95
May	295.9	1.63	209.7	1.46	142.8	1.42
Jun	205.8	1.14	150.6	1.05	76.6	0.76
Jul	194.0	1.07	131.1	0.91	70.6	0.70
Aug	219.3	1.21	146.8	1.02	83.7	0.83
Sep	178.3	0.98	119.5	0.83	69.2	0.69
Oct	164.4	0.91	127.0	0.88	84.2	0.84
Nov	158.3	0.87	119.8	0.83	106.8	1.06
Dec	91.7	0.51	91.7	0.64	70.2	0.70

Pectora roborant cultus recti

The mean annual precipitation for sub-catchments is given in Table 5-3 –MAP.

The simulation uses the entire length of records from 1950 to 2004 – IYSTRT, IYREND.

The monthly means of the daily maximum and minimum temperatures for the Nyando Catchment are given in Table 5-4 – TMAX (I), TMIN (I).

The expert system on reference potential evaporation (E_i) was defined on a day-by-day basis. Monthly means of daily wind runs (km.day-1), sunshine duration (h) are available are shown in Table 5-13. There was no evaporation data available on the first Nyando Catchment model configuration, the evaporation data was collected later during the model calibration. Thus A-pan equivalent values of evaporation did not need adjustment for the very first module. The base temperature station value also did not need altitude correction –E (i), EQPET, IWDF, ISNF, WIND (i), ASSH (i), PANCOR, CORPAN (i).

Table 5-13 Monthly values at Nyando catchment of the meteorological variables used in the expert system

	Unit	Jan	Feb	Mar	Apr	May	Jun	Jul	Aug	Sep	Oct	Nov	Dec
Wind runs	km/day	123.3	155.8	154.6	134.7	115	101.2	109.6	120.4	125.9	123.9	109.8	106.1
Sunshine	hr/day	9	9	8	8	8	8	7	7	8	8	7	8

With respect to the soil types, inadequate field data was available and therefore default values were used –PEDINF.

The texture of the soil was classified as sandy clay loam, which covers the entire catchments (i.e. 100%) –ITEXT.

The thicknesses of the A- and B- horizons were both approximately 0.2m for the first model set up –PEDDEP.

The soil types were assumed not to have shrink-swell properties –ICRACK.

The initial soil water contents for the top- and subsoil horizons were assumed at permanent wilting point. No statistical analysis of the soil water regime was required – SMAINI, SMBINI, SWLOPT.

All of the current land use and cover could be estimated from similar land cover in the ACRU manual CROP number system. The forest effect was not considered in the first model set up – LCOVER.

Plant interception loss was to be determined indirectly by the Von Hoyningen-Huene equation

Pectora roborant cultus recti

using average monthly crop coefficients K_{cm} (CAY), input month-by-month –INTLOS.

Neither monthly nor daily values of leaf area indices were known –LAIND.

A single crop covers each sub-catchment. The crop coefficients (i.e. the proportion of water "consumed" by a plant in relation to that evaporated by an A-pan in a given period) for the various months are shown in Table 5-14, and these are representative of the entire sub-catchment (i.e. 100%) --CAY (I=1, 12)

Table 5-14 Average monthly crop coefficients (CAY) of sub-catchments

Sub-catchment	Jan	Feb	Mar	Apr	May	Jun	Jul	Aug	Sep	Oct	Nov	Dec
1	0.8	0.8	0.6	0.4	0.2	0.2	0.2	0.2	0.2	0.4	0.65	0.8
2	0.8	0.8	0.6	0.4	0.2	0.2	0.2	0.2	0.2	0.4	0.65	0.8
3	0.8	0.8	0.8	0.8	0.8	0.8	0.8	0.8	0.8	0.8	0.8	0.8
4	0.8	0.8	0.8	0.8	0.8	0.8	0.8	0.8	0.8	0.8	0.8	0.8
5	0.8	0.8	0.8	0.8	0.8	0.8	0.8	0.8	0.8	0.8	0.8	0.8
6	0.8	0.8	0.8	0.8	0.8	0.8	0.8	0.8	0.8	0.8	0.8	0.8
7	0.8	0.8	0.8	0.8	0.8	0.8	0.8	0.8	0.8	0.8	0.8	0.8
8	0.8	0.8	0.6	0.4	0.2	0.2	0.2	0.2	0.2	0.4	0.65	0.8
9	0.8	0.8	0.6	0.4	0.2	0.2	0.2	0.2	0.2	0.4	0.65	0.8
10	0.8	0.8	0.8	0.8	0.8	0.8	0.8	0.8	0.8	0.8	0.8	0.8

Interception losses (mm.rainday-1) of each sub-catchment –VEGINT (I=1, 12), and the fractions of the root mass in the A-horizon (topsoil) of the soil –ROOTA (I=1, 12) were not needed in the model.

The effective total rooting depth of the vegetation of each sub-catchments are given in Table 5-15 – EFRDEP.

Table 5-15 Estimated effective rooting depth of vegetation of each sub-catchment

Sub-catchment	1	2	3	4	5	6	7	8	9	10
Effective depth (m)	0.5	0.5	0.8	0.8	0.8	0.8	0.8	0.5	0.8	0.8

The total evaporation was determined by considering the components of soil water evaporation and plant transpiration jointly –EVTR.

The fraction of available plant water at which the total evaporation is assumed to drop below the maximum evaporation, is 0.4, and the critical leaf water potential of the vegetation was not known – FRAW, CONST.

There are three sub-catchments (1, 2, and 4), of which more than 50% are covered by forest, therefore the forest option was required for these three sub-catchments –FOREST.

Simulation under enhanced atmospheric CO2 levels and a threshold temperature to output active plant transpiration was not required -- CO2TRA, TMPCUT.

Unsaturated redistribution of soil water was not simulated and no lysimeter data was available. Simulated storm flow was thus not to be re-infiltrated –IUNSAT, LYSIM.

With regards to the simulated runoff, the storm flow response factor (i.e. the fraction of the total storm flow running off on the day of the event) was assumed as 0.2. The fraction of the groundwater store which becomes base flow on a particular day was assumed as 0.01. The effective depth of the soil to be considered in generating storm flow was taken as the depth of the A-horizon (topsoil horizon), and the simulated runoff statistics are for storm flow and base flow combined. It was assumed that there is no adjunct or disjunct impervious area which may increase the response of the catchment. Thus the initial abstraction of the impervious areas was 1.00 mm – QFRESP, COFRU, SMDDEP, IRUN, ADJIMP, DISIMP, and STOIMP.

Pectora roborant cultus recti

The coefficient of initial abstraction for the dry-land portion of the catchment remains unaltered from one month to the next. These are presented in Table 5-16 –COIAM (I=1, 12).

Table 5-16 Coefficient of initial abstraction for dry land portion

	Jan	Feb	Mar	Apr	May	Jun	Jul	Aug	Sep	Oct	Nov	Dec
Initial abstraction	0.2	0.2	0.2	0.1	0.1	0.1	0.1	0.2	0.2	0.2	0.1	0.1

The peak discharge estimation is required for the catchment before activating the sediment yield module. For this simulation, lag is calculated from the sub-catchment time of concentration. The sub-catchments time of concentrations are shown in Table 5-7 –PEAK, LAG and TCON.

Sediment yield analysis is carried out using the MUSLE. The upper and lower limit of soil erodibility factors were assumed 1.20 and 0.17, and the specific actual slope length and steepness factors (SL) were calculated previously as shown in Table 5-7. Limited support practices information was available. No daily values of the canopy cover factors were available, but the estimated monthly cover factor was available, which uses the entire catchment and covers both winter and summer seasons. All the sediment produced from daily rainfall events reach the sub-catchments outlet within 24 hours, thus SEDIST are 1.0. The runoff energy, as expressed in MUSLE, has a multiplication factor (constant) of 8.934 and an exponent of 0.560 for all ten sub-catchments –MUSLE, SOIFC1, SOIFC2, ELFACT, PFACT, ICOVRD, COVER, SEDIST, ALPHA, BETA.

- The estimation of soil erodibility factors and subcatchment cover factors will be introduced in chapter 8 (ACRU model sediment yield module calibration).
- The support practice factor can be estimated at two levels of information availability. Level 1 is limited support practice information available, while level 2 is detailed support information available. The Nyando model only has limited information available, and from Table 5-17 and Figure 5-21 to the estimated values of the support practice factors were determined (Table 5-18)

Table 5-17 P-values for contour tilled lands and lands with contour banks (after Wischmeier and Smith, 1978, ACRU User Manual)

Land Slope (%)	Contour Tilled	Contour Banks with Grassed Waterways
1--2	0.6	0.12
3--8	0.5	0.1
9--12	0.6	0.12
13--16	0.7	0.14
17--20	0.8	0.16
21--25	0.9	0.18

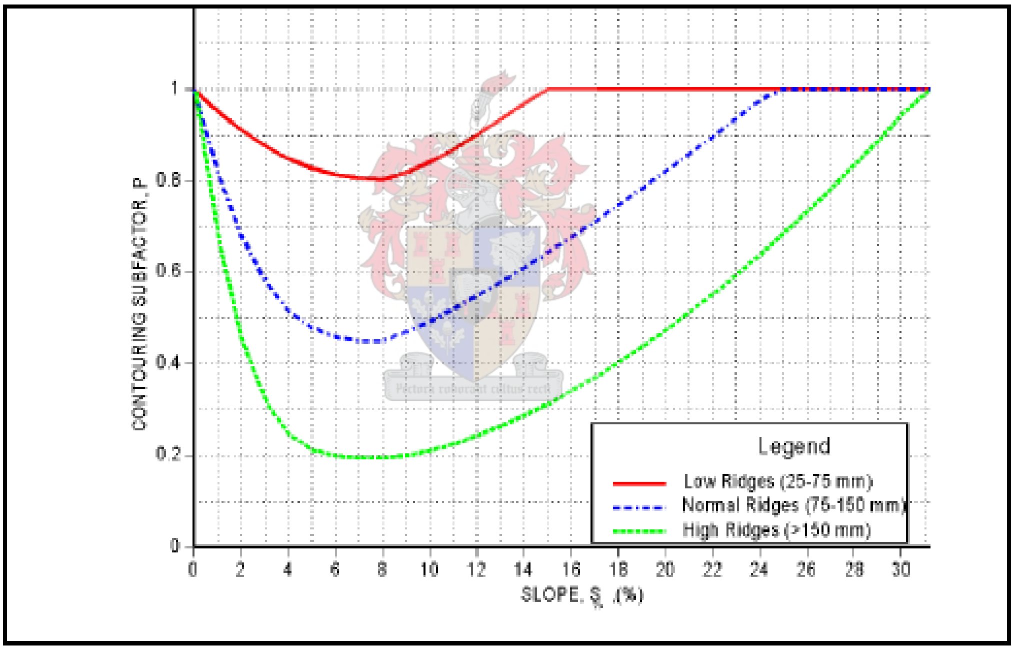

Figure 5-21 Support practice factor for contour (ACRU User Manual)

Table 5-18 Support practice value of Nyando catchment

Sub-catchment	Unit	1	2	3	4	5	6	7	8	9	10
Land slope	%	1.35	2.86	2.53	1.64	2.31	1.07	0.31	0.3	1.44	0.3
P-value		0.6	0.5	0.5	0.6	0.5	0.6	1.0	1.0	0.6	1.0

* Note: normal ridges curve was used for study models

Sub-catchment 10 has a wetland and therefore the wetland option was activated in this sub-catchment. The maximum flow rate capacity of the main channel through the wetland was assumed to be 20.8m^3/s (data determined by using observed daily discharge in main channel) – IVLEL, CAPM3S.

No shallow groundwater analysis was required –IGWATR.

No irrigation occurs in the catchment. –IRRIGN.

No domestic abstractions were taking place in the catchment –IDOMR.

No reservoir analysis was required –RESYLD.

No crop yield analysis was required –CROP.

No extreme value analysis was required –IEVD.

5.4.3 Nzoia River catchment model configuration

The Nzoia River catchment study model covers 13693 km^2, which is slightly larger than the area recorded in other documents of about 12842 km^2, the model study area was measured directly from a topographic map. As few research projects have carried out in the Nzoia catchment, but the useful detail for the ACRU model set up is even less than for the Nyando catchment's model study. According to this scenario, a number of items had to adopt the default values or relevant Nyando catchment values.

The Nzoia catchment ACRU model was configured as follows:

A MENU file for the Nzoia Catchment was to be prepared to enable the ACRU model to generate the streamflow from the distributed catchment –ICELL.

The 26 sub-catchments make up the Nzoia catchment (Figure 5-16) and the model were run for all 26 sub-catchments. Further sub-catchment information is given in Table 5-8 --ISUBNO, MINSUB and MAXSUB. The loopback mode was not be used at this stage –LOOPBK. No hydrograph routing was to be performed –IROUTE.

The sub-catchment configuration is depicted in Figure 5-22, from which the sub-catchment layout could be determined –ICELLN, IDSTRM.

Pectora roborant cultus recti

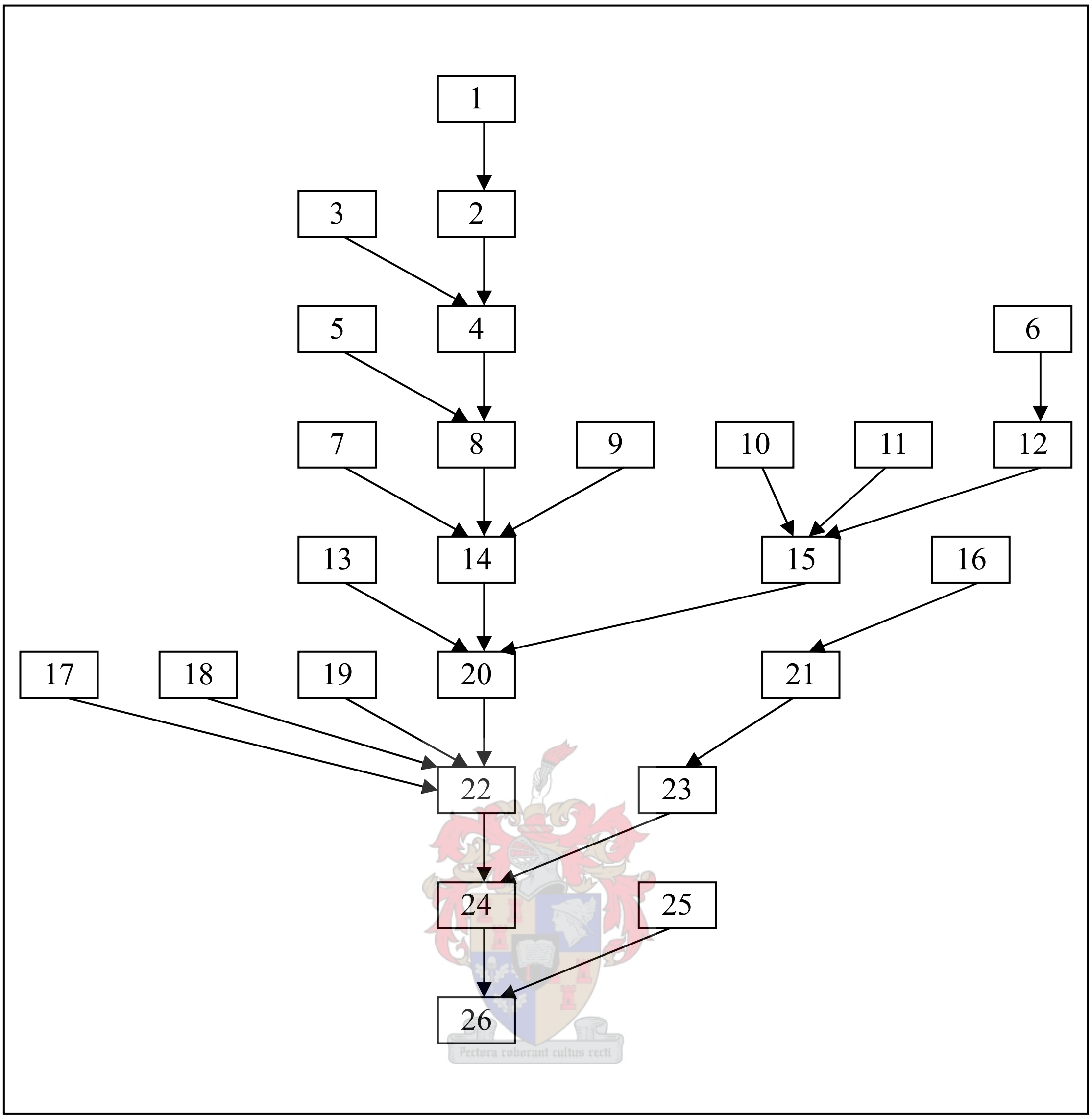

Figure 5-22 Nyando sub-catchment configuration

The climate data files containing daily rainfall are single format which were named as "A1.dat, A2.dat, etc." – IRAINF.

Monthly precipitation factors were used to account for the spatial variability of the sub-catchments, and the rainfall data had to be prepared in the single ACRU format –PPTCOR, CORPPT (I), FORMAT.

Monthly precipitation factors per sub-catchment are available and estimated by using Equation

5.5. Calculated results of the sub-catchments monthly precipitation factors are also presented in Table 5-19.

Table 5-19 Monthly precipitation adjustment factors for Nzoia catchment

Rainfall station	Eldoret		Bungoma		Kitale	
$P_{S_i}\,(mm)$	85		127		103	
	P_m	f_A	P_m	f_A	P_m	f_A
Jan	31	0.37	47	0.37	46	0.45
Feb	38	0.45	67	0.53	39	0.38
Mar	75	0.88	129	1.01	98	0.95
Apr	134	1.56	221	1.74	161	1.56
May	123	1.44	223	1.75	144	1.40
Jun	100	1.18	122	0.96	139	1.36
Jul	153	1.80	121	0.95	119	1.15
Aug	151	1.77	133	1.04	136	1.32
Sep	67	0.79	125	0.98	95	0.92
Oct	61	0.72	150	1.18	153	1.49
Nov	60	0.70	125	0.98	73	0.71
Dec	30	0.35	65	0.51	31	0.30

Pectora roborant cultus recti

The mean annual precipitations for sub-catchments are given in Table 5-9 –MAP.

No observed daily values of streamflow or peak discharge are available, except at the river mouth, and therefore the simulated streamflow could not be overwritten. A dynamic input file is not used –IOBSTQ, IOBSPK, DANMIC.

The simulation used the entire length of record from 1950 to 2004 – IYSTRT, IYREND.

The monthly means of the daily maximum and minimum temperatures for the Nzoia Catchment are given in Table 5.4. – TMX (I), TMIN (I)

The expert system on reference potential evaporation (E_i) was determined on a day-to-day basis.

Monthly means of the total of pan evaporation was available, which also used the same data as used in Nyando Catchment, which were given in Table 5-20. Thus an A-pan equivalent value of evaporation adjustment factor was assumed as 1.00 for the very first module, which covers the entire catchment; the base temperature station values did not need altitudinal correction –E (i), EQPET, IWDF, ISNF, PANCOR, CORPAN (i).

Table 5-20 Mean monthly total evaporation values at Nzoia catchment of the meteorological variables used in the expert system

Month	Jan	Feb	Mar	Apr	May	Jun	Jul	Aug	Sep	Oct	Nov	Dec
Evaporation(mm)	68	68	72.5	57.5	54	51	50	58	67.5	69	70	70

With respect to the soils, only inadequate information was available and therefore default values were used –PEDINF.

The texture of the soil was classified as sandy clay loam, which covers the entire catchment – ITEXT.

The thicknesses of the A- and B- horizons were approximately 0.25m and 0.50m for first model set up –PEDDEP.

The soils were assumed not to have shrink-swell properties –ICRACK.
The initial soil water contents for the topsoil and subsoil horizons are assumed to be at permanent wilting point. No statistical analysis of the soil water regime was required – SMAINI, SMBINI and SWLOPT.

The Nzoia catchment land use and cover were estimated for a combined condition, which consisted of different single land use conditions, and each of these are estimated from similar land covers in the ACRU manual CROP number system, so that, the similar default land cover values had to be selected. Every sub-catchment land cover and percentage distribution is presented in Table 5-10 –LCOVER.

Plant interception loss was determined indirectly by the Von Hoyningen-Huene equation using average monthly crop coefficients Kcm (CAY), input month-by-month –INTLOS.

Neither monthly nor daily values of leaf area indices are known –LAIND.

Depending on the combined land cover conditions, area-weighting had to be used for sub-catchment crop coefficients estimation -CAY (I=1, 12).

An additional program was used to calculate combined crop coefficients. This program is called LCOVER (area-weighting program). When using the program to estimate the mixed catchment crop coefficients, the default value of each single component had to be checked before area-weighting, as well as the percentages (according to Table 5-21).

Table 5-21 Combined average monthly crop coefficients of sub-catchments

Sub-catchment	Jan	Feb	Mar	Apr	May	Jun	Jul	Aug	Sep	Oct	Nov	Dec
1	0.8	0.8	0.71	0.58	0.44	0.41	0.41	0.41	0.47	0.6	0.72	0.8
2	0.8	0.8	0.72	0.59	0.45	0.42	0.42	0.42	0.48	0.61	0.72	0.8
3	0.8	0.8	0.8	0.77	0.71	0.69	0.69	0.69	0.72	0.77	0.78	0.8
4	0.78	0.78	0.78	0.75	0.71	0.68	0.67	0.67	0.7	0.73	0.75	0.77
5	0.79	0.79	0.7	0.56	0.4	0.37	0.35	0.35	0.38	0.54	0.68	0.78
6	0.78	0.78	0.64	0.48	0.3	0.27	0.27	0.27	0.29	0.47	0.66	0.78
7	0.81	0.81	0.69	0.54	0.38	0.37	0.37	0.37	0.39	0.55	0.71	0.81
8	0.78	0.78	0.78	0.76	0.73	0.71	0.7	0.7	0.71	0.74	0.76	0.78
9	0.78	0.78	0.78	0.73	0.67	0.62	0.6	0.6	0.63	0.68	0.71	0.75
10	0.78	0.78	0.66	0.5	0.32	0.28	0.27	0.27	0.29	0.47	0.64	0.77
11	0.79	0.79	0.68	0.53	0.35	0.33	0.32	0.32	0.36	0.52	0.68	0.78
12	0.76	0.76	0.76	0.72	0.65	0.62	0.61	0.61	0.65	0.71	0.73	0.76
13	0.8	0.8	0.68	0.52	0.35	0.34	0.33	0.33	0.36	0.52	0.69	0.8
14	0.79	0.79	0.79	0.79	0.77	0.76	0.76	0.76	0.77	0.78	0.79	0.79
15	0.75	0.75	0.75	0.71	0.64	0.6	0.6	0.6	0.65	0.71	0.73	0.75
16	0.83	0.83	0.83	0.8	0.74	0.73	0.73	0.73	0.76	0.81	0.82	0.83
17	0.79	0.79	0.79	0.78	0.76	0.75	0.75	0.75	0.75	0.77	0.78	0.79
18	0.79	0.79	0.79	0.78	0.76	0.74	0.74	0.74	0.74	0.76	0.77	0.78
19	0.81	0.81	0.68	0.52	0.36	0.36	0.34	0.34	0.36	0.52	0.69	0.81
20	0.8	0.8	0.8	0.79	0.77	0.76	0.76	0.76	0.77	0.79	0.79	0.8
21	0.76	0.76	0.76	0.73	0.66	0.63	0.63	0.63	0.67	0.72	0.73	0.76
22	0.77	0.77	0.61	0.43	0.22	0.2	0.2	0.2	0.22	0.42	0.63	0.77
23	0.77	0.77	0.61	0.43	0.22	0.2	0.2	0.2	0.22	0.42	0.63	0.77
24	0.75	0.75	0.62	0.45	0.24	0.2	0.2	0.2	0.24	0.44	0.61	0.75
25	0.75	0.75	0.62	0.45	0.24	0.2	0.2	0.2	0.24	0.44	0.61	0.75
26	0.75	0.75	0.63	0.48	0.28	0.24	0.24	0.24	0.28	0.47	0.63	0.75

Interception losses (mm.rainday-1) of each sub-catchment –VEGINT (I=1, 12) and the fractions of the root mass in the A-horizon (topsoil) of the soil –ROOTA (I=1, 12) were not needed.

The effective total rooting depth of the vegetation was selected as 0.75 m for the first model set up, which value covers the entire catchment –EFRDEP.

Total evaporation was determined by considering the components of soil water evaporation and plant transpiration jointly –EVTR.

The fraction of plant available water, at which the total evaporation is assumed to drop below the maximum evaporation, is 0.4, and the critical leaf water potential of the vegetation is not known – FRAW, CONST.

There is no sub-catchment forest cover and the forest option was not required in this model – FOREST.

Simulation under enhanced atmospheric CO_2 levels was not required, nor is a threshold temperature to output active plant transpiration- CO2TRA, TMPCUT.

Unsaturated redistribution of soil water was not simulated and no lysimeter data was available. The simulated stormflow was therefore not re-infiltrated –IUNSAT, LYSIM.

With regards to simulated runoff, the stormflow response factor (i.e. the fraction of the total stormflow running off on the day of the event) was assumed 0.3. The fraction of the groundwater store which becomes baseflow on a particular day was assumed 0.012. The effective depth of the soil to be considered in generating stormflow was, in this case, taken as the depth of the A-horizon (topsoil horizon), and the simulated runoff statistics are for stormflow and baseflow combined. It is assumed that there are no adjunct or disjunct impervious areas which may increase the response of the catchment. Thus the initial abstraction of the impervious areas is 1.00 mm – QFRESP, COFRU, SMDDEP, IRUN, ADJIMP, DISIMP, and STOIMP.

The coefficient of initial abstraction for the dryland portion of the catchment remains unaltered from one month to the next and was estimated as 0.2, for the entire catchment –COIAM (I=1, 12).

The peak discharge estimation is required for the catchment before the sediment yield can be determined. For this simulation, lag was calculated from the sub-catchment time of concentration. The results of each sub-catchments time of concentration are shown in Table 5-11 –PEAK, LAG, and TCON.

A sediment yield analysis was carried out using the MUSLE. The upper and lower limit of soil erodibility factors were assumed as 0.52 and 0.51, and also, the specific actual slope length and steepness factors (S_L) were calculated previously as shown in Table 5-11. Limited support practices information was available for the study model (Table 5-22). No daily values of the canopy cover factors were available and the default value of 0.50 was used to estimate the monthly cover factor for the first model set up, for the entire catchment, and covers both winter and summer seasons (i.e. 100%). All the sediments produced from daily rainfall events reach the sub-catchments outlet within 24 hours, thus SEDIST is 1.0. The runoff energy, as expressed in MUSLE, has a multiplication factor (constant) of 8.934 and an exponent of 0.560, in all 26 sub-catchments –MUSLE, SOIFC1, SOIFC2, ELFACT, PFACT, ICOVRD, COVER, SEDIST, ALPHA, BETA.

Soil erodibility factors and canopy cover factors area-weighting were introduced in the sediment yield module calibration.

Table 5-22 The Nzoia catchment practices factors

Sub-catchment	Land slope (%)	P-value	Sub-catchment	Land slope (%)	P-value
1	2.6	0.5	14	0.86	0.9
2	0.52	0.9	15	1.98	0.6
3	1.23	0.6	16	0.6	0.9
4	0.76	0.9	17	0.6	0.9
5	1.07	0.6	18	1.76	0.6
6	3.18	0.5	19	3.68	0.5
7	0.22	1	20	0.76	0.9
8	0.87	0.9	21	1.27	0.6
9	1.24	0.6	22	0.52	0.9
10	1.31	0.6	23	0.64	0.9
11	1.04	0.6	24	0.23	1
12	4.37	0.5	25	0.52	0.9
13	0.82	0.9	26	0.06	1

There are several sub-catchments which do have wetlands. Most of them are however very small (< 10% of the sub-catchment area). In addition, the maximum flow rate capacities of the main channel through the wetlands were unknown. Hence, the wetland option was ignored in this model –IVLEL, CAPM3S.

No shallow groundwater analysis was required –IGWATR.

No irrigation occurs in the catchment. --IRRIGN

No domestic abstractions were taking place in the catchment. --IDOMR

No reservoir analysis was required. --RESYLD

No crop yield analysis was required. --CROP

No extreme value analysis was required. –IEVD

5.5 PROBLEMS ENCOUNTERED DURING MODEL SET UP

The accuracy and stability of the calculations depend on the reliability of the input variables. Most of the problems encountered during the test runs were due to these variables.

- As previously mentioned, the data of too many necessary variables are not available for this model study and default values had to be used in many cases. Hence, the model accuracy will inevitably be affected.
- Both Nyando and Nzoia are large catchments, and the numbers of rainfall stations are not enough (three stations each). The sub-catchment daily rainfall had to be calculated by using equation 5.1 which this also affect the simulations.
- The sub-catchment plotted areas are relatively large. According to the ACRU manual, the suggested sub-catchment areas should be smaller than 50 km^2, however, the model sub-catchment is much larger than this: maximum 1078 km^2 (sub-catchment 5, Nzoia catchment), and minimum 162.5 km^2 (sub-catchment 8, Nyando catchment).
- Detailed annual evaporation is 756 mm which less than MAP. Generally, the evaporation does not vary much and almost equals the rainfall, except during the rainy seasons where rainfall exceeds evaporation. The monthly evaporation adjustment factor was initially 1.00 in the model configuration but was adjusted during calibration.
- The model used topographic maps published in the early 1970s. From then on, in less than 30 years; the Kenyan population increased from 4 million rapidly to more than 20 million today. The increased population induces greater land use pressures, hence the land use factors had to be adjusted during the model calibration.

CHAPTER 6 FLOW MODEL CALIBRATION AND SENSITIVITY ANALYSIS

6.1 INTRODUCTION

Following the model configuration, other important steps in modelling are: calibration, verification and sensitivity analysis. The sediment yield aspect of the model is dependent on the calibrated hydraulic component, and every error introduced in the streamflow assessment will influence the sediment yield calculations. This thesis separates the calibration and verification of the hydraulic and sediment yield module into two chapters. Unfortunately, no flow model verification information is available for the study model. This step was only completed for the sediment yield module. This chapter deals with the hydraulic module calibration, while the following chapter will introduce the sediment yield module calibration and verification.

6.2 INTRODUCTION OF THE ACRU OUTPUTBUILDER AND ACRU VIEW

6.2.1 ACRU Outputbuilder

According to the ACRU User Manual that ACRU model requires an input file containing details on which variables to store during a simulation for output and analysis following the simulation. In order to conserve disk storage and to reduce the time required to perform the simulation, users of the modelling system may choose to store only relevant variables. The Outputbuilder lists all the variables available for storage during the simulation with description of the variables, and the user may toggle on, and thus choose to store the variable, for either a subset or the entire set of variables. A listing and a description of the variables which may be output is contained in Appendix A.

6.2.2 ACRU VIEW

"Goodness of fit" between the simulated values and the observed data is calculated by objective functions. It is desirable that a streamflow simulation should be as "good", in other words, as accurate as possible. This chapter discusses how the comparison of observed vs. simulated streamflow was done following the ACRU VIEW program.

ACRU VIEW is a Microsoft Excel based application designed to analyze and view data produced by the ACRU model. The simulated result data is converted to a specific form and processed internally for statistical and graphical analysis. The ACRU VIEW application consists of 7 main forms; Home, Statistics, Graphs, Comparative Statistics, Extreme Value Analysis (EVD), EVD graph and Flow Duration Curve (FDC) graph. The streamflow results viewer focuses on graphs and comparative statistical aspects.

6.2.3 Integration and utilization

After the output variables setup and model simulation, the simulated result can be called into the ACRU VIEW to view the streamflow graph. The study models were aimed at determining the Nyando catchment and Nzoia catchment soil erosion and sediment yields, and for output, two relevant variables are selected by using Outputbuilder, and these are: Streamflow (CELRUN) with its unit mm/day and Sediment yield from sub-catchments (SEDYLD), with unit ton/day.

As described previously, the Ahero flow gauging station on the Nyando River is located in sub-catchment 8 and not at the downstream end of the catchment. The Nzoia River flow gauging station is at the downstream end of the river, so that the total of 26 sub-catchments could be used.

6.3 EXPLANATION OF THE MODEL CALIBRATION, VERIFICATION AND SENSITIVITY ANALYSIS

6.3.1 Introduction

There are three definitions that must be clarified at the first stage:

a) Calibration

The process of adjusting parameters by running the model at different parameter values until a satisfactory result is obtained is called calibration (Grijsen, 1986).

b) Verification

According to Nitsche (2000) that verification is used to describe the process of ensuring that the model applied to the specific catchment for a particular set of calibration data can be applied to another situation; this is to ensure that the errors in the simulated values are acceptable.

The model calibration actually is a circular running process in the ACRU utilities system. Once a model is configured it should run to achieve certain purposes. Then the simulated result can be called into the ACRU VIEW to get the corresponding graphs and comparative statistics. The graph form is used to plot time series or variable vs. variable graphs. The comparative form enables statistical comparison of two variables (observed variable vs. simulated variable). If comparative statistics are too low or too high, ACRU VIEW will indicate the problems and the model should be taken back to ACRU Menu builder to change the relevant parameters, and the model must be run again. This process may be repeated several times by adjusting the different parameters until a satisfactory result is achieved. The statistical criteria and calibration data can then be applied to other scenarios. During model calibration and verification, sensitivity analysis could be implemented to determine which parameters have a significant impact on the model result.

c) Sensitivity analysis

The sensitivity of parameters means the relative significance of each parameter in the performance of the whole model (Görgens, 1983). As the model is supposed to represent the situation in reality, a sensitivity analysis is therefore important for the calibration process, as it determines which parameters have a significant impact on the model results (Nitsche, 2000).

6.3.2 The description of the steps of the ACRU model calibration

As the ACRU User Manual describes, the above process can be divided into 7 steps:

Step 1: Check mean annual precipitation, MAP

Precipitation is the major driving force of most hydrological responses. Errors in rainfall data are magnified in simulated runoff. Rainfall data has to be as accurate as possible.

Step 2: Check mean annual runoff, MAR, and its stationarity

According to the ACRU User Manual, streamflow increases curvilinearly with rainfall, but responses are different from region to region, mainly as a result of the type and distribution of rainfall as well as physiographic factors (soil, slope, geology).

Step 3: Check mean annual reference potential evaporation, MAE_r

For both the Nyando Catchment model and Nzoia Catchment model the option for estimation of total evaporation as an entity which consisted of soil water evaporation (E_s) and plant transpiration (E_t) was chosen. These characteristics determine that MAE_r will relate to meteorological factors (sunshine, windy, temperature) as well as land use and cover condition.

Step 4: Output and interpret a time series of monthly totals of observed vs. simulated streamflow

In the circular process of calibration and verification, this step always obtains a time series of daily/monthly observed and simulated streamflow following on the checks of step1 to 3. Actually it is a transitional step which is not only the end of the model running, but also the beginning of statistical comparison.

Step 5: Check the overall water budget by using a statistical comparison

From this step the model verification starts and statistical package is invoked for the first time. The ACRU User Manual describes the estimation of 'goodness-of- fit' as actually checking that the sum of simulated streamflow (Q_s) differs from the sum of observed flows (Q_o), with the difference aimed at less than 5%, but 10% is acceptable. Sensitivity testing of parameters in this step is the kind of parameters which could evidently influence the Q_s. A description of these sensitivity parameters and their analysis is presented in Table 6-1.

Table 6-1 Relational sensitivity parameter analysis of overall water budget checking

If $Q_s > Q_o$		
sensitivity parameter	**description**	**comment**
precipitation	too high	
Q_o	too low	incorrect rating tables
evaporation	too low	
top soil depth	too shallow	cause high stormflow and baseflow
crop coefficients	too low	
If $Q_s < Q_o$		
sensitivity parameter	**description**	**comment**
precipitation	too low	
Q_o	too high	incorrect rating tables
evaporation	too high	
total soil depth	too deep	cause low stormflow and baseflow
critical soil depth	too deep	cause low stormflow
crop coefficients	too high	

Pectora roborant cultus recti

Step 6: Check the overall streamflow trends from the monthly statistical comparison

The ACRU model verification also can check the overall streamflow by using streamflow monthly statistical comparison trend lines. The following seven general trends (Figure 6-1) obtained from perusal of the mean, slope and intercept values occur most frequently in streamflow simulation (ACRU User Manual). The characteristics and the relative parameters of the trend lines are described in Appendix B.

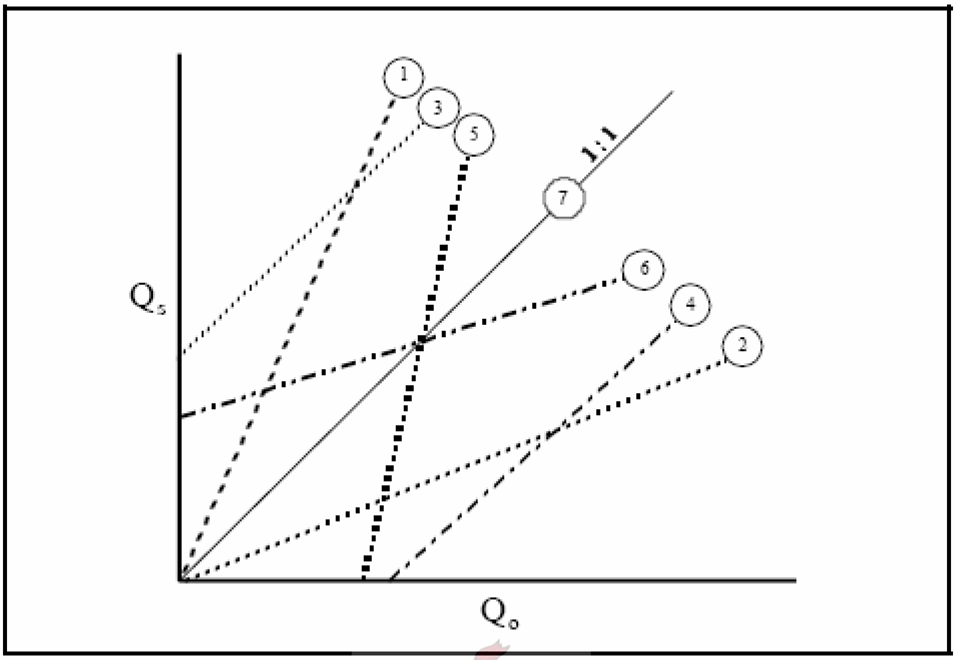

Figure 6-1 General trends in streamflow simulation

<u>Step 7: Daily output analysis</u>

Generally, daily output analysis follows the monthly statistical analysis to achieve more accurate verification. A short period (2-5 years) should be selected, which should include at least one rainfall/runoff season well above the average and another well below the average, and then repeat the above steps by using daily output.

6.4 CALIBRATION AND SENSITIVITY ANALYSIS

6.4.1 The Nyando catchment model calibration

a) The total amount of observed streamflow is 12626mm for the whole Nyando Catchment between 1950 and 2004 which is much less than that of the first configured model simulated value of 15079mm (16 % difference). The graph (Figure 6-2) of simulated monthly total of daily streamflow vs. observed monthly total of daily streamflow also indicates that the simulated values of low flows are much higher than for observed values.

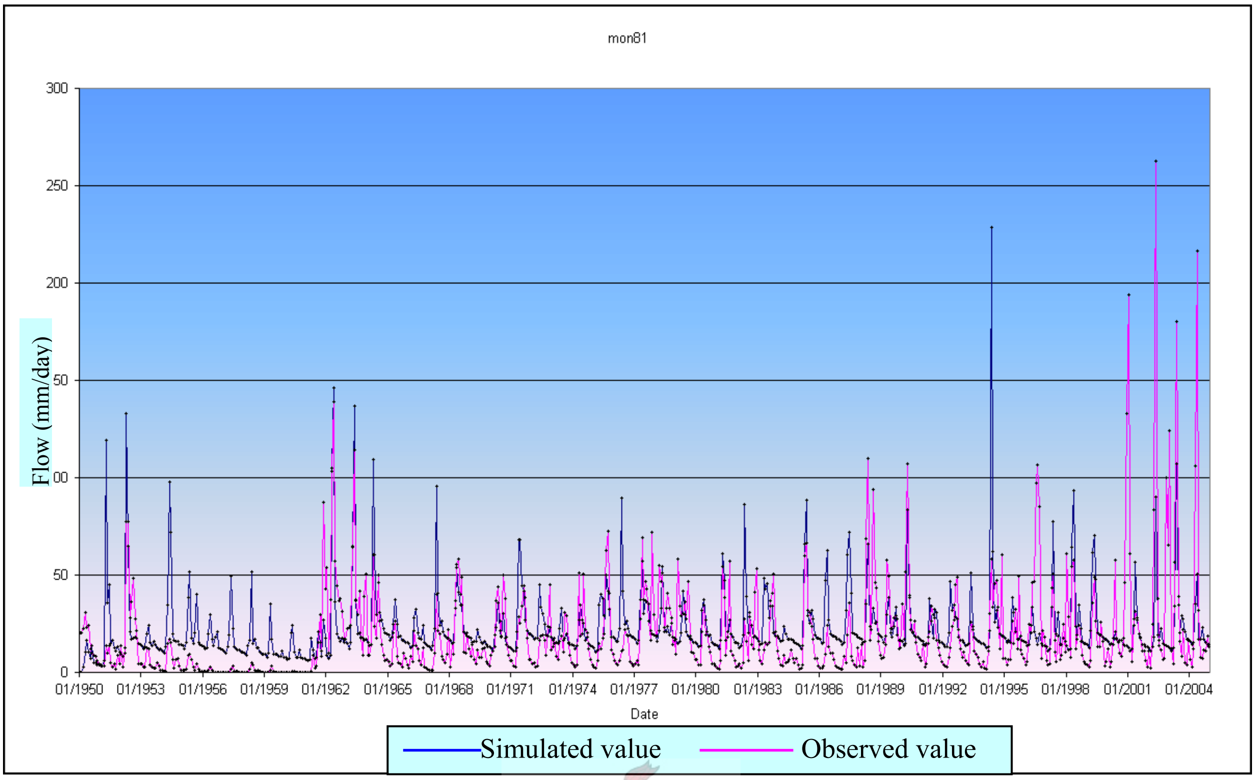

Figure 6-2 The Nyando catchment model simulated vs. observed monthly total streamflow – before calibration

b) After the first model simulation, the corresponding graph indicates that streamflow vs. time series contained large errors from 1950 to 1961 (which is patched in the observed record); and from 2000 to 2004 (which was data obtained from another source). Hence, it was decided that for the actual simulation series to use a shorter time period from 1962 to 1999. Therefore, the rainfall stations' MAP had to be recalculated by using a shorter period daily rainfall. The sub-catchment daily rainfall (refer to Equation 5.1) and sub-catchment monthly precipitation adjustment factors (refer to Equation 5.5) were also readjusted since the rainfall stations MAP changed. The results of recalculated MAP and precipitation factors are showed in Table 6-2 and 6-3.

Table 6-2 Rainfall stations MAP- Before calibration vs. after calibration

MAP (mm)	Time series	Rainfall station		
		Kericho	Koru	Kano
Before calibration	1950-2004	2122	1708	1194
After calibration	1962-1999	2175	1726	1207

Table 6-3 Recalculated monthly precipitation adjustment factors *

Rainfall Station	**Kericho**		**Koru**		**Kano**	
P_{S_i} (mm)	181		144		101	
	P_m	f_A	P_m	f_A	P_m	f_A
Jan	97.3	0.54	104.7	0.73	84.8	0.84
Feb	110.2	0.61	109.7	0.76	94.1	0.94
Mar	177.2	0.98	171.8	1.19	127.5	1.27
Apr	282.3	1.56	243.2	1.69	196.1	1.95
May	295.9	1.63	209.7	1.46	142.8	1.42
Jun	205.8	1.14	150.6	1.05	76.6	0.76
Jul	194.0	1.07	131.1	0.91	70.6	0.70
Aug	219.3	1.21	146.8	1.02	83.7	0.83
Sep	178.3	0.98	119.5	0.83	69.2	0.69
Oct	164.4	0.91	127.0	0.88	84.2	0.84
Nov	158.3	0.87	119.8	0.83	106.8	1.06
Dec	91.7	0.51	91.7	0.64	70.2	0.70

* compare with Table 5-12

The observed value of total streamflow was also reduced to 9288mm since the simulated period was shortened (1962-1999).

c) As section 5.4.2 mentioned, observed evaporation data was not available during the first model configuration. Daily sunshine and windruns data were used to estimate evaporation. Actual monthly evaporation data was collected and put into the model calibration (refer to Table 5-4). Generally, the annual evaporation of Nyando catchment is more or less equal to the MAP, but is less during the rainy season. In this scenario, monthly evaporation adjustment factors were required to achieve the total balance by trail and error. The estimated factors are presented in Table 6-4.

Table 6-4 Modified monthly evaporation adjustment factors

Sub-catchment	Jan	Feb	Mar	Apr	May	Jun	Jul	Aug	Sep	Oct	Nov	Dec
1	1.26	1.26	1.26	2.2	2.2	2.2	1.26	1.26	1.26	1.26	1.26	1.26
2	1.52	1.52	1.52	3.2	3.2	3.2	1.52	1.52	1.52	1.52	1.52	1.52
3	1.52	1.52	1.52	3.2	3.2	3.2	1.52	1.52	1.52	1.52	1.52	1.52
4	1.65	1.65	1.65	3.2	3.2	3.2	1.65	1.65	1.65	1.65	1.65	1.65
5	1.92	1.92	1.92	3.2	3.2	3.2	1.92	1.92	1.92	1.92	1.92	1.92
6	1.65	1.65	1.65	3.2	3.2	3.2	1.65	1.65	1.65	1.65	1.65	1.65
7	1.52	1.52	1.52	3.2	3.2	3.2	1.52	1.52	1.52	1.52	1.52	1.52
8	1.26	1.26	1.26	2.2	2.2	2.2	1.26	1.26	1.26	1.26	1.26	1.26
9	1.26	1.26	1.26	2.2	2.2	2.2	1.26	1.26	1.26	1.26	1.26	1.26
10	1.26	1.26	1.26	2.2	2.2	2.2	1.26	1.26	1.26	1.26	1.26	1.26

Pectora roborant cultus recti

d) The forest land use factor wasn't considered in the model configuration whereas there are forest stand in these sub-catchments. This factor was added in during calibration by using area-weighting, and thus, the sub-catchments monthly crop coefficients (CAY) were also changed (Table 6-5).

Table 6-5 Modified monthly crop coefficients (CAY) *

Sub-catchment	Jan	Feb	Mar	Apr	May	Jun	Jul	Aug	Sep	Oct	Nov	Dec
1	0.8	0.8	0.6	0.3	0.1	0.1	0.2	0.2	0.2	0.4	0.65	0.8
2	0.8	0.8	0.6	0.3	0.1	0.1	0.2	0.2	0.2	0.4	0.65	0.8
3	0.8	0.8	0.8	0.7	0.7	0.7	0.8	0.8	0.8	0.8	0.8	0.8
4	0.8	0.8	0.8	0.7	0.7	0.7	0.8	0.8	0.8	0.8	0.8	0.8
5	0.8	0.8	0.8	0.7	0.7	0.7	0.8	0.8	0.8	0.8	0.8	0.8
6	0.8	0.8	0.8	0.7	0.7	0.7	0.8	0.8	0.8	0.8	0.8	0.8
7	0.8	0.8	0.8	0.7	0.7	0.7	0.8	0.8	0.8	0.8	0.8	0.8
8	0.8	0.8	0.6	0.3	0.1	0.1	0.2	0.2	0.2	0.4	0.65	0.8
9	0.8	0.8	0.6	0.3	0.1	0.1	0.2	0.2	0.2	0.4	0.65	0.8
10	0.8	0.8	0.8	0.7	0.7	0.7	0.8	0.8	0.8	0.8	0.8	0.8

* compare with Table 5-14

Most of the factors were estimated quite a few times to try to improve the simulated result. The total calibrated simulated streamflow is 11990mm which is overestimated with 29.1 %, which is above the observed value for 9288mm (Figure 6-3). The monthly streamflow distribution and its simulation statistical comparison trend are presented in Figure 6-4.

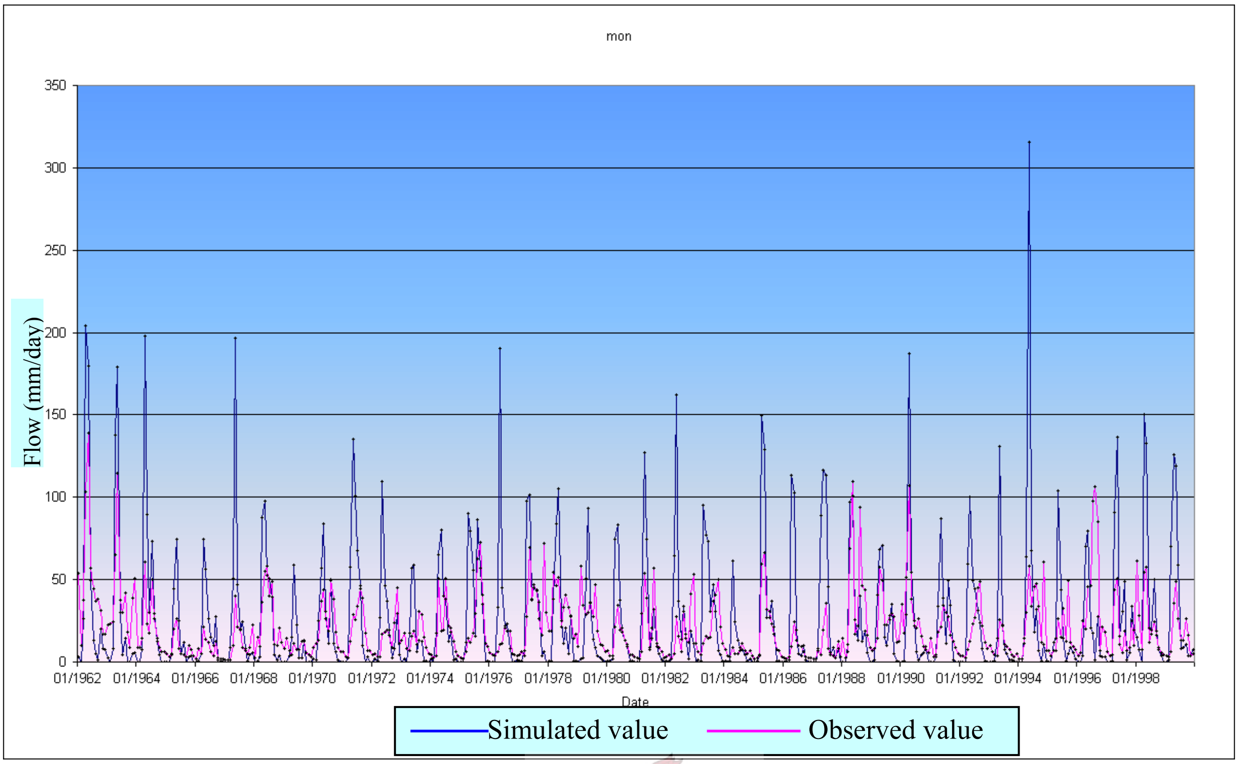

Figure 6-3 The Nyando catchment model simulated vs. observed monthly total streamflow – after first calibration

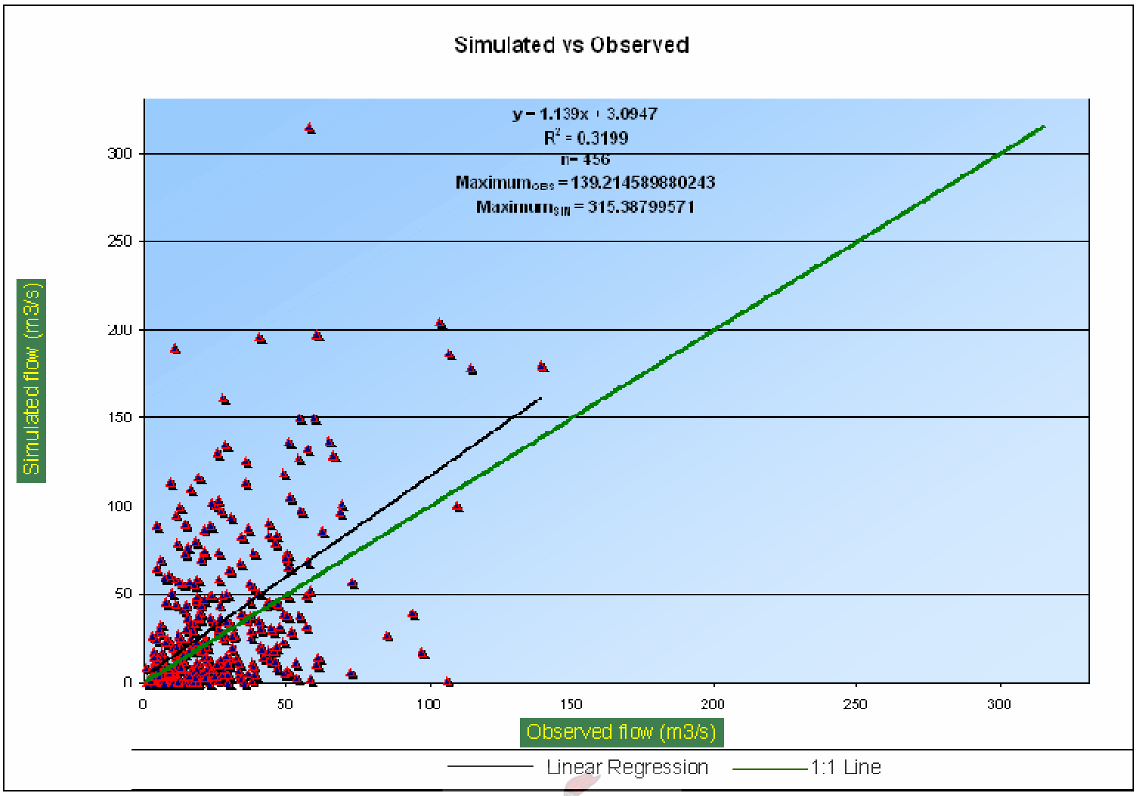

Figure 6-4 The Nyando model simulated vs. observed streamflow statistical comparison trend line

6.4.2 The Nyando catchment model sensitivity analysis

During the first round of the model calibration, it was mainly aimed to check the accuracy of MAP, MAR, and MAE. After this, the model calibration was refined by adjusting streamflow control variables, effective total rooting depth, coefficient of initial abstraction, the soil type and depth information.

According to the above simulation result (Figure 6-3), the simulated streamflow was still higher than observed values. The distribution trend was close to the general trend 1 (Figure 6-1). Therefore, the following changes were carried out to refine the accuracy of the model.

a) Soil type default value for sand-clay-loam soils was replaced by sand for more infiltration to reduce the stormflow.

b) Too much stormflow would be obtained if the total soil depth was too shallow. Therefore, both the topsoil depth and subsoil depths were increased respectively to 0.3m and 0.8m, which both were previously estimated at a depth of 0.2m.

c) To reduce the simulated streamflow, the immediate approach was to reduce the baseflow and stormflow. There are two coefficients that can be used to achieve this purpose. One coefficient is the stormflow response fraction for the catchment, i.e. the fraction of the total stormflow that will cause runoff from the catchment/sub-catchment on the same day as the rainfall event; the other coefficient is baseflow response. It is the fraction of water from the intermediate/groundwater store which becomes streamflow on a particular day (ACRU User Manual). The model assumed these two coefficients at 0.2 and 0.001. Finally, the stormflow response fraction dropped from 0.2 to 0.1, and baseflow response fraction was set at 0.00.

d) The coefficient of initial abstraction is used to estimate the rainfall abstracted by interception, surface storage and infiltration before stormflow commences. The study model configuration used a default initial abstraction value of 0.2 through the rainy season and dry season. The calibration simulation obtained trend line indicates that too much rainfall is converted to streamflow during the wet season. The main rainy season in Nyando Catchment occurs between April and July, and another shorter period occurs between November and December. In order to reduce the streamflow, the rain season abstraction coefficient increased to 0.3 instead of 0.2, while the default value of 0.2 was retained for the dry season (Table 6-6), through out the entire catchment.

Table 6-6 Modified Nyando catchment initial abstraction coefficients

Jan	Feb	Mar	Apr	May	Jun	Jul	Aug	Sep	Oct	Nov	Dec
0.2	0.2	0.2	0.3	0.3	0.3	0.3	0.2	0.2	0.2	0.3	0.3

The model calibration included adjustment of many adjustable variables which relate to streamflow. A trail and error approach was followed to obtain the final calibration. The final calibration simulation resulted in 9759mm total streamflow which is 5.1 % higher than the observed value: 9288mm (see comparison graph Figure 6-5). The generated trend line and 1:1

line overlap significantly (Figure 6-6). Thus an acceptable simulation result was achieved, which meant the model could be used for other scenarios.

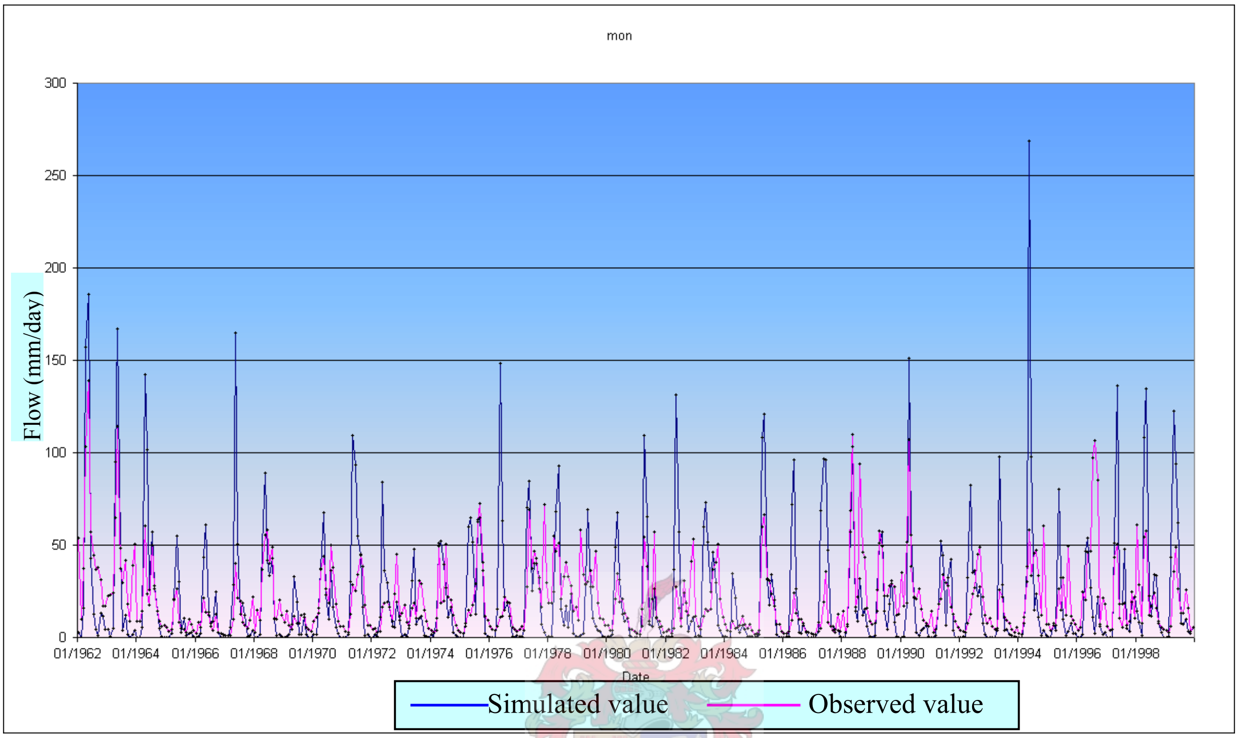

Figure 6-5 Nyando catchment model simulated vs. observed monthly total streamflow – after second calibration

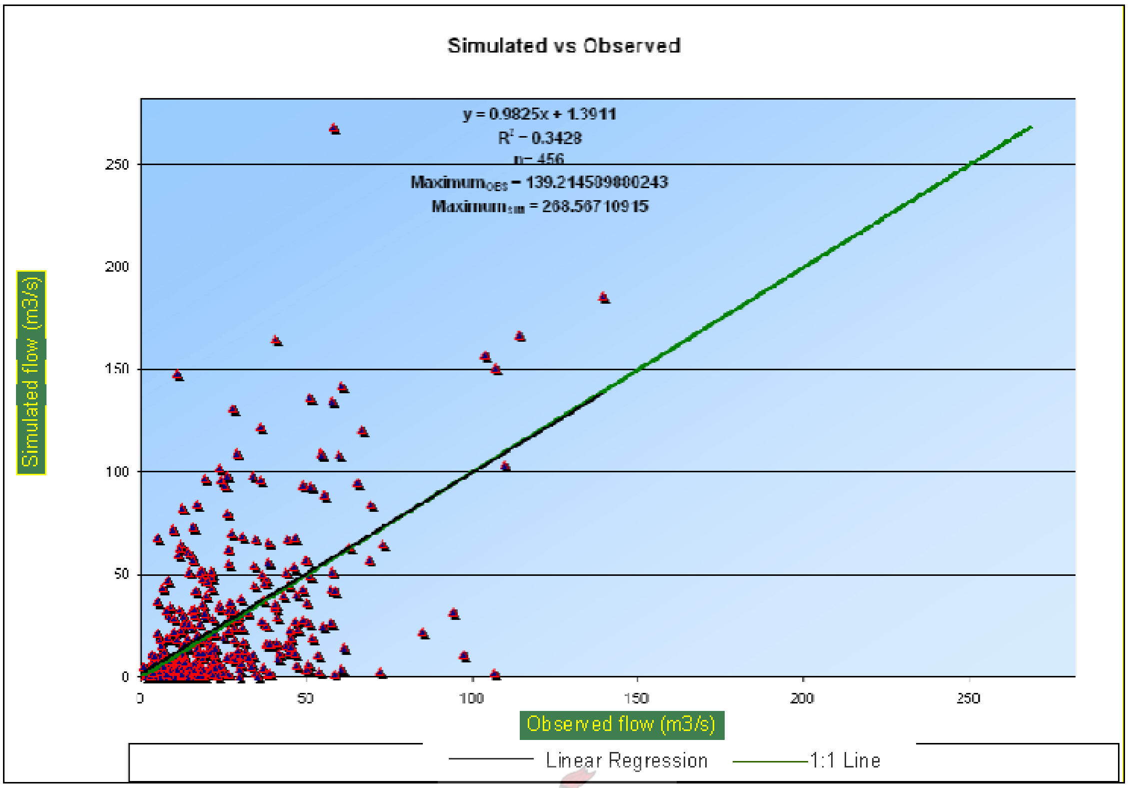

Figure 6-6 Nyando model simulated vs. observed streamflow statistical comparison trend line

6.4.3 The Nzoia catchment model calibration and sensitivity analysis

The Nzoia Catchment is over four times the size of Nyando Catchment and with a large number of default values. This could lead to a poor calibration and verification. The whole calibration process and sensitivity analysis were similar to those for the Nyando catchment model, which adopted 7 steps starting from the main factors (viz. MAP, MAR, MAE). The process is presented below:

a) The first Nzoia model simulation after configuration resulted in a simulated total streamflow of 59686mm for the period 1950 to 2004, which overestimated the observed streamflow by 297 % (Figure 6-7).The simulation was similar to the general trend 3 (refer to Figure 6-1), which indicated that both low flow and high flow were oversimulated (Figure 6-8).

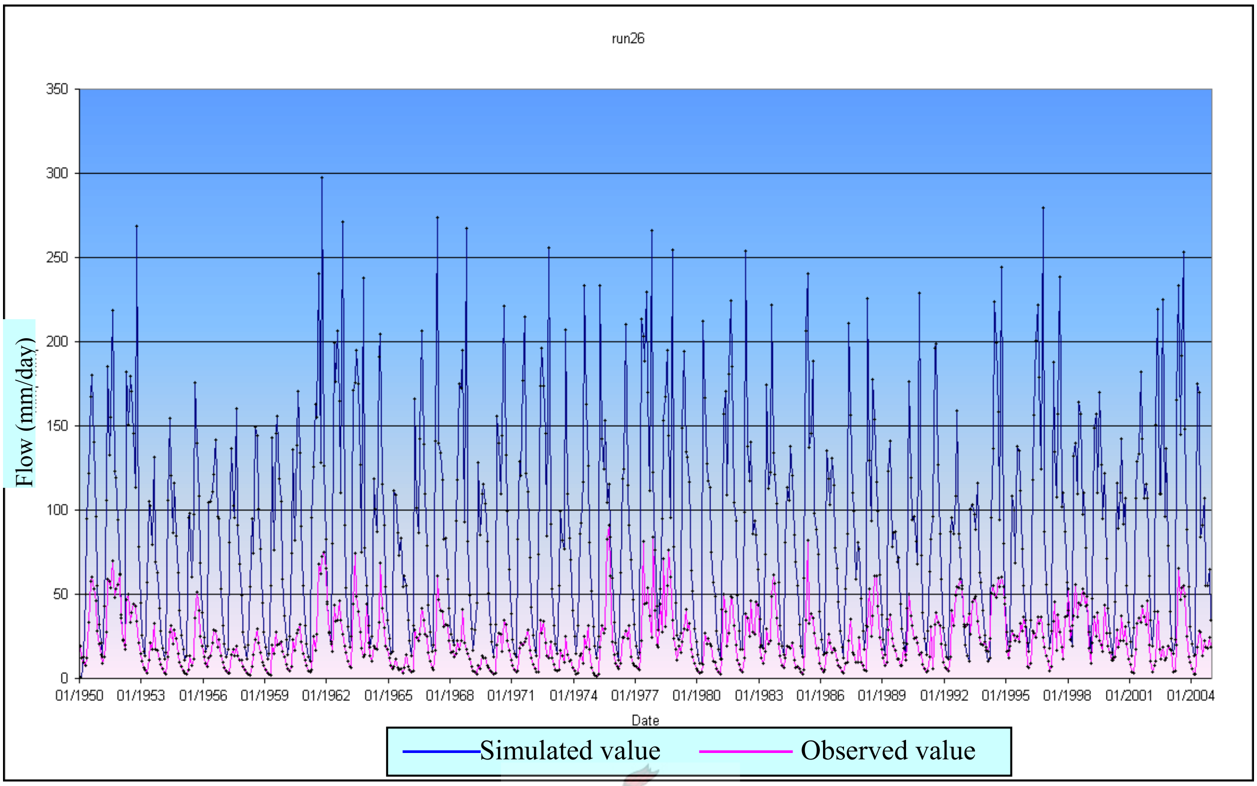

Figure 6-7 Nzoia catchment model simulated vs. observed monthly total streamflow – before calibration

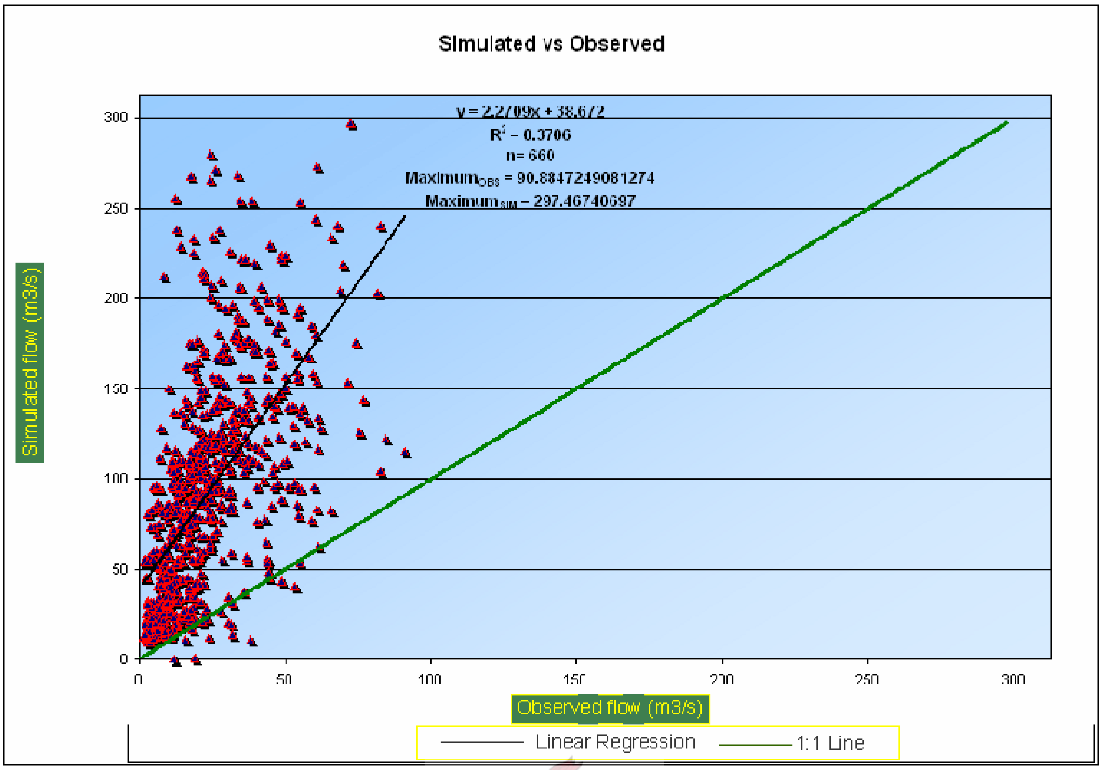

Figure 6-8 Nzoia model simulated vs. observed streamflow statistical comparison trend line – before model calibration

b) The Nzoia Catchment model was configured after the Nyando Catchment. Therefore, the available monthly evaporation could be used in the set up, but relevant adjustment factors were required as well during the model configuration. The values of these factors were initially assumed to be 1.00, for a whole year and covered the entire the catchment. Finally, the adjustment factors were calibrated to an acceptable range through different trails. The adopted factors are shown in Table 6-7.

Table 6-7 Calibrated monthly evaporation adjustment factors

Sub-catchment	Jan	Feb	Mar	Apr	May	Jun	Jul	Aug	Sep	Oct	Nov	Dec
1	1.00	1.00	1.00	2.46	2.46	2.46	2.46	2.46	2.46	1.46	1.00	1.00
2	1.00	1.00	1.00	2.32	2.32	2.32	2.32	2.32	2.32	1.32	1.00	1.00
3	1.00	1.00	1.00	2.46	2.46	2.46	2.46	2.46	2.46	1.46	1.00	1.00
4	1.00	1.00	1.00	2.32	2.32	2.32	2.32	2.32	2.32	1.32	1.00	1.00
5	1.00	1.00	1.00	2.46	2.46	2.46	2.46	2.46	2.46	1.46	1.00	1.00
6	1.00	1.00	1.00	2.46	2.46	2.46	2.46	2.46	2.46	1.46	1.00	1.00
7	1.00	1.00	1.00	2.46	2.46	2.46	2.46	2.46	2.46	1.46	1.00	1.00
8	1.00	1.00	1.00	2.32	2.32	2.32	2.32	2.32	2.32	1.32	1.00	1.00
9	1.00	1.00	1.00	2.32	2.32	2.32	2.32	2.32	2.32	1.32	1.00	1.00
10	1.00	1.00	1.00	2.46	2.46	2.46	2.46	2.46	2.46	1.46	1.00	1.00
11	1.00	1.00	1.00	2.46	2.46	2.46	2.46	2.46	2.46	1.46	1.00	1.00
12	1.00	1.00	1.00	2.46	2.46	2.46	2.46	2.46	2.46	1.46	1.00	1.00
13	1.00	1.00	1.00	2.59	2.59	2.59	2.59	2.59	2.59	1.59	1.00	1.00
14	1.00	1.00	1.00	2.46	2.46	2.46	2.46	2.46	2.46	1.46	1.00	1.00
15	1.00	1.00	1.00	2.46	2.46	2.46	2.46	2.46	2.46	1.46	1.00	1.00
16	2.00	2.00	2.00	3.25	3.25	3.25	3.25	3.25	3.25	2.25	2.00	2.00
17	1.00	1.00	1.00	2.99	2.99	2.99	2.99	2.99	2.99	1.99	1.00	1.00
18	1.00	1.00	1.00	2.99	2.99	2.99	2.99	2.99	2.99	1.99	1.00	1.00
19	1.00	1.00	1.00	2.99	2.99	2.99	2.99	2.99	2.99	1.99	1.00	1.00
20	2.00	2.00	2.00	3.25	3.25	3.25	3.25	3.25	3.25	2.25	2.00	2.00
21	2.00	2.00	2.00	3.38	3.38	3.38	3.38	3.38	3.38	2.38	2.00	2.00
22	2.00	2.00	2.00	3.12	3.12	3.12	3.12	3.12	3.12	2.12	2.00	2.00
23	2.00	2.00	2.00	3.38	3.38	3.38	3.38	3.38	3.38	2.38	2.00	2.00
24	2.00	2.00	2.00	3.12	3.12	3.12	3.12	3.12	3.12	2.12	2.00	2.00
25	1.00	1.00	1.00	2.99	2.99	2.99	2.99	2.99	2.99	1.99	1.00	1.00
26	1.00	1.00	1.00	2.72	2.72	2.72	2.72	2.72	2.72	1.72	1.00	1.00

c) According to Figure 6-7, the general trend line 3 indicates that total soil depth is too shallow, causing too much stormflow to be generated, especially when the subsoil horizon thickness is too shallow, which cause too much baseflow. According to this, several trials runs were performed to approach the satisfactory total soil depth. The value of the topsoil depth was increased from 0.25m to 0.3m, while the subsoil depth was increased to 0.6m, from 0.5m previously.

d) The streamflow control variables always play important roles in the flow model. For the Nzoia model the stormflow response fraction was reduced to 0.06 which was lower than the previous fraction of 0.3. The baseflow response fraction was also decreased from 0.012 to 0.00.

After the calibration, the Nzoia catchment model simulated result finally could be accepted to simulate other scenarios. The calibrated result of the total streamflow was 16996mm, which was 12.98% (slightly higher than 10%) greater than the observed value. The comparison graph is shown in Figure 6-9 and the trend line is very close 1:1 line (Figure 6-10).

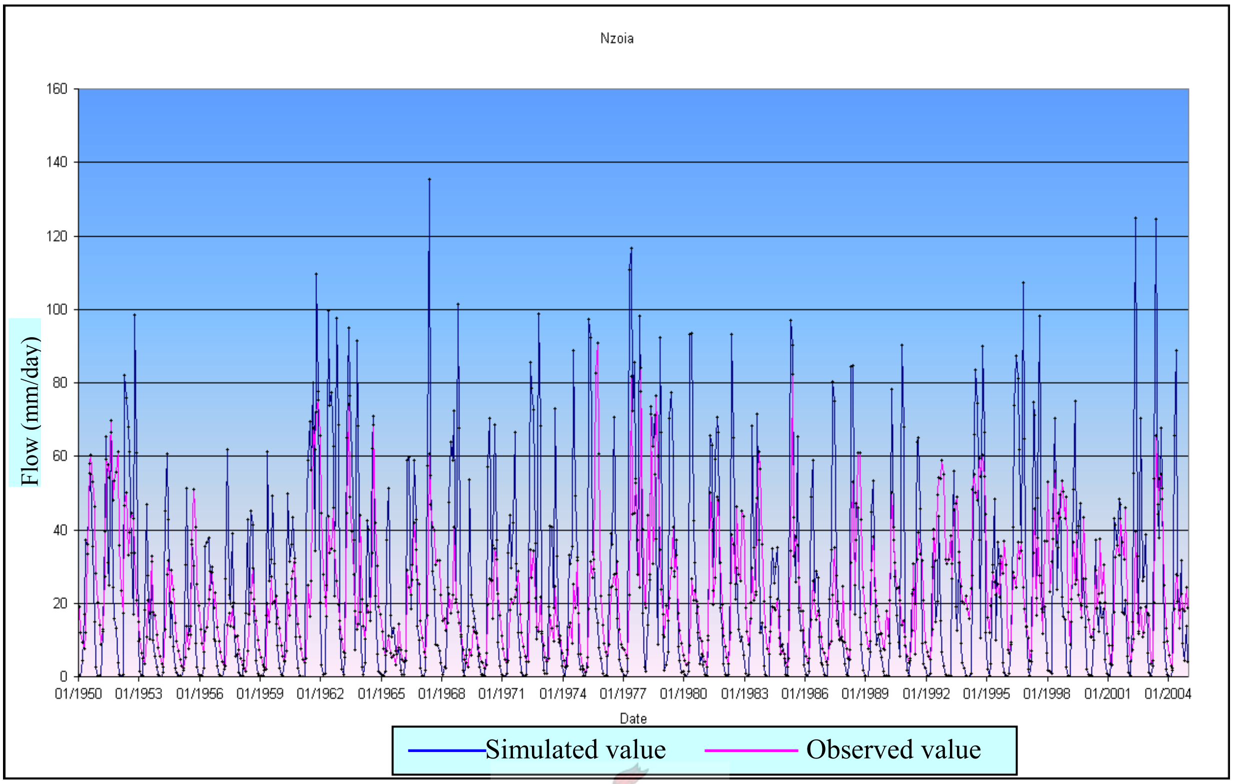

Figure 6-9 Nzoia Catchment model simulated vs. observed monthly total streamflow – after calibration

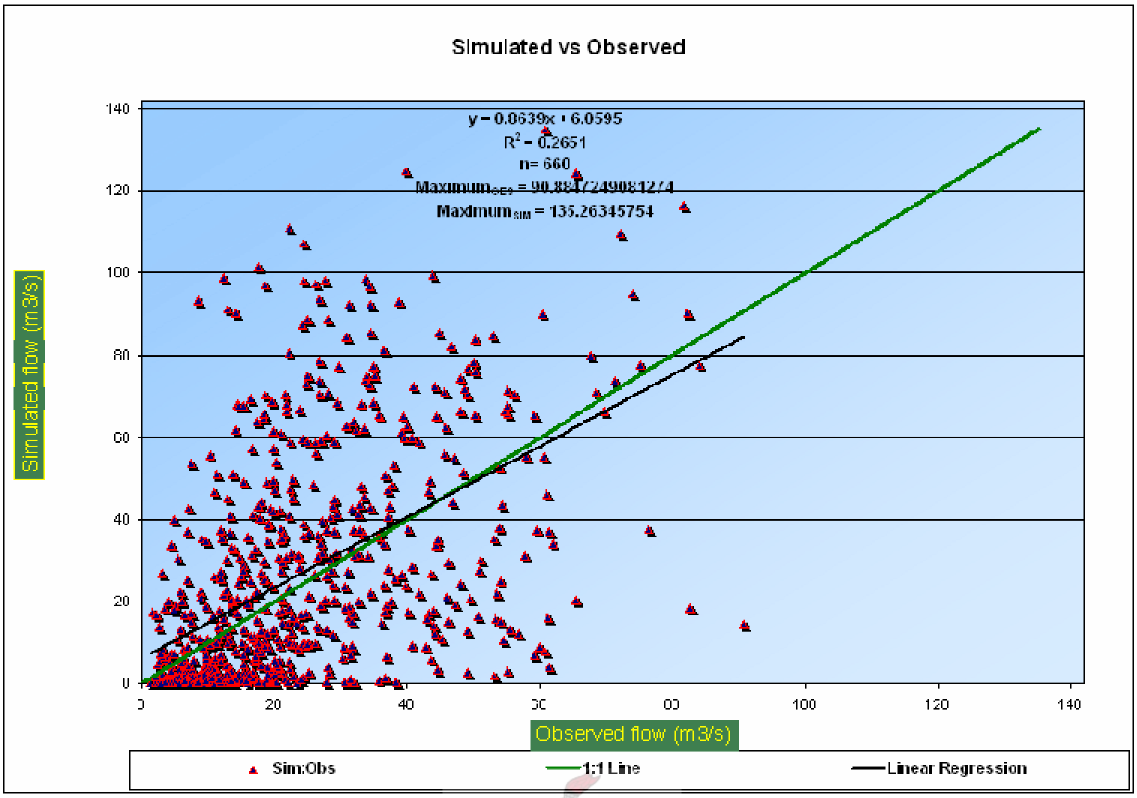

Figure 6-10 Nzoia model simulated vs. observed streamflow statistical comparison trend line – after model calibration

6.5 DISCUSSION OF FINAL MODEL RESULTS

The objective in this chapter was to develop water budget models which are capable of indicating the real situations in specific catchments. The model has an ability to predict, with acceptable accuracy, the relationship between precipitation, runoff and evaporation in the catchment/sub-catchments. The accuracy mainly depends on the accuracy of the input observed MAP, MAR and MAE values. However, other factors, such as the correctness of the soil information and land use condition are also important to obtain accurate module runs.

By checking the overall water budget and monthly total precipitation, the model could accurately predict the mass balance in the system. Generally, daily output analysis follows the monthly statistical analysis to achieve the most accurate predictions. However, daily water input analysis was not used in detail, since most of the daily input information was unknown, with the exception of daily rainfall and daily runoff. This is also the reason for the errors of underestimation of low flow and overestimation of high flow.

Although both the Nyando Catchment and Nzoia catchment are large area catchments, the ACRU program has handled flow model simulation successfully. Apparently, two aspects can be concluded after the model calibration: no matter how big the total catchment is, sub-catchments should not be plotted at too large a scale. The uncertainties and inaccuracies will be increased if the sub-catchment size is too big. Another aspect is that the sub-catchment data must be very detailed.

Unfortunately in this study, only a few large scaled and outdated topographic maps were available for sub-catchment plots and a number of factors were unknown which had to be replaced by default values.

CHAPTER 7 SEDIMENT YIELD MODULE CALIBRATION, SENSITIVITY ANALYSIS AND VERIFICATION

7.1 INTRODUCTION

The focus of this chapter is on sensitivity analyses of the sediment yield parameters and the calibration and verification of the sediment yield modules. The accuracy of the sediment yield parameters is largely dependent on the accuracy of the flow simulation; therefore, the errors in the sediment yield simulation already existed since flow model errors are present. The sensitivity analysis of the sediment yield parameters determines the adjustments of these parameters in order to obtain a satisfactory fit which is reasonable compared to observed data.

Sediment yields of the Nzoia and Nyando Rivers were calculated from suspended sediment data of LVEMP and data obtained during this study. The sediment yields obtained in this study are considerably higher than those obtained in other LVEMP projects (Table 7-1)

Table 7-1 Measured sediment yields at Nyando River mouth and Nzoia River mouth (Basson, 2005)

River	Catchment area (km^2)	Mean runoff (1950 to 2004) (m^3/s)	Sediment yield ($t/km^2.a$)	Sediment load (t/a)
Nyando	3655	21	142 (Probable) 346 (High Probable)	519969 1265309
Nzoia	*12842 (13691)	119	80 (Probable) 218 (High Probable)	1029820 2795892

* Notes: a) as described before, the model used a Nzoia catchment area of 13691km^2, measured from topographic maps, which is larger than the official value of 12842km^2.

b) “Probable” and “high probable” values are given due to the limited suspended sediment data available, especially for medium to large floods. The sediment yields include suspended and bed load.

Mathematical modelling of the sediment transport and deposition processes in Winam Gulf and opposite the Nzoia River have been carried out and the sediment deposition patterns that can be expected are shown in Figures 7-1 and 7-2 respectively. It is expected that the delta (above water) at Nzoia River mouth will reach the Uganda border in 115 years. At Winam Gulf the water depth near Kisumu could become less than 2 m deep over a distance of 30 km if the water level drops below the current 1134 masl (Basson, 2005).

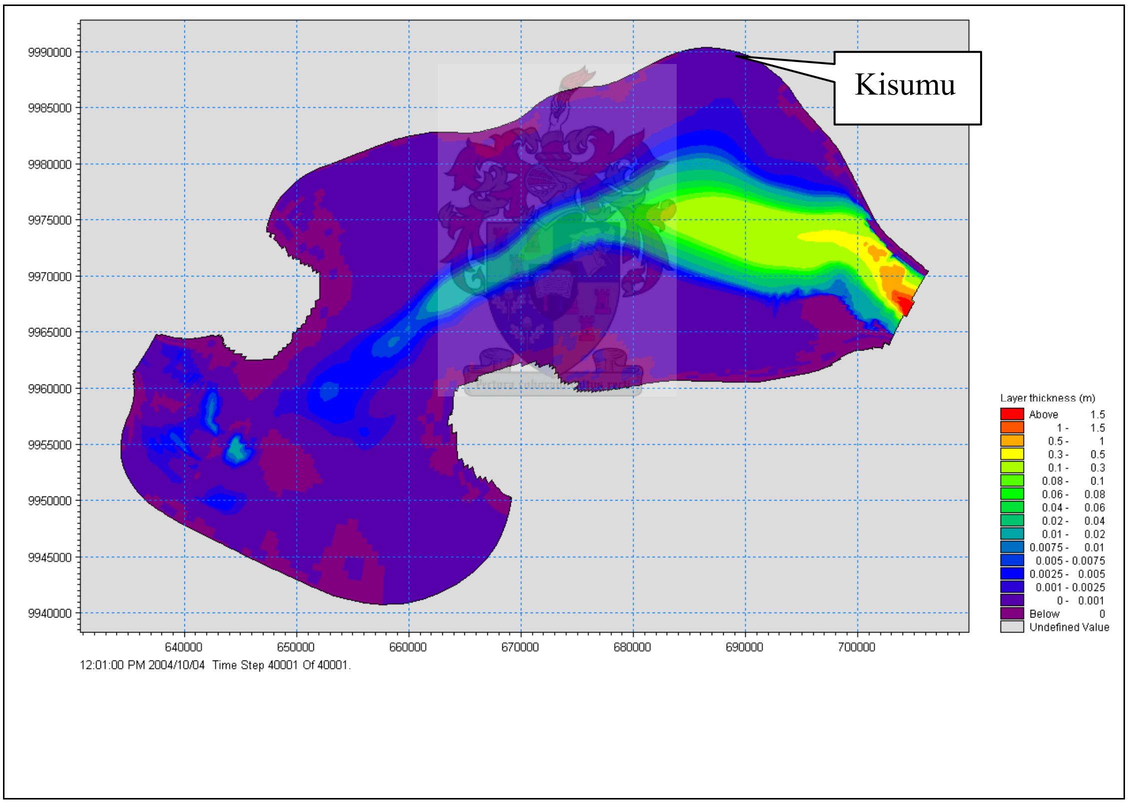

Figure 7-1 Sediment deposition thickness pattern as simulated for the next 50 years in Winam Gulf (Basson, 2005)

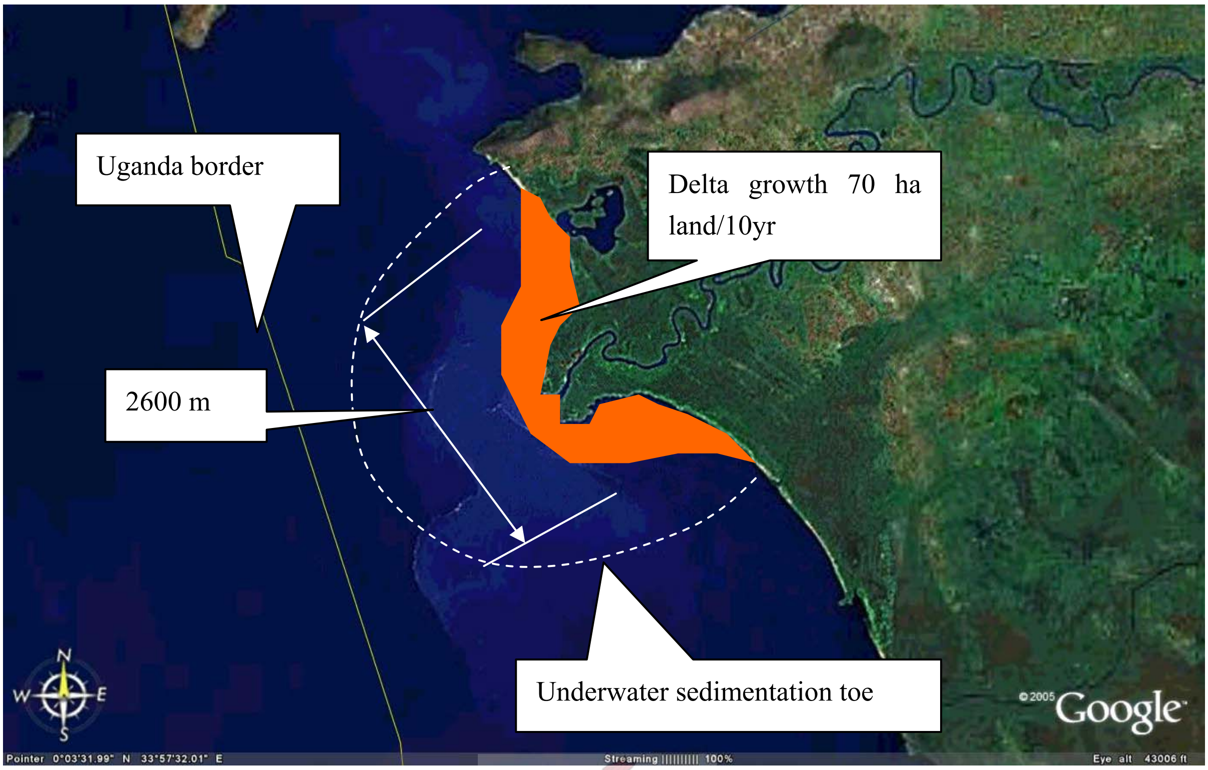

Figure 7-2 Predicted Nzoia deposition pattern over next 10 years (Basson, 2005)

According to Table 7-1, the mean annual sediment yield of the catchments, are also the values that the models were calibrated against. The ACRU model estimates each sub-catchment sediment yield, and the total catchment sediment load must be added up after every simulation in order to compare with the observed total catchment sediment yield.

7.2 SENSITIVITY PARAMETERS

According to the ACRU User Manual, the MUSLE estimates the bulk delivery of sediment out a catchment outlet (refer to Equation 3.3). Having selected this option, there are several factors used to characterise the state of the catchment in terms of its runoff energy (viz. the ALHPA and BETA parameters) and in terms of its inherent soil loss potential (viz. the soil erodibility factors SOIFC1 and SOIFC2, the cover factor, input either monthly as COVER(I) or daily as CFACTD(K)), and the support practice factor PFACT. The states and effects of related factors are described below:

- **ALPHA** - Runoff erosivity constant.
- **BETA** - Runoff erosivity exponent.

According to Simons and Senturk (1992), the MUSLE coefficients ALPHA and BETA are located specifically, hence must be determined for specific catchments in specific climatic regions. Kienzle and Lorentz (1993) reported that very little research has been undertaken on calibrating these coefficients. Default values of 8.934 and 0.56 for ALPHA and BETA respectively, have been used in southern Africa. Having been originally calibrated for catchments in selected catchments in the USA by Williams (1975), these values for ALPHA and BETA have been adopted extensively with varying degrees of success (Williams and Berndt, 1977; Williams, 1991; Kienzle et al., 1997). These values have also been used in the Nyando model and Nzoia model simulations.

- **SOIFC1** - Maximum soil erodibility factor (K_{max}).
- **SOIFC2** - Minimum soil erodibility factor (K_{min}).

Three methods for estimating the soil erodibility factors which are supplied for different levels of available information on soil characteristics could be used to estimate the soil erodibility factor:

1. Soil form and series of the Binomial Soil Classification system, or the soil form, family and textural class of the Taxonomic Classification system, is known.
2. Limited Soil physical data available
3. Detailed Soil physical data available

Soil textural class and physical data was unknown for the study models and the default texture class (sand-loam-clay) were used in the model configuration and replaced by sand texture in the Nyando catchment during the flow model calibration. The Nzoia catchment still continued to use sand-loam-clay as its catchment soil texture during the flow model calibration. According to this scenario, method 1 was selected to estimate the soil erodibility factors. The processes are presented as follows are described in the ACRU User Manual):

1a) Determine the soil erodibility class for the Taxonomic or Binomial Soil Classification respectively.

1b) Estimate the nominal K-factor, K_{nom} from Table 7-2

Table 7-2 Soil erodibility factors (K_{nom}) for various erodibility classes

Soil erodibility class	**K_{nom}**
very high	> 0.70
high	0.50 - 0.70
moderate	0.25 - 0.50
low	0.13 - 0.25
very low	< 0.13

1c) Determine, the ratio r_k of K_{max} to K_{min} using Table 7-3.

Pectora roborant cultus recti

Table 7-3 K_{max} / K_{min} ratios, r_k

K_{max}/K_{min} Ratio, r_k	**Seasonal variation in rainfall erosivity, R**
1	Virtually no seasonal variation in R
3	Seasonal variation in R = low
7	Seasonal variation in R = high

1d) Determine K_{min} (SOIFC2) and K_{max} (SOIFC1) from Equation 7.1 and 7.2.

$$K_{\min} = \frac{2 \times K_{nom}}{1 \times r_K} \qquad \text{Eq 7.1}$$

$$K_{\max} = K_{\min} \times r_K \qquad \text{Eq 7.2}$$

1e) If no variation in K-factor is required, set SOIFC1 = SOIFC2 = K_{nom}.

- **COVER (I) or CFACTD (K)** – The cover factor, C, as COVER(I) or CFACTD(K) can be estimated in three different ways depending on the level of information available.

Level 1 An estimation of the C-factor can be made from knowledge of the initial SCS Runoff Curve Number, CNII.

Level 2 Limited Vegetation Information Available; such as canopy cover, height of canopy, mulch cover and residual effects, then the cover factor can be estimated separately for cultivated land and uncultivated land.

Level 3 Detailed Vegetation Information Available; cover factor can be estimated from the five sub-factors, viz. period land use, canopy cover, surface vegetation or mulch cover, surface roughness and soil moisture for different times of the year.

The Level 1 was selected to estimate the C-factors, similar to selecting the estimation method of soil erodibility. Where there is no detailed daily cover information available, the C-factor had to be estimated on a monthly basis (COVER(I)) via the following steps:

1a) Determine the initial SCS Curve Number (CNII) from Appendix C of the ACRU manual.
1b) Calculate the C-factor (COVER(I)) from Equation 7.3 or read the C-factor from Figure 7-3.

$$C = EXP\left(\frac{CNII \times 97.5}{10.9}\right) \qquad \text{Eq 7.3}$$

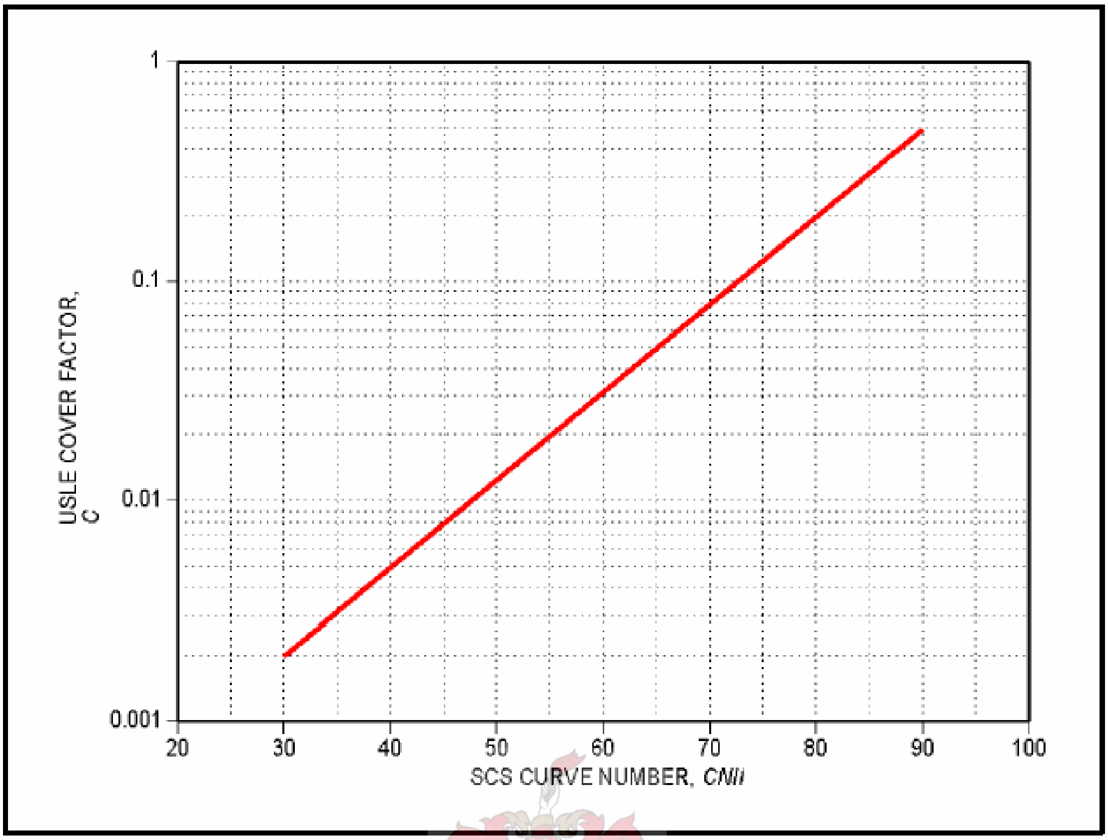

Figure 7-3 Relationship between initial SCS Curve Number, CNII, and MUSLE Cover Factor, C (after Øverland 1990)

- **PFACT** - Support practice factor (P) in MUSLE. The estimation of this factor was discussed in section 5.4.2, and the results presented in section 5.4.2 for Nyando Catchment (refer to Table 5-18) and section 5.4.3 for Nzoia Catchment (refer to Table 5-22).

- **SEDIST** - The fraction of the event based sediment yield from the catchment that reaches the outlet on the day of the event. According to the calculated time of concentration of Nyando sub-catchments and Nzoia sub-catchments, all the sediments produced from daily rainfall events reach the catchment outlet within 24 hours. Thus SEDIST is 1.0.

7.3 MODEL CALIBRATION

7.3.1 Nyando model calibration

The Nyando model aims to calibrate the adjustable factors from sensitivity parameters. There are only two factors adjustable to achieve the measured sediment yield, viz. soil erodibility factor and cover factor; the rest of the factors were already adjusted during the stream flow model calibration and verified directly or indirectly.

<u>The cover factor</u>

Actually, the cover factor should first be checked for the study model, depending on the level of available information of the land use conditions. These factors have already been confirmed during the flow model calibration. Hence the calibration of the cover factor should be based on the confirmed flow model. The Nyando Catchment/sub-catchments' general land use is given in Table 7-4:

Table 7-4 Current land use condition in Nyando catchment – after flow model calibration

Sub-catchment	Current land use (%)			
	crops	sugarcane	forest	wetland
1	50.00		50.00	
2	50.00		50.00	
3		100.00		
4		50.00	50.00	
5		100.00		
6		100.00		
7		100.00		
8	100.00			
9		100.00		
10				100.00

Following the Level 1 C-factor estimation process, the CNII values under the specific land uses was first determined using Appendix C of the ACRU model. The seasonal stormflow potential also needs to be considered to achieve the related CNNII. The C-factors read from Figure 7-3 stand for each single land use, so the area-weighting has to be completed to get the combined sub-catchment monthly C-factors. The estimated results are shown in Table 7-5.

Table 7-5 Calibrated Sub-catchment combined cover factors – Nyando catchment

Sub-catchment	Jan	Feb	Mar	Apr	May	Jun	Jul	Aug	Sep	Oct	Nov	Dec
1	0.05	0.05	0.08	0.08	0.08	0.08	0.05	0.05	0.05	0.08	0.08	0.08
2	0.05	0.05	0.08	0.08	0.08	0.08	0.05	0.05	0.05	0.08	0.08	0.08
3	0.01	0.01	0.01	0.01	0.01	0.01	0.01	0.01	0.01	0.01	0.01	0.01
4	0.01	0.01	0.01	0.01	0.01	0.01	0.01	0.01	0.01	0.01	0.01	0.01
5	0.01	0.01	0.01	0.01	0.01	0.01	0.01	0.01	0.01	0.01	0.01	0.01
6	0.01	0.01	0.01	0.01	0.01	0.01	0.01	0.01	0.01	0.01	0.01	0.01
7	0.01	0.01	0.01	0.01	0.01	0.01	0.01	0.01	0.01	0.01	0.01	0.01
8	0.05	0.05	0.08	0.08	0.08	0.08	0.05	0.05	0.05	0.08	0.08	0.08
9	0.01	0.01	0.01	0.01	0.01	0.01	0.01	0.01	0.01	0.01	0.01	0.01
10	0.00	0.00	0.00	0.00	0.00	0.00	0.00	0.00	0.00	0.00	0.00	0.00

Pectora roborant cultus recti

Soil erodibility factors

The Nyando River Basin is a major source of sediment flows into Lake Victoria in Kenya. Severe soil erosion and land degradation problems occur throughout the Nyando River basin. Accelerated runoff sheet erosion over much of the Nyando catchment area has led to severe rill, gully and stream bank erosion in the lower parts of the river basin. The soil type for the study catchment in sand, and the soil erodibility class should therefore be high. The erodibility factor K_{nom} range lies between 0.5 and 0.7 (Table 7-2). It is assumed that K_{nom} = 0.595 for the first stage, then the maximum erodibility factor K_{max} and minimum erodibility factor were calculated as 1.20 and 0.17. Assuming that the seasonal variation in rainfall erosivity remains within a high level, then $r_k = 7$. For this trial, the simulated sediment yield was 395 ton/km^2.annum, which was an oversimulation of 14.2% if compared to the measured sediment yield of 346 ton/km^2.annum (based on high probable data).

The simulated calibration sediment yield is higher than the measured values. Assuming that sediment yield linearly relates to the soil erodibility factor and that the model uses a low level erodibility factor to recalculate the K_{max}, K_{min}, while seasonal variation in rainfall erosivity still stays at a high level (viz. $r_k = 7$), then it can result in a low sediment yield. The next step is to find out the linear relationship by using the simulated high and low results.

According to the above, the erodibility factor of Nyando model was re-estimated to modify: $K_{nom}= 0.42$; $K_{max} = 0.84$ and $K_{min} = 0.12$ with these factors simulated sediment yield was 280 ton/km^2.annum. The linear relationship could be set up as shown in Figure 7-4:

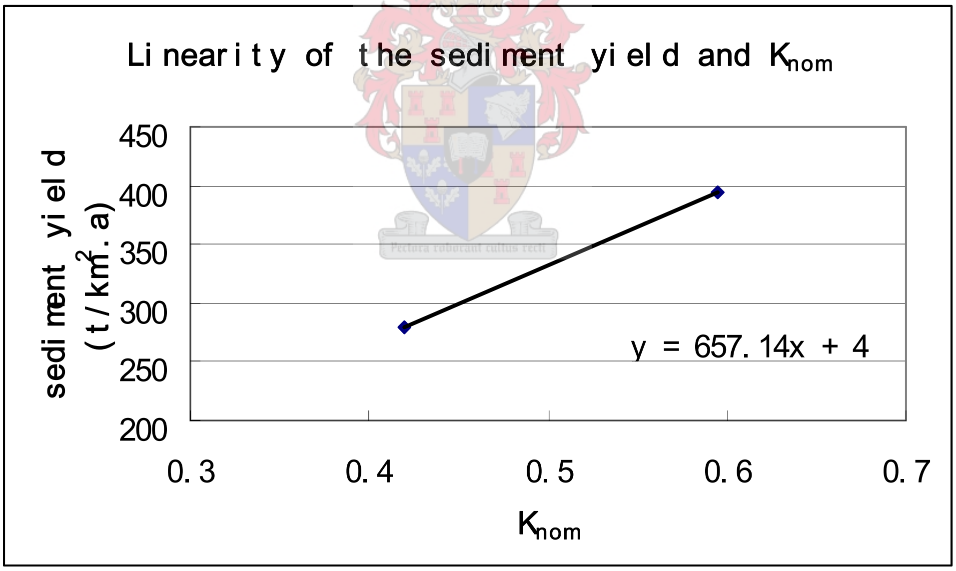

Figure 7-4 Estimated linear relationship between sediment yield and K_{nom} – Nyando catchment

The Nyando sediment yield module calibration aims to achieve the measured yield of 346 ton/km^2.annum. If this value is put into the trend line equation, then the related erodibility factors will be K_{nom} = 0.525, K_{max} = 1.20 and K_{min} = 0.17. The simulated sediment yield was 350 ton/km^2.annum by using these factors, which was only 1.16% above the measured value. Therefore the sediment yield module calibration was also accurate enough to carry out scenarios analysis.

The Ahero gauging station is also available to measure the sediment load of the Nyando River, but only few isolated sediment load measurement was carried out. From Figure 7-5 it can be seen that simulated values are higher than observed values when discharges are less than 50 m^3/s.

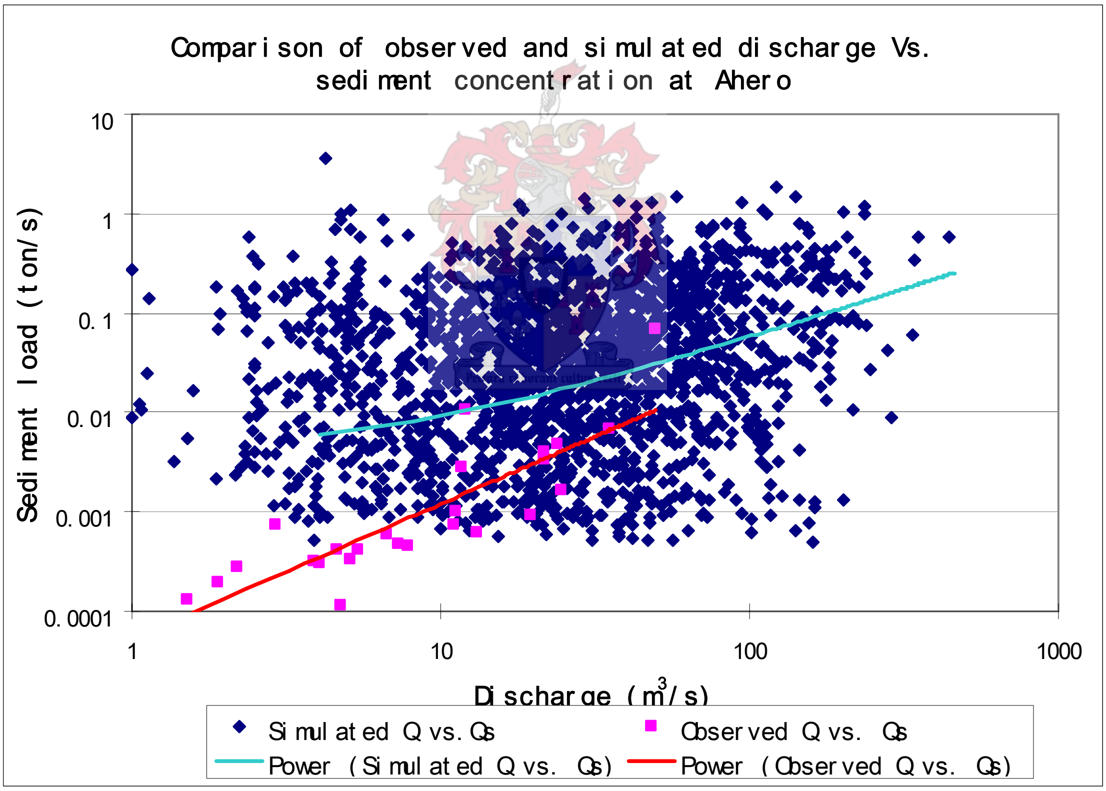

Figure 7-5 Comparison of observed and simulated discharge vs. sediment load at Ahero

7.3.2 Nzoia model calibration and result

The Nzoia catchment sediment yield module calibration was done in the same way as that done for the Nyando sediment yield module calibration.

<u>The cover factor</u>

The estimation of cover factor in the Nzoia model was more complicated than that for the Nyando model, because the Nzoia catchment land cover has used more distributions. Table 7-6 clearly indicates this situation. The Level 1 C-factor estimation process as well as the area-weighting process was also used on the Nzoia model.

Pectora roborant cultus recti

Table 7-6 Calibrated Sub-catchment combined cover factors – Nzoia catchment

Sub-catchment	Jan	Feb	Mar	Apr	May	Jun	Jul	Aug	Sep	Oct	Nov	Dec
1	0.21	0.21	0.21	0.17	0.17	0.17	0.17	0.17	0.17	0.21	0.21	0.21
2	0.23	0.23	0.23	0.18	0.18	0.18	0.18	0.18	0.18	0.23	0.23	0.23
3	0.27	0.27	0.27	0.23	0.23	0.23	0.23	0.23	0.23	0.27	0.27	0.27
4	0.26	0.26	0.26	0.26	0.26	0.26	0.26	0.26	0.26	0.26	0.26	0.26
5	0.24	0.24	0.24	0.21	0.21	0.21	0.21	0.21	0.21	0.24	0.24	0.24
6	0.26	0.26	0.26	0.25	0.25	0.25	0.25	0.25	0.26	0.26	0.26	0.26
7	0.27	0.27	0.27	0.23	0.23	0.23	0.23	0.23	0.23	0.27	0.27	0.27
8	0.28	0.28	0.28	0.28	0.28	0.28	0.28	0.28	0.28	0.28	0.28	0.28
9	0.18	0.18	0.18	0.18	0.18	0.18	0.18	0.18	0.18	0.18	0.18	0.18
10	0.25	0.25	0.25	0.24	0.24	0.24	0.24	0.24	0.24	0.25	0.25	0.25
11	0.26	0.26	0.26	0.23	0.23	0.23	0.23	0.23	0.23	0.26	0.26	0.26
12	0.26	0.26	0.26	0.26	0.26	0.26	0.26	0.26	0.26	0.26	0.26	0.26
13	0.27	0.27	0.27	0.24	0.24	0.24	0.24	0.24	0.24	0.27	0.27	0.27
14	0.30	0.30	0.30	0.30	0.30	0.30	0.30	0.30	0.30	0.30	0.30	0.30
15	0.26	0.26	0.26	0.26	0.26	0.26	0.26	0.26	0.26	0.26	0.26	0.26
16	0.25	0.25	0.25	0.18	0.18	0.18	0.18	0.18	0.18	0.25	0.25	0.25
17	0.29	0.29	0.29	0.29	0.29	0.29	0.29	0.29	0.29	0.29	0.29	0.29
18	0.28	0.28	0.28	0.28	0.28	0.28	0.28	0.28	0.28	0.28	0.28	0.28
19	0.26	0.26	0.26	0.23	0.23	0.23	0.23	0.23	0.23	0.23	0.26	0.26
20	0.30	0.30	0.30	0.29	0.29	0.29	0.29	0.29	0.29	0.30	0.30	0.30
21	0.28	0.28	0.28	0.28	0.28	0.28	0.28	0.28	0.28	0.28	0.28	0.28
22	0.30	0.30	0.30	0.30	0.30	0.30	0.30	0.30	0.30	0.30	0.30	0.30
23	0.30	0.30	0.30	0.30	0.30	0.30	0.30	0.30	0.30	0.30	0.30	0.30
24	0.30	0.30	0.30	0.30	0.30	0.30	0.30	0.30	0.30	0.30	0.30	0.30
25	0.30	0.30	0.30	0.30	0.30	0.30	0.30	0.30	0.30	0.30	0.30	0.30
26	0.28	0.28	0.28	0.28	0.28	0.28	0.28	0.28	0.28	0.28	0.28	0.28

Soil erodibility factors

According to Table 7-1 the Nzoia River Basin sediment yield is 230 ton/km^2 annum (high probable), which is less than Nyando River Basin sediment yields. The Nzoia River flow is however much greater than the Nyando River mean annual flow. The sand-loam-clay used as soil texture in the Nzoia catchment was already proved in flow model calibration. Assuming that the seasonal variation in rainfall erosivity is very high (r_k = 7), and the soil erodibility class also stays at a moderate level, K_{nom} = 0.42, then Equations 7.1 and 7.2 were used calculate the K_{max} = 0.42, K_{min} = 0.06. The simulated sediment yield was 752 ton/km^2.annum, this value was an oversimulation of 226.1 %. The sediment module had to be readjusted to achieve an acceptable sediment yield value.

The Nzoia model obtains a linear trend as shown in Figure 7-5, which is the same as the Nyando model sediment yield module:

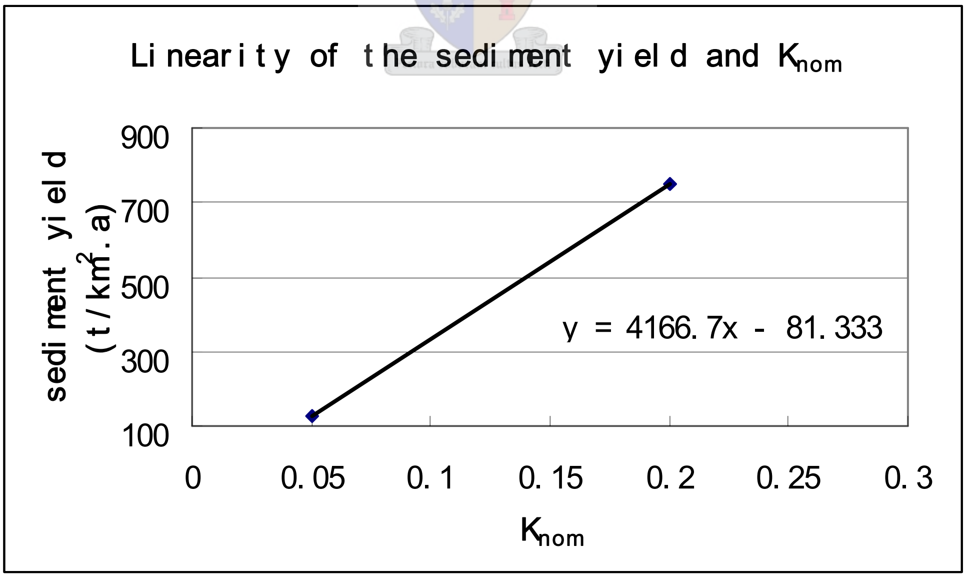

Figure 7-6 Estimated linear relationship between sediment yield and K_{nom} – Nzoia catchment

The final calibrated sediment yield simulation result was 249 ton/km^2.annum, which was above the measured value by 8.26 %. This is acceptable. With K_{nom} = 0.07, K_{max} = 0.14, and K_{min} = 0.02, the soil erodibility factor stays at a very low level.

The station Rwambwa (Figure 7-7) which is located at the Nzoia River mouth was used to measure the sediment load for Nzoia River. The relationship between the sediment load and discharge was used to calibrate the sediment yield which was simulated by the ACRU model. Figure 7-8 indicates that the gradients of the measured and simulated.

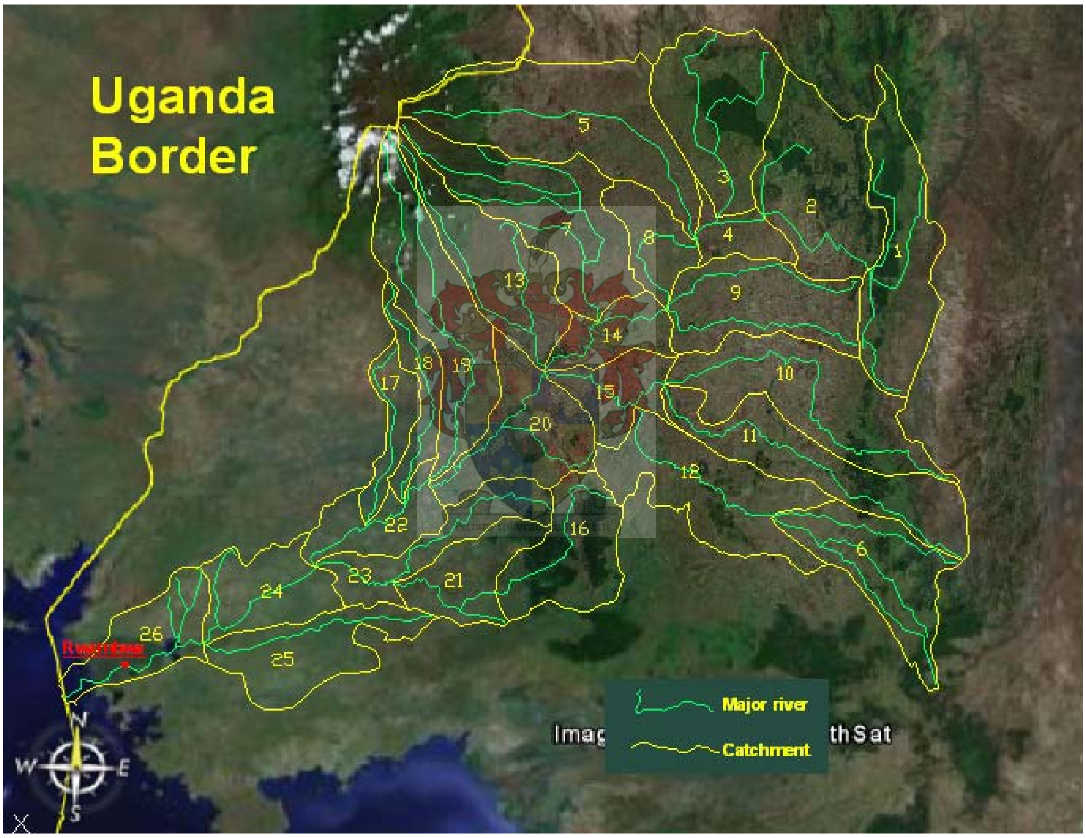

Figure 7-7 Sediment load survey point in Nzoia catchment

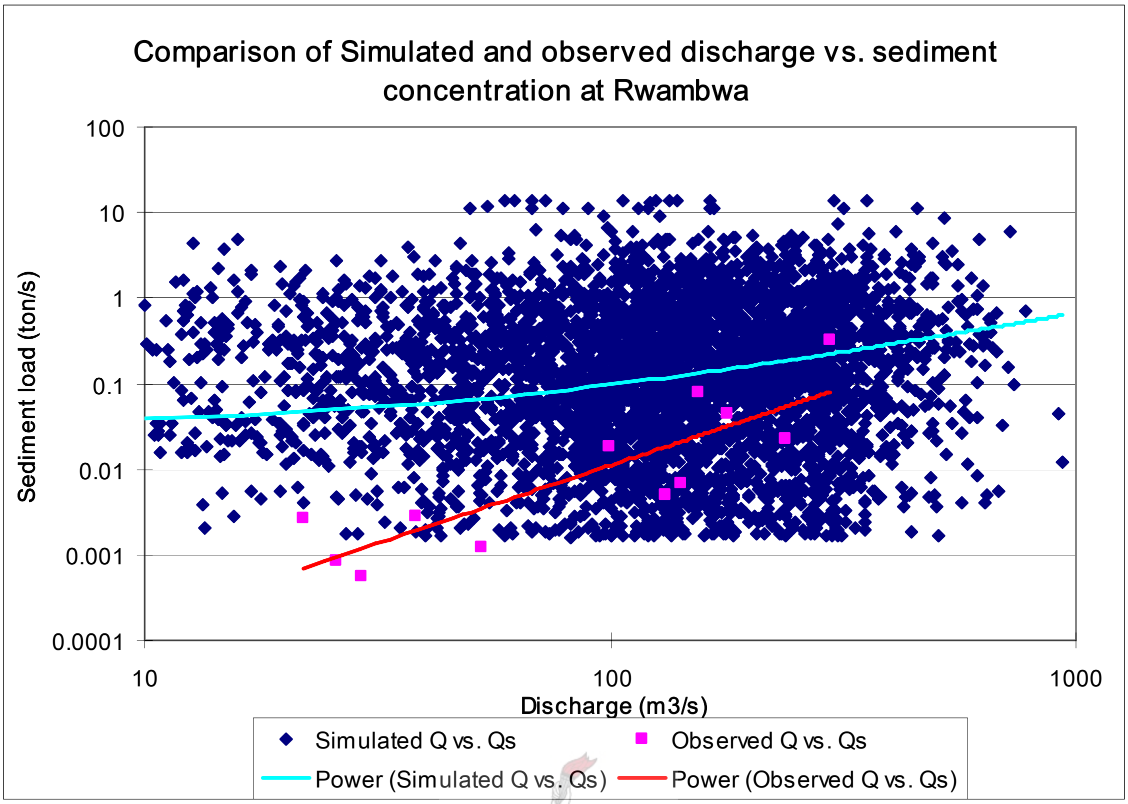

Figure 7-8 Comparison of Simulated and observed discharge vs. sediment concentration at Rwambwa

7.4 MODEL VERIFICATION

7.4.1 Nyando catchment model verification

The lack of data prevented any real verification of the calibration of the sediment yield and soil erosion. However there are two aspects of the sediment yield and soil erosion in Nyando catchment that could be verified. The ACRU model simulated that soil erosion potential reaches quite a high level in sub-catchment 9. The first aspect of verifying the soil erosion is to compare the simulated sediment yield in sub-catchment 9 with the result collected from other researchers who have worked in the same area. The other aspect is to use measured discharge and sediment yield relationships to verify the sediment yield in specific sub-catchments.

a) During the period of March 1999 to 2000, a case-control, designed to assess the prevalence and impacts of soil degradation problems, was undertaken (Walsh, Shepherd, 2000). The method evaluated the extent and locations of high active sediment sources using a combination of Landsite TM satellite imagery, ground survey, etc. The study clearly indicated the soil erosion risk area in Nyando catchment (Figure 7-6). A further study also shows the high soil erosion risk area. The hotspots have been highlighted in red in Figure 7-7. This result is quite similar to the ACRU model simulated result where the sub-catchment 9 in the Nyando catchment is a high soil erosion area (Figure 7-8).

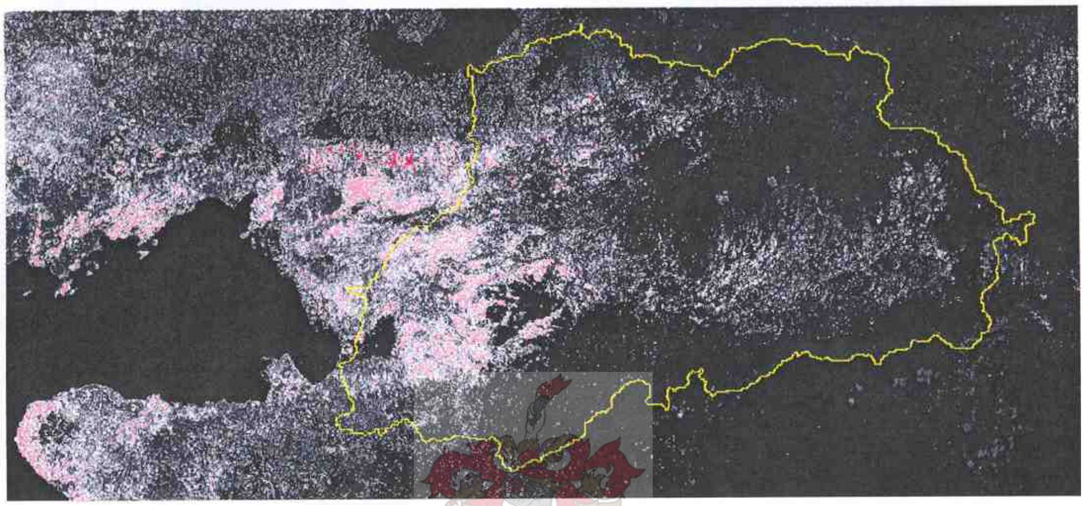

Figure 7-9 Image processed to reveal areas with elevated phosphorus erosion risk in the Nyando catchment (Shepherd & Walsh), 2000)

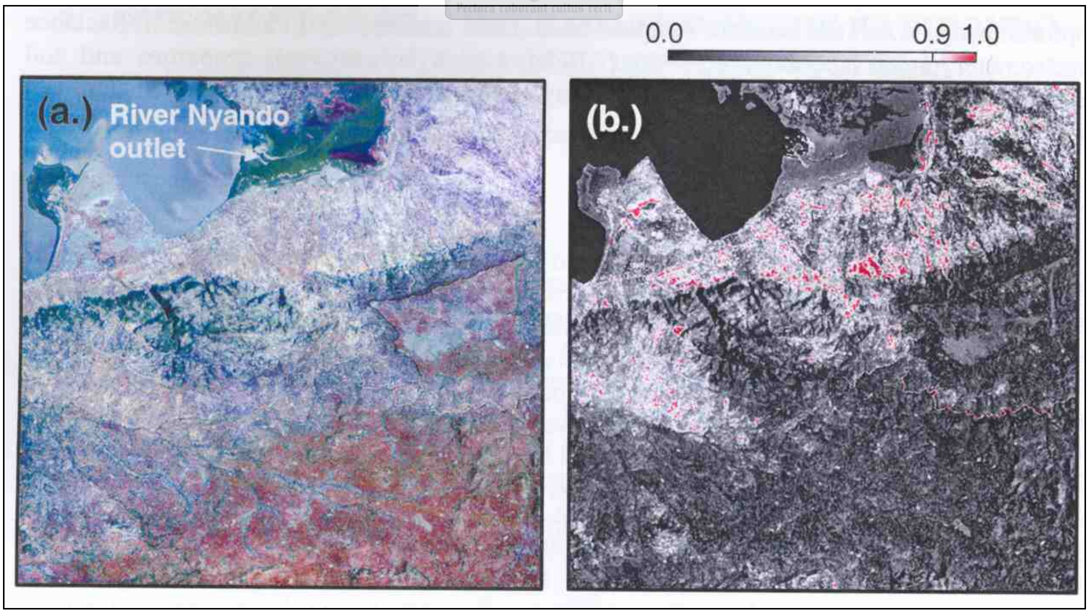

Figure 7-10 Prevalence of severely accelerated soil erosion in the Nyakach Bay area of Lake Victoria (Shepherd & Walsh, 2000)

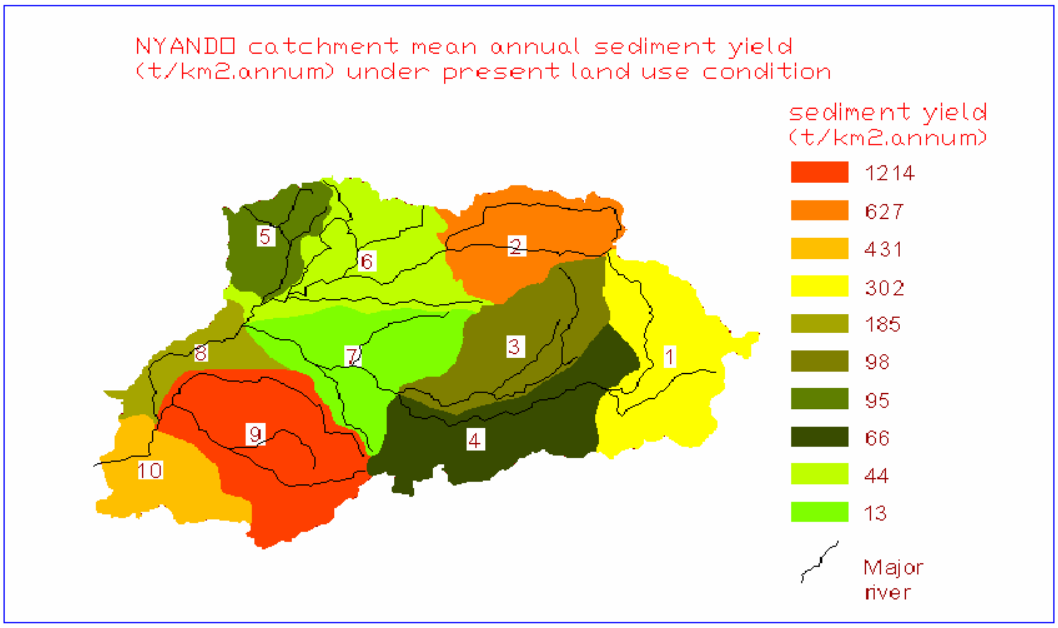

Figure 7-11 Nyando catchment simulated sediment yields under current conditions

b) A gauging station is available in the field that measures the sediment load from the tributary of the Nyando River, which is located at Muhoroni (Figure 7-12). Figure 7-13 indicates that simulated values are higher than observed values but mainly at small flows, which is a similar result as for Ahero Gauge.

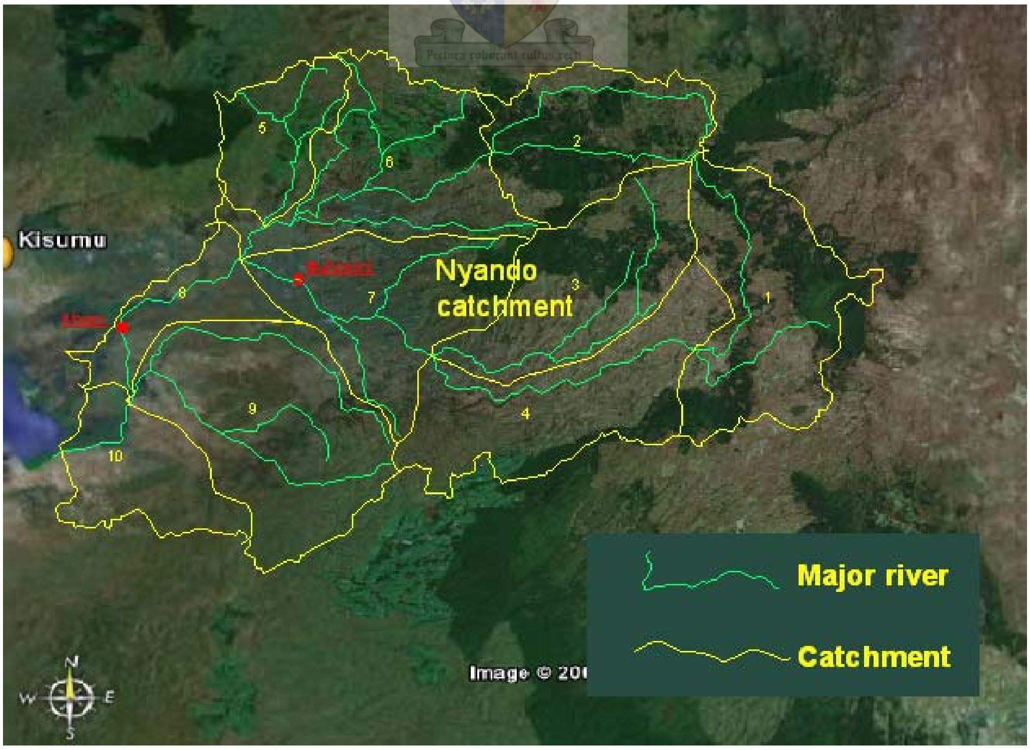

Figure 7-12 Sediment load survey points in Nyando catchment

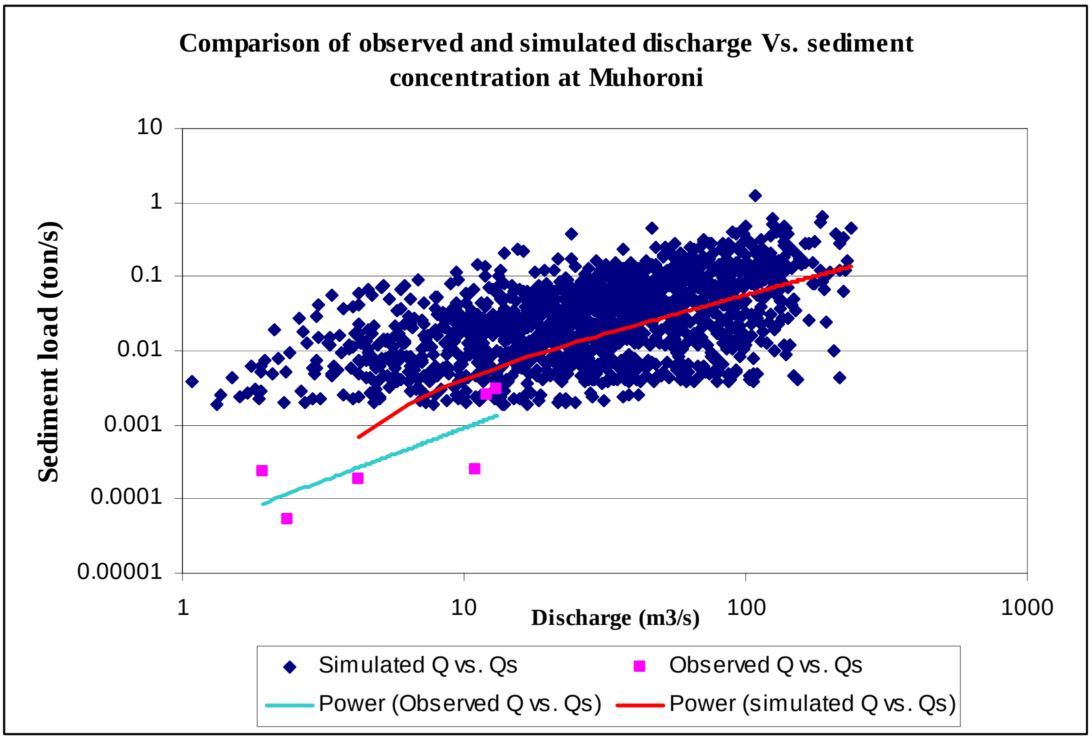

Figure 7-13 Comparison of observed and simulated discharge vs. sediment load at Muhoroni

7.4.2 Nzoia catchment model verification

No similar data/information was found to verify the Nzoia catchment results, and only Rwambwa gauging station was available along the Nzoia River and was used for model calibration.

7.5 DISCUSSION OF RESULTS

The ACRU model sediment yield module calibration basically could be approached in two ways : to check the soil erodibility characteristics and to adjust the land cover factors. The accuracy of sediment yield module simulation largely depends on the accuracy of the flow model. Many factors which affect both the flow model and the sediment module should first be adjusted in the flow model to achieve accurate streamflow, such as cover factors which are determined by land use as has already been confirmed in the flow model simulation.

The accuracy of the sediment yield simulation also depends on the level of available information. There are different methods which could be used to estimate soil erodibility factors as well as cover factors. However, these specific methods can only be used with particular data. Since these data were not available, the sediment yield module had to use simpler methods to estimated soil erodibility and cover factors.

The soil erodibility factor played an important role during the sediment yield calibration. It successfully reduced the simulated sediment yield from a large difference to an acceptable range (Table 7-7). The cumulative graphs of simulated sediment yields for Nyando catchment and Nzoia catchment are shown in Figure 7-14 and Figure 7-15. After verifying the calibrated model by comparing it with satellite imagery and observed data, the model could be used for different scenario simulations.

Table 7-7 Result of sediment yield module calibration

<table>
<tr><th colspan="2">Catchment</th><th>Unit</th><th>Nyando</th><th>Nzoia</th></tr>
<tr><td colspan="2">Measured sediment yield</td><td>t/km^2.a</td><td>346</td><td>230</td></tr>
<tr><td rowspan="4">Simulated sediment yield</td><td>Before calibration</td><td>t/km^2.a</td><td>395</td><td>752</td></tr>
<tr><td>Initial difference with measured data</td><td>%</td><td>14.2</td><td>226.1</td></tr>
<tr><td>After calibration</td><td>t/km^2.a</td><td>350</td><td>249</td></tr>
<tr><td>Final difference with measured data</td><td>%</td><td>1.2</td><td>8.3</td></tr>
</table>

Figure 7-14 and 7-15 show cumulative sediment load (simulated) versus cumulative runoff volumes which indicate linear relationship, especially in the case of the Nyando catchment. Although the scatters in the calibration graphs are high (Figure 7-5 and 7-8), the cumulative graphs provide more confidence in the results, given the limited field data.

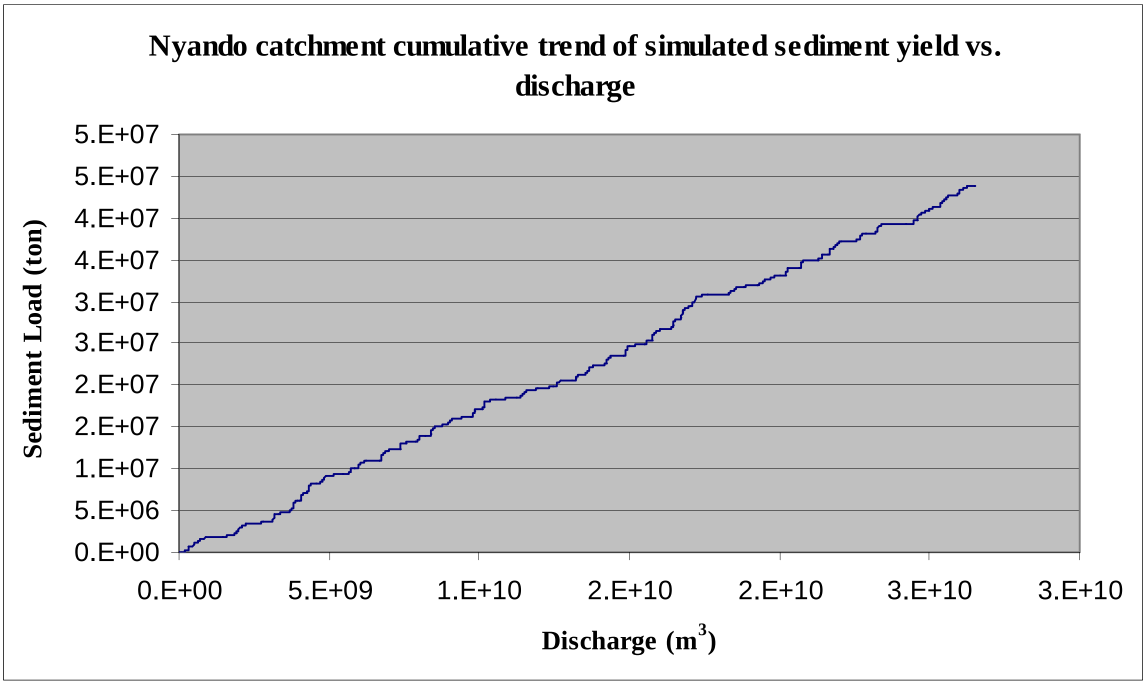

Figure 7-14 Nyando catchment cumulative simulated sediment load vs. cumulative runoff volume

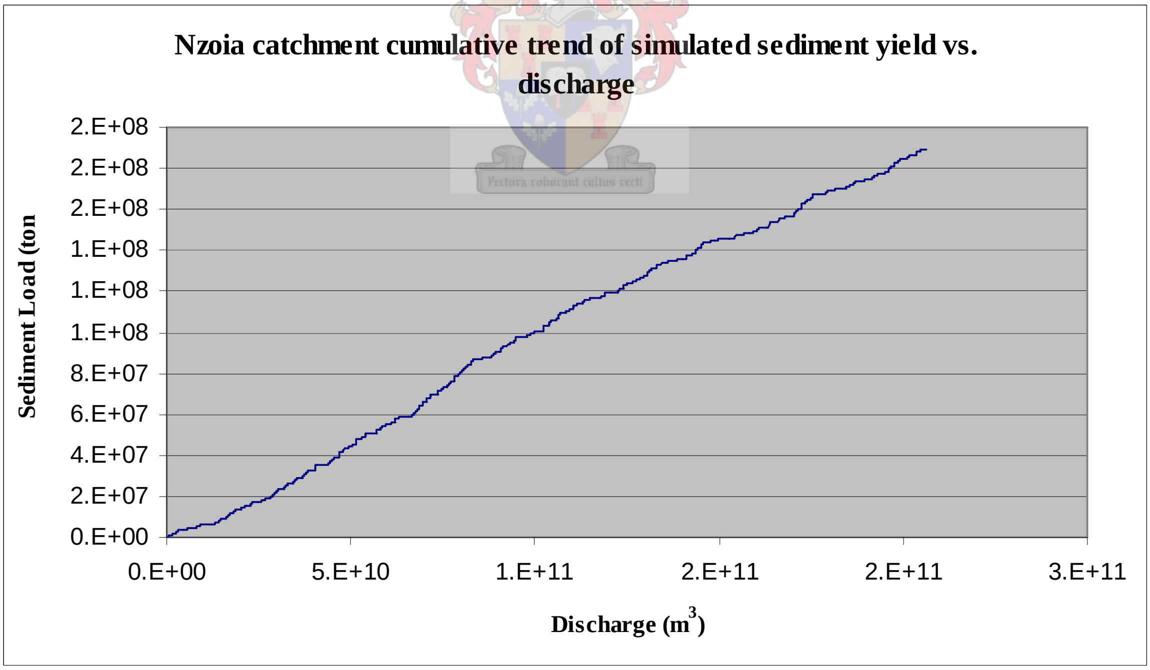

Figure 7-15 Nzoia catchment cumulative simulated sediment load vs. cumulative runoff volume

CHAPTER 8 SCENARIO ANALYSIS

8.1 INTRODUCTION

Several research projects have studied the severe soil erosion and land degradation problems throughout the Nyando and Nzoia River basins (Swallow, 2000). Accelerated run off sheet erosion over much of the Nyando catchment area has led to severe rill, gully and stream bank erosion in the lower parts of the river basin. The principal causes of erosion include deforestation of headwaters and overuse of extensive areas of fragile lands on both hillslopes and plains, coupled with loss of watershed filtering functions through encroachment on wetlands and loss of riverine vegetation. Associated with soil erosion, there has been substantial depletion of soil quality over much of the basin.

A regional assessment identified the Nyando River Basin and Nzoia River Basin as major source of sediment flow into Lake Victoria from Kenya. Sediment and nutrient transport and mixing undoubtedly influence the water quality and ecology of Lake Victoria.

For effective catchment management and land care programs, it is important to model catchment soil erosion processes. In this chapter different scenarios are examined in order to determine the model's ability to predict the outcome of different situations that would be important in a soil erosion-sediment yield control program. The scenarios for the Nyando catchment and the Nzoia Catchment are presented separately.

8.2 NYANDO RIVER

8.2.1 Current condition scenario simulation

The Nyando catchment is shown in Figure 8-1, with sub-catchment 9 known for severs gully erosion.

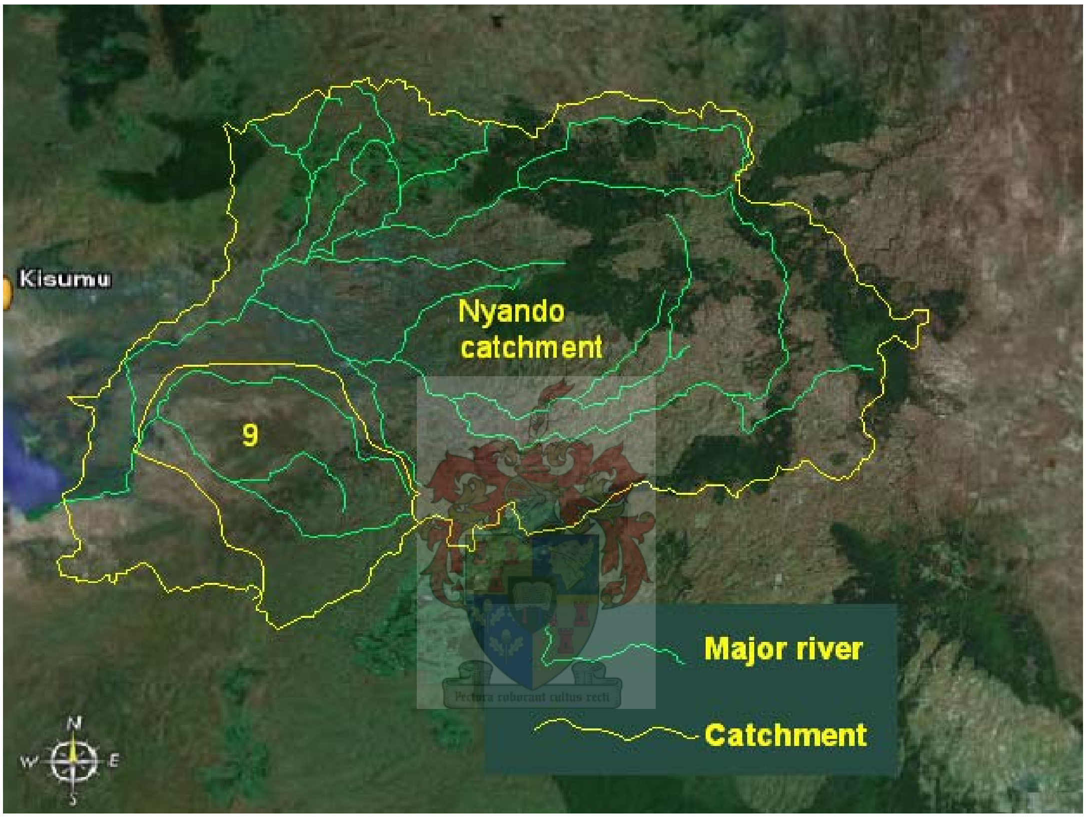

Figure 8-1 Nyando catchment satellite image

The current land uses are shown in Figure 8-2 (note natural forests were included in the calculations but not shown in the Figure), with catchment rainfall given in Figure 8-3.

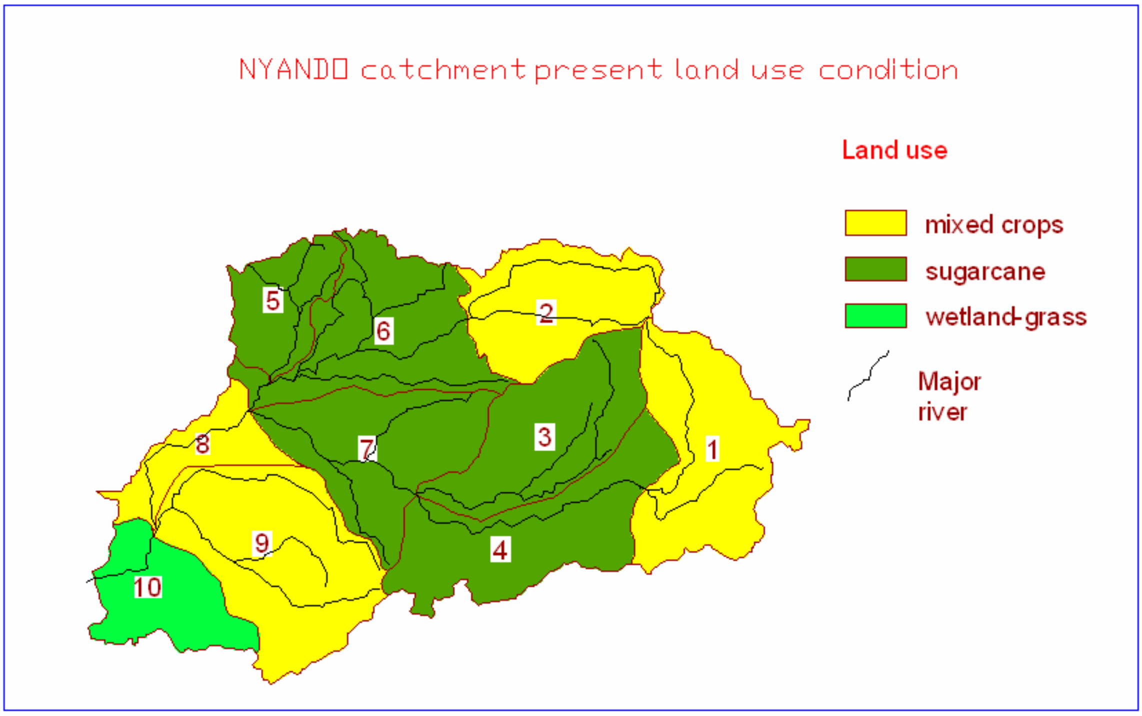

Figure 8-2 Nyando catchment current land use (natural forests not shown)

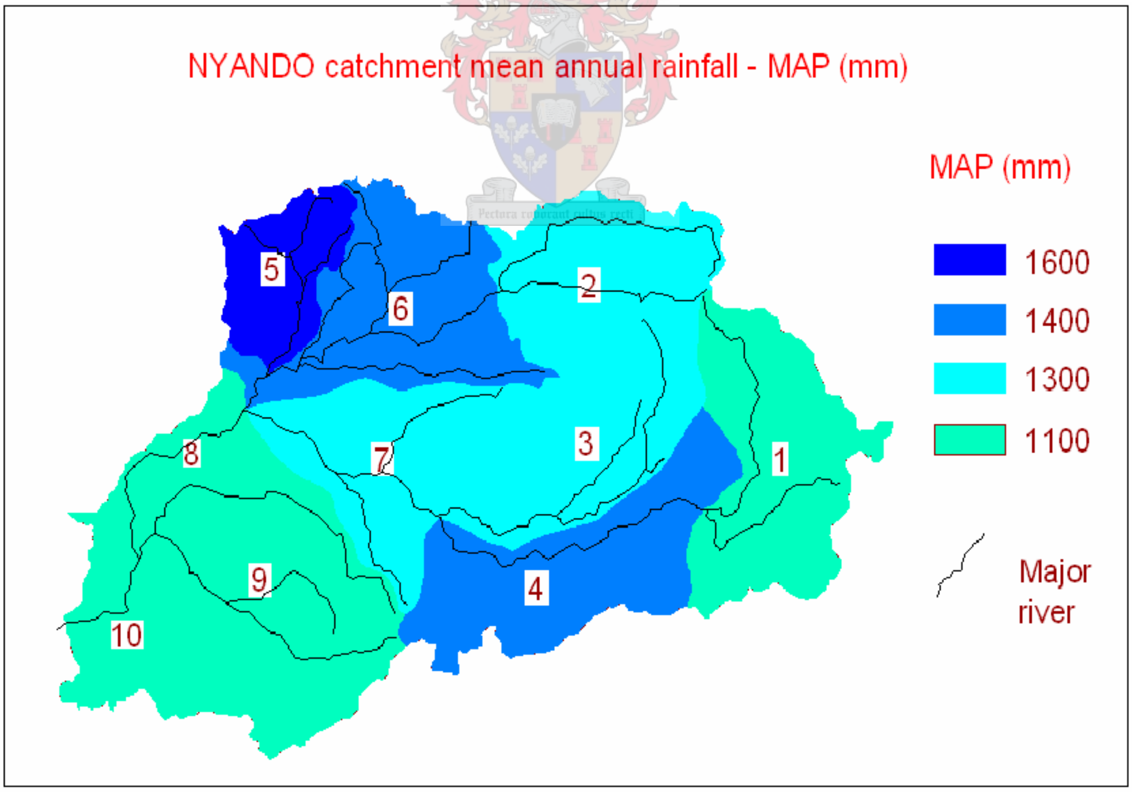

Pectora roborant cultus recti

Figure 8-3 Nyando River catchment rainfall

The current land use conditions were first simulated to identify a holistic situation of the catchment as well as the several situations of each sub-catchment. The results are given in Table 8-1 and 8-2. Figure 8-4 gives the sub-catchment sediment yields that were simulated. At least four sub-catchments (viz. sub-catchments 1, 2, 9 and 10) have relatively high sediment yields (Figure 8-5). Sub-catchments 1, 2, 9 and 10 are relatively steep leading to relatively high sediments yield, which is aggravated with degradation in sub-catchment 8 and 10. A satellite image of sub-catchment 9 shows the gully area with severe degradation where the simulated sediment yield is extremely high (Figures 8-6). The simulation indicated that more than half of the sediment loads are from this area (52.9% of total sediment load). The sediment loads are shown in Figure 8-7, while Figure 8-8 shows clearly that most of the sediment load is generated during April and May.

Table 8-1 Nyando sub-catchment current sediment yield

Sub-catchment		**A1**	**A2**	**A3**	**A4**	**A5**	**A6**	**A7**	**A8**	**A9**	**A10**	**Total**
Area	**km^2**	460.4	348.1	394.6	444.0	193.8	445.8	406.1	162.5	557.8	241.7	3654.7
Sediment yield	**$t/km^2.a$**	302	627	98	66	95	44	13	185	1214	431	350
Sediment load	**t/a**	139122	218281	38568	29129	18342	19658	5276	30050	676967	104073	1279363
Percentage of total sediment load	**%**	10.9	17.1	3.0	2.3	1.4	1.5	0.4	2.3	52.9	8.1	100

Table 8-2 Nyando catchment current monthly sediment yield distribution

		Apr	**May**	**Jun**	**Jul**	**Aug**	**Sep**	**Oct**	**Nov**	**Dec**	**Jan**	**Feb**	**Mar**	**Total**
Monthly sediment yield	**$t/km^2.m$**	1845	1071	166	77	153	51	77	158	39	55	94	419	350
Monthly rainfall (adjusted by ACRU)	**mm**	260	234	106	93	119	79	75	78	30	38	47	107	1259

Pectora roborant cultus recti

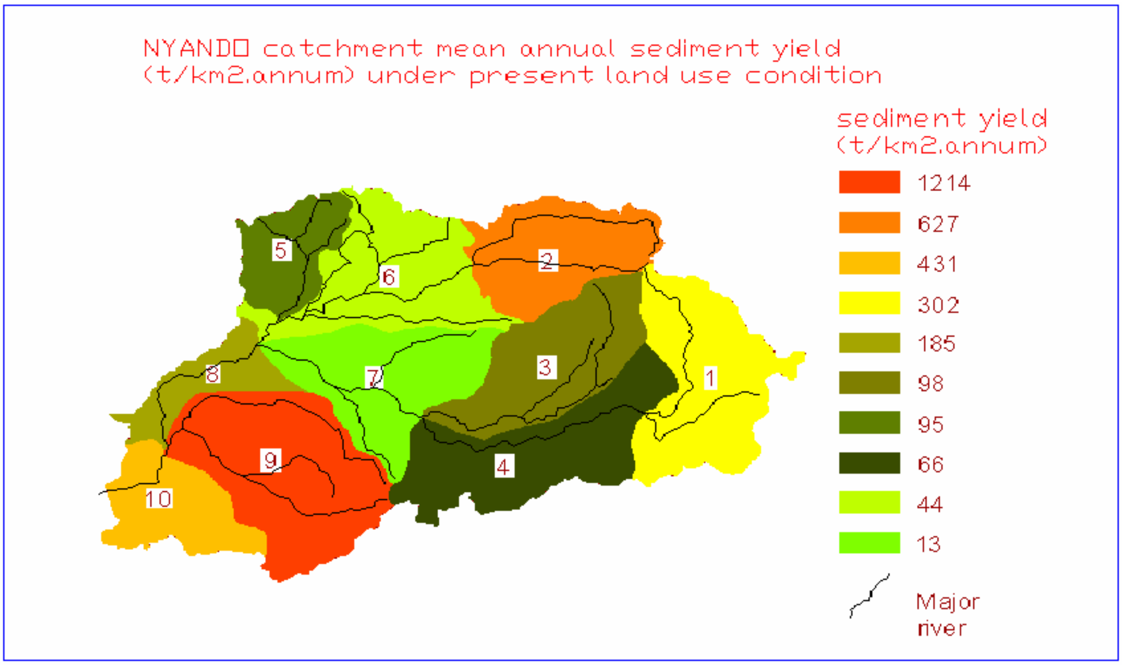

Figure 8-4 Nyando catchment sediment yields under current condition

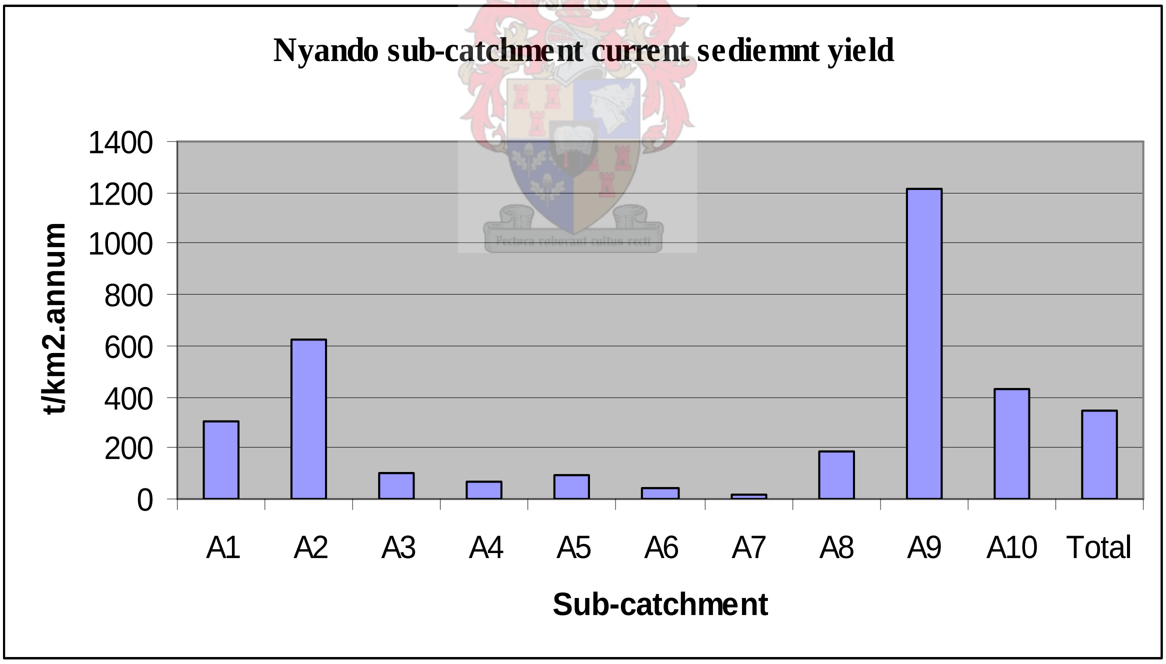

Figure 8-5 Nyando sub-catchment sediment yields

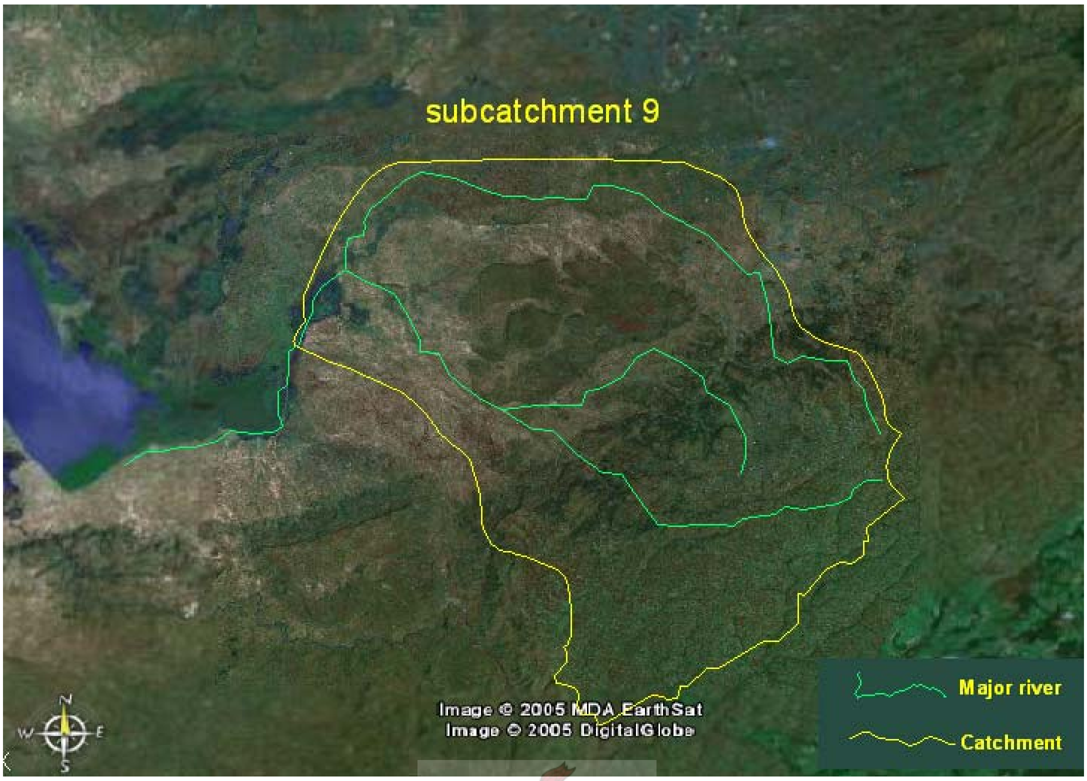

Figure 8-6 Nyando sub-catchment 9 – gully erosion area

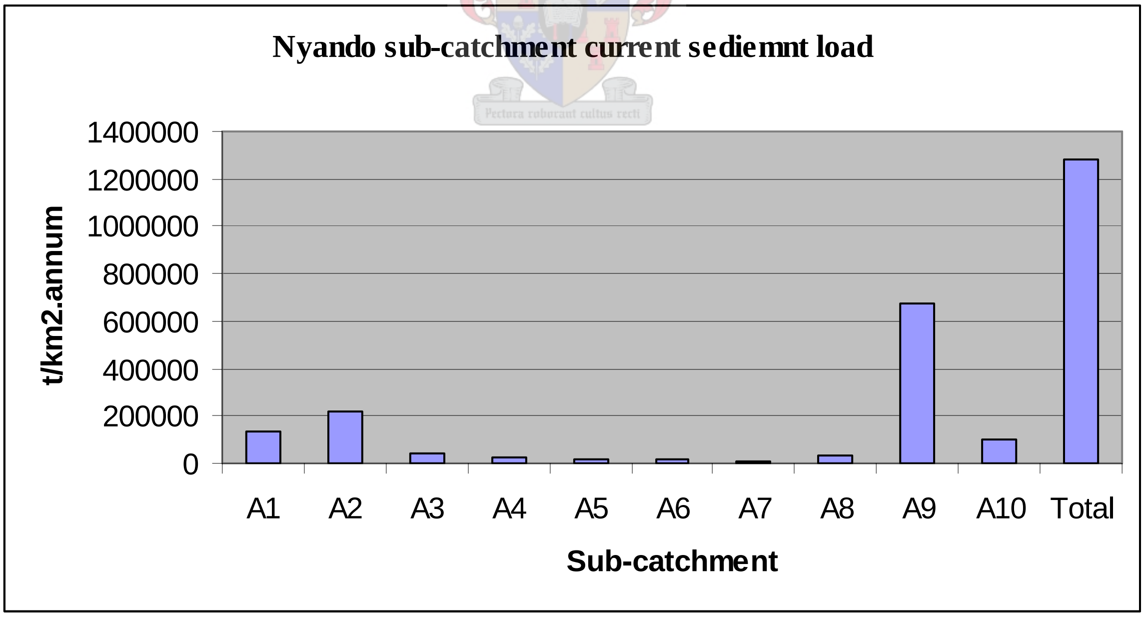

Figure 8-7 Nyando sub-catchment sediment loads

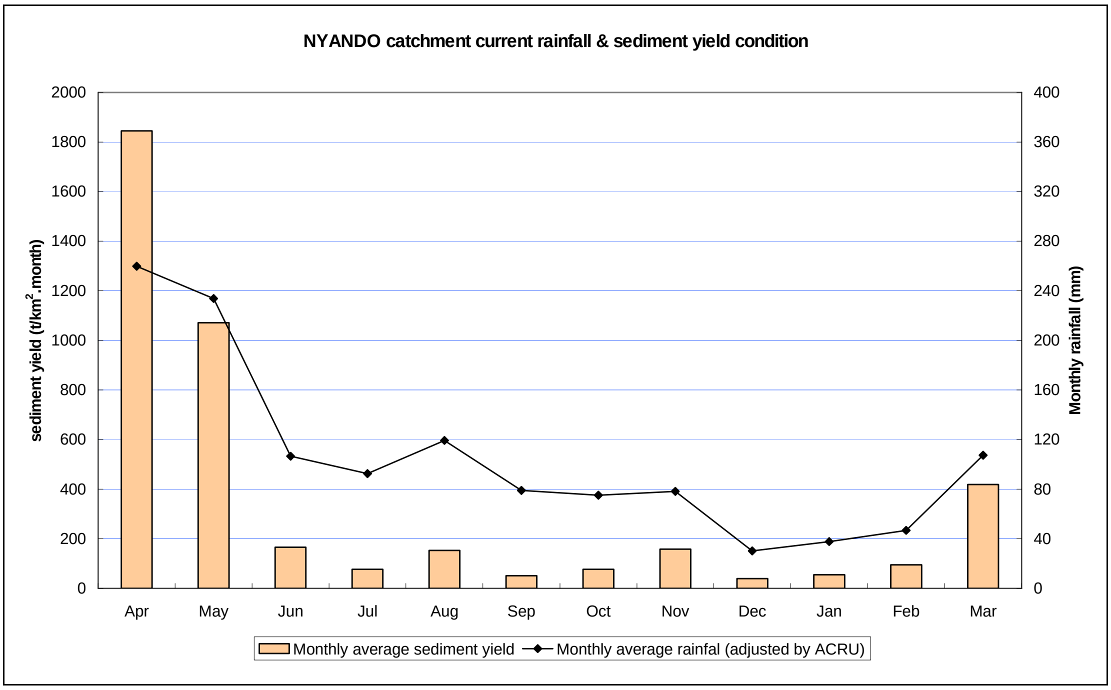

Figure 8-8 Nyando catchment simulated monthly sediment yields

8.2.2 Rehabilitation/land use change scenarios

The simulation done for the Nyando Catchment's current condition clearly shows that sub-catchment 9 is the main cause of the high sediment yield. Most of the soil erosion occurs in it. The following rehabilitation or land use change scenarios were considered:

- Scenario 1: Nyando with riparian vegetation restored* and sub-catchments 8 and 9 irrigated mixed crops (subsistence farming currently) (Figures 8-9 and 8-10).
- Scenario 2: Nyando with sub-catchment 9 land use changed to 100 % grassland (Figures 8-11 and 8-12).
- Scenario 3: Nyando with sub-catchment 9 land use changed to 50 % grassland (Figures 8-13 and 8-14). The other 50% land use is mixed crop.
- Scenario 4: Nyando with sub-catchments 8 and 9 irrigated sugarcane (Figures 8-15 and 8-16).

Note *: the riparian areas 20m from the river banks were calculated and in the model it was specified as forest.

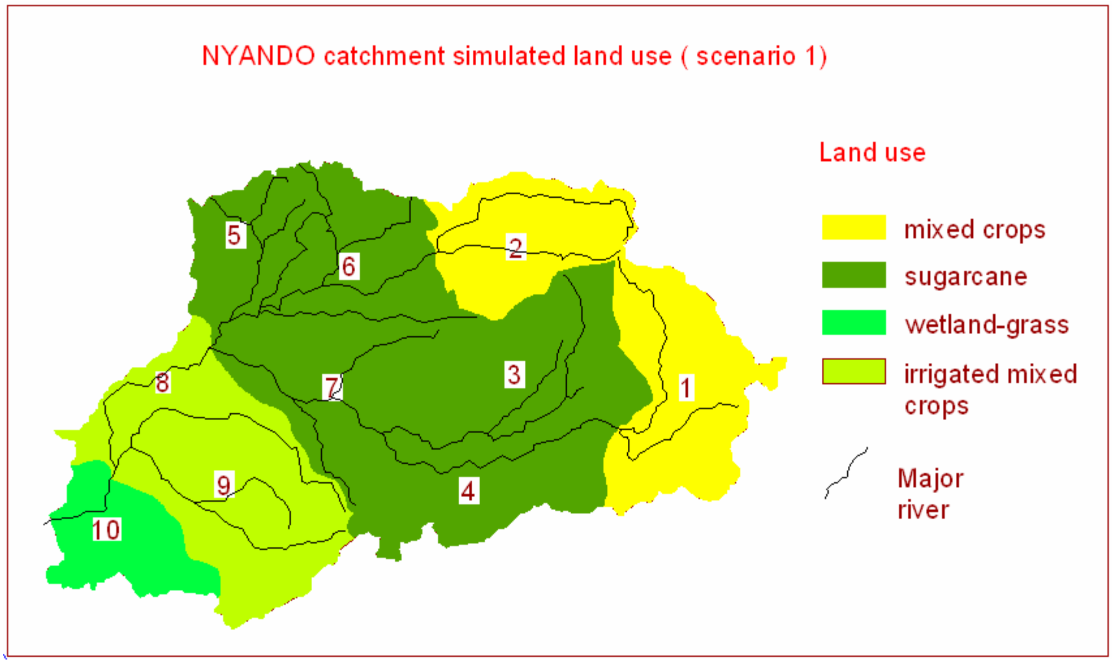

Figure 8-9 Nyando with riparian vegetation restored & sub-catchments 8 & 9 irrigated

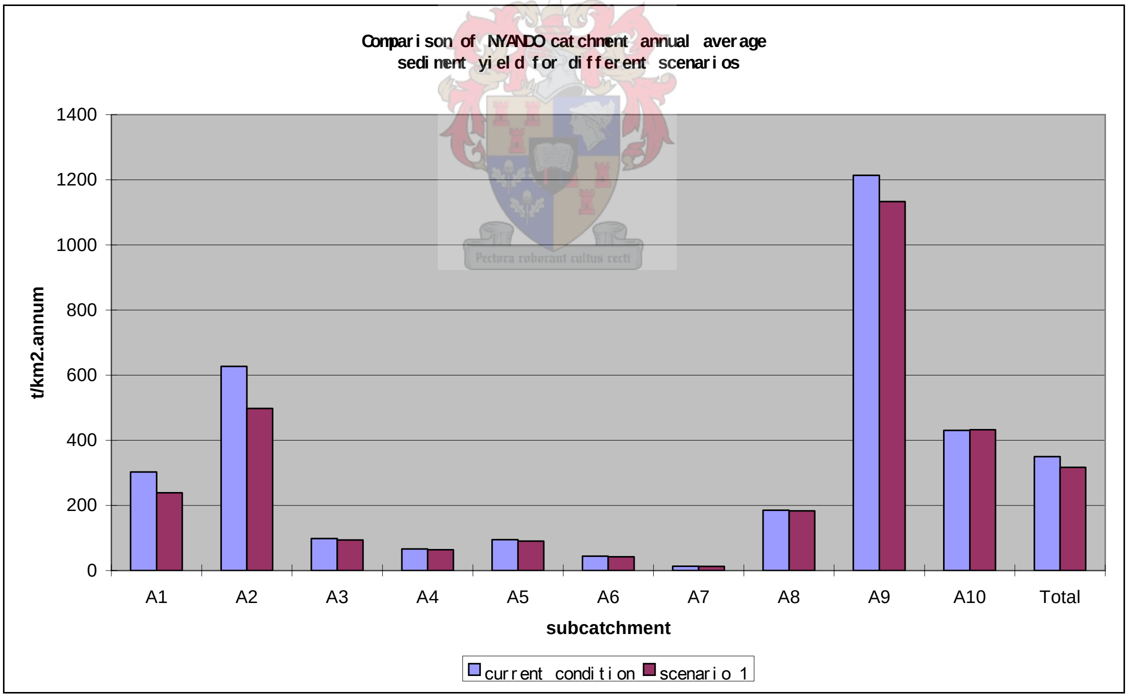

Figure 8-10 Nyando with riparian vegetation restored & sub-catchments 8 & 9 irrigated

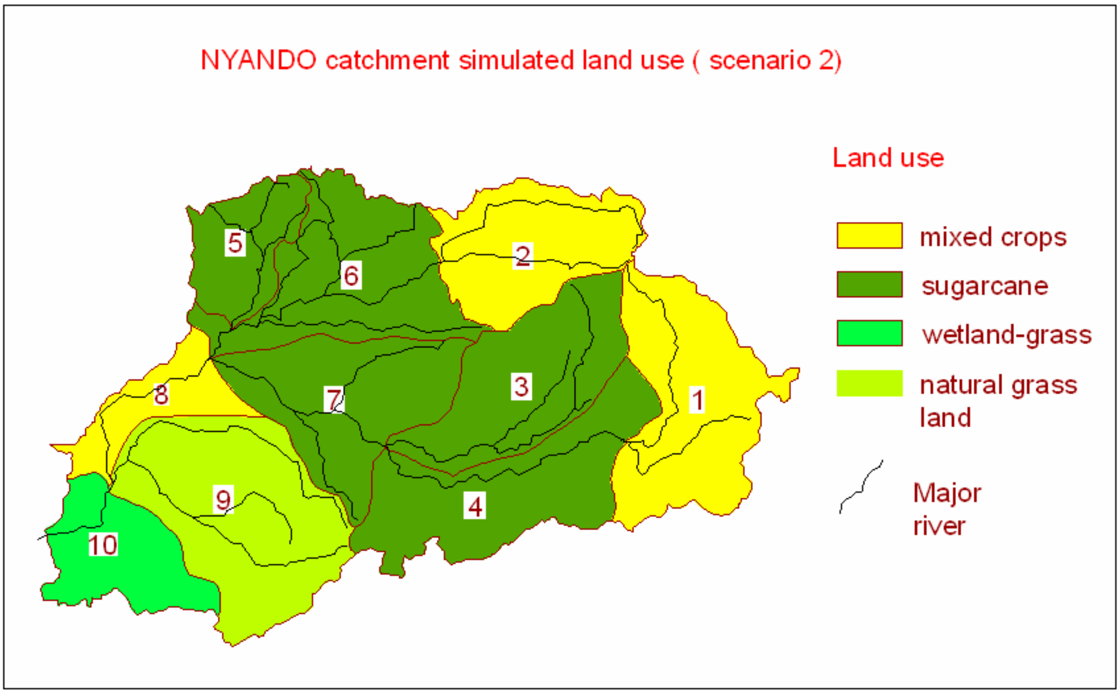

Figure 8-11 Nyando with sub-catchment 9 land use changed to 100% grassland

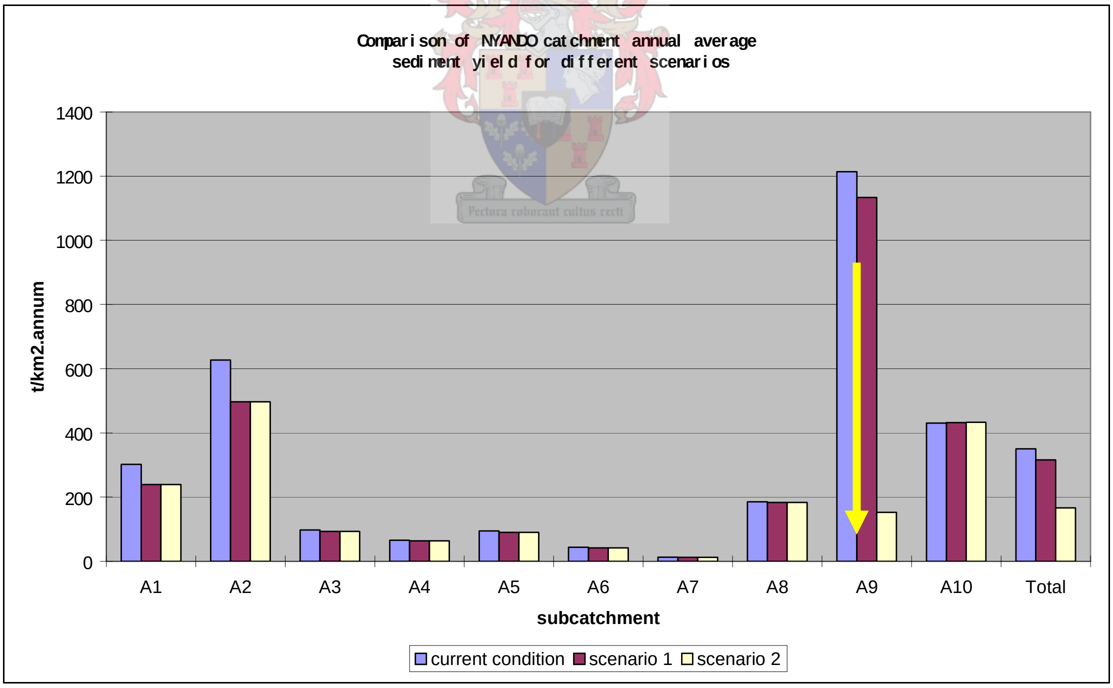

Figure 8-12 Nyando with sub-catchment 9 land use changed to 100% grassland

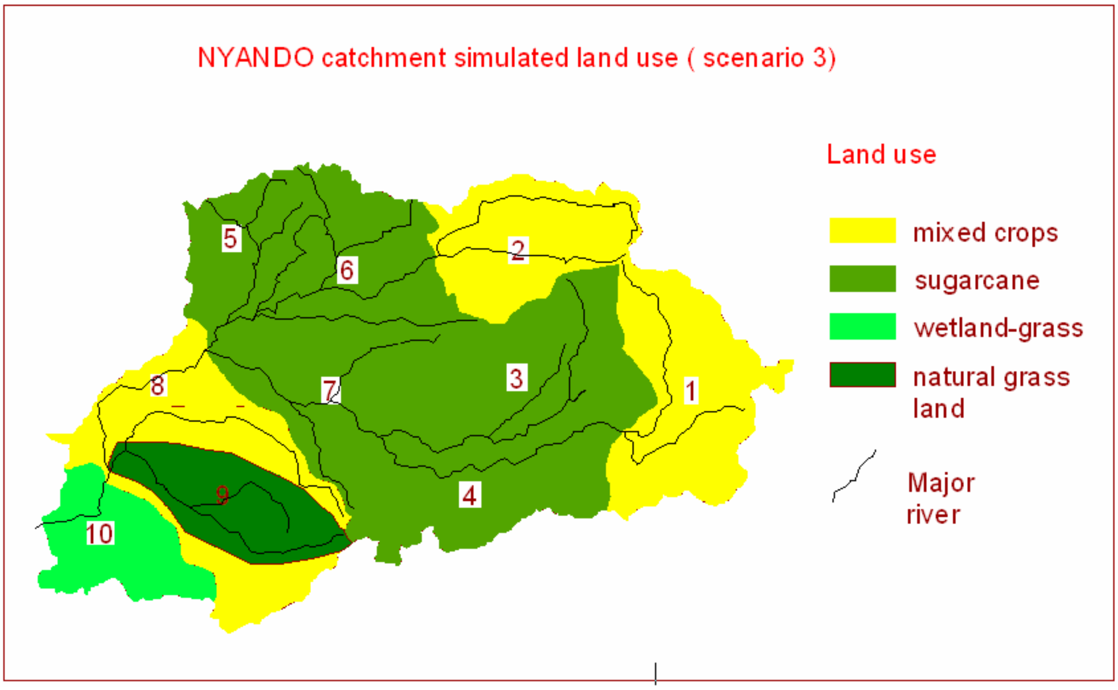

Figure 8-13 Nyando with sub-catchment 9 land use change to 50% grassland

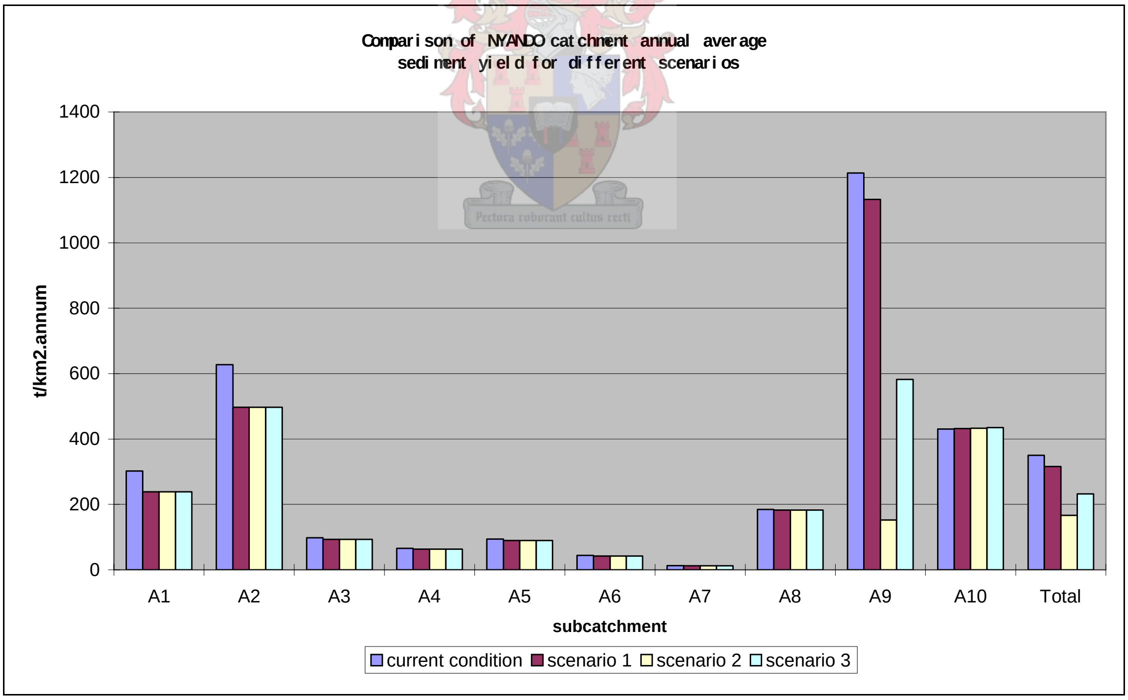

Figure 8-14 Nyando with sub-catchment 9 land use change to 50% grassland

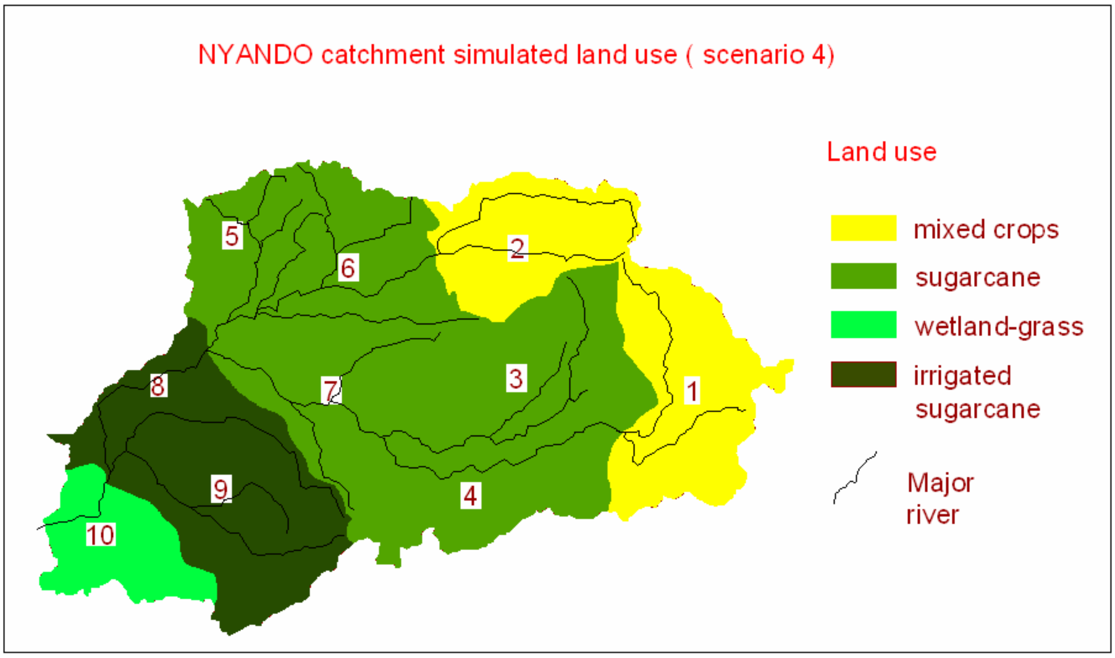

Figure 8-15 Nyando with sub-catchments 8 & 9 irrigated sugarcane

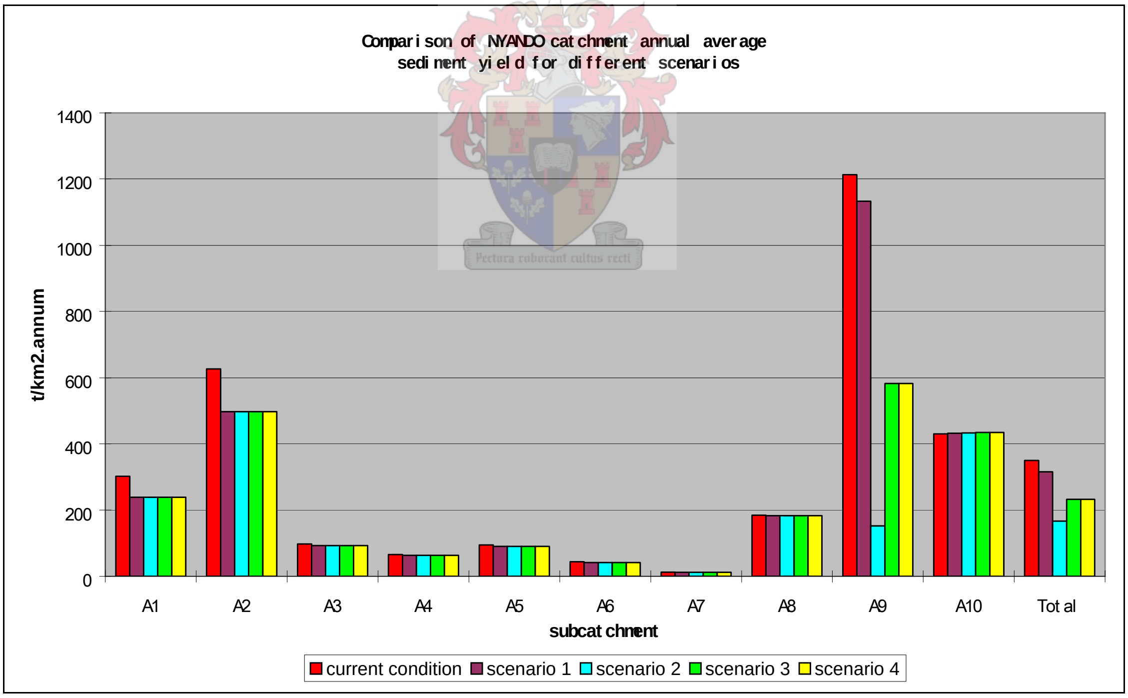

Figure 8-16 Nyando with sub-catchments 8 & 9 irrigated sugarcane

8.2.3 Discussion of the results

The scenarios were aimed at reducing the stream bank erosion and gully erosion risk. The simulated results are shown in Table 8-3 and show that revegetation by grassland could have a major impact on decreasing the sediment yield (scenario 2). The result also indicates that sub-catchment 9 is in a state of serious soil loss and excessive land development. The natural vegetation was grassland before subsistence farming started in the region.

Table 8-3 Result of scenario simulations

Sub-catchment	Unit	A1	A2	A3	A4	A5	A6	A7	A8	A9	A10	Total	Percentage decrease
Area	**km^2**	460	348	395	444	194	446	406	163	558	242	3655	
current condition	**t/km^2.a**	302	627	98	66	95	44	13	185	1214	*431	350	**%**
scenario 1	**t/km^2.a**	239	497	93	64	90	42	12	183	1133	432	316	9.7
*** scenario 2**	**t/km^2.a**	239	497	93	64	90	42	12	183	153	433	167	52.4
scenario 3	**t/km^2.a**	239	497	93	64	90	42	12	183	*583	435	232	33.6
scenario 4	**t/km^2.a**	239	497	93	64	90	42	12	183	*583	435	232	33.6

Note *: the option of Scenario 2 is sub-catchment 9 land use changed to 100 % grassland, which results in the greatest change compared with other options. Grassland seems to be the best way to reduce the soil erosion risks.

*: in sub-catchment 9, the scenario 3 and 4 had same simulated result, which means the 100% irrigated sugarcane has the same effect as 50% grassland for the sediment yield.

*: in sub-catchment 10, the simulated scenario results were slightly bigger than current condition, but the reason is unknown.

8.3 NZOIA RIVER

8.3.1 Current condition scenario simulation

The Nzoia River catchment was divided into 26 sub-catchments for the ACRU modelling (Figure 8-17). The catchment rainfall is shown in Figure 8-18.

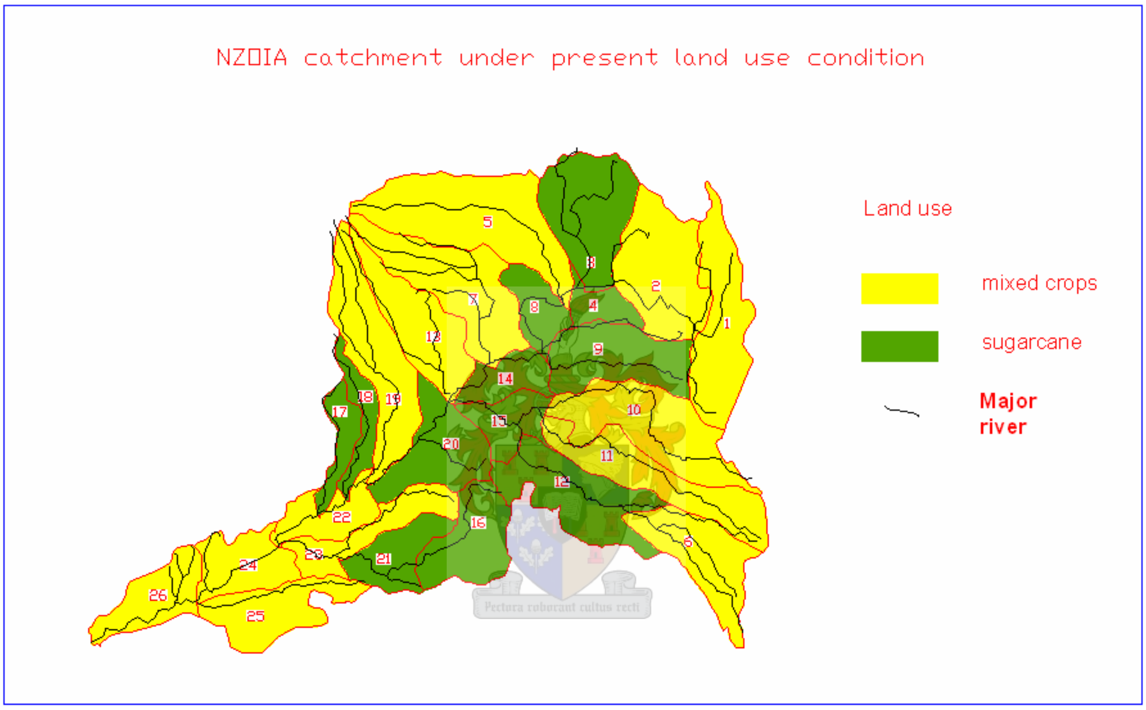

Figure 8-17 Nzoia River catchment current land use (natural forests not shown)

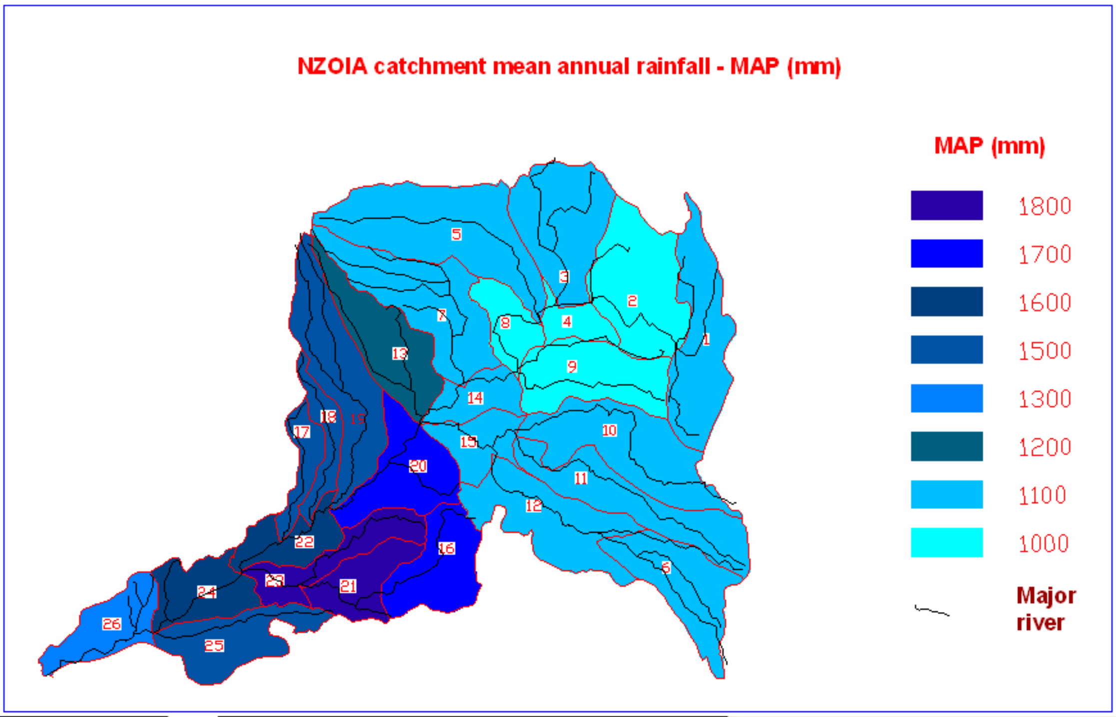

Figure 8-18 Nzoia River annual rainfall

The Catchment current condition simulation results are given in Table 8-4 and 8-5, the simulated sub-catchment sediment yields are shown in Figure 8-19. In eleven of the sub-catchments the sediment yields are higher than the average values: sub-catchment 1, 6, 12, 14, 15, 16, 18, 19, 20, 21 and 23 (Figure 8-20). Figure 8-21 shows clearly that most of the sediment loads are generated in the rainy season.

Table 8-4 Nzoia catchment sediment yield

Sub-catchment	Area	Sediment yield	Sub-catchment	Area	Sediment yield
	km^2	t/km^2.a		km^2	t/km^2.a
A1	711	318	**A14**	258	260
A2	780	79	**A15**	290	354
A3	727	169	**A16**	505	343
A4	178	146	**A17**	204	218
A5	1078	111	**A18**	222	416
A6	570	376	**A19**	770	647
A7	804	48	**A20**	556	340
A8	267	136	**A21**	351	540
A9	613	134	**A22**	311	197
A10	820	198	**A23**	395	283
A11	670	139	**A24**	402	93
A12	714	665	**A25**	509	148
A13	589	216	**A26**	397	9
			Total	13691	251

Table 8-5 Nzoia catchment monthly sediment yields

Description	Unit	Apr	May	Jun	Jul	Aug	Sep	Oct	Nov	Dec	Jan	Feb	Mar	Total
Monthly sediment yield	t/km^2.m	734	426	263	436	429	55	490	40	2	2	5	109	249
Monthly rainfall (adjusted by ACRU)	mm	285	256	151	191	211	88	153	71	17	17	22	98	1559

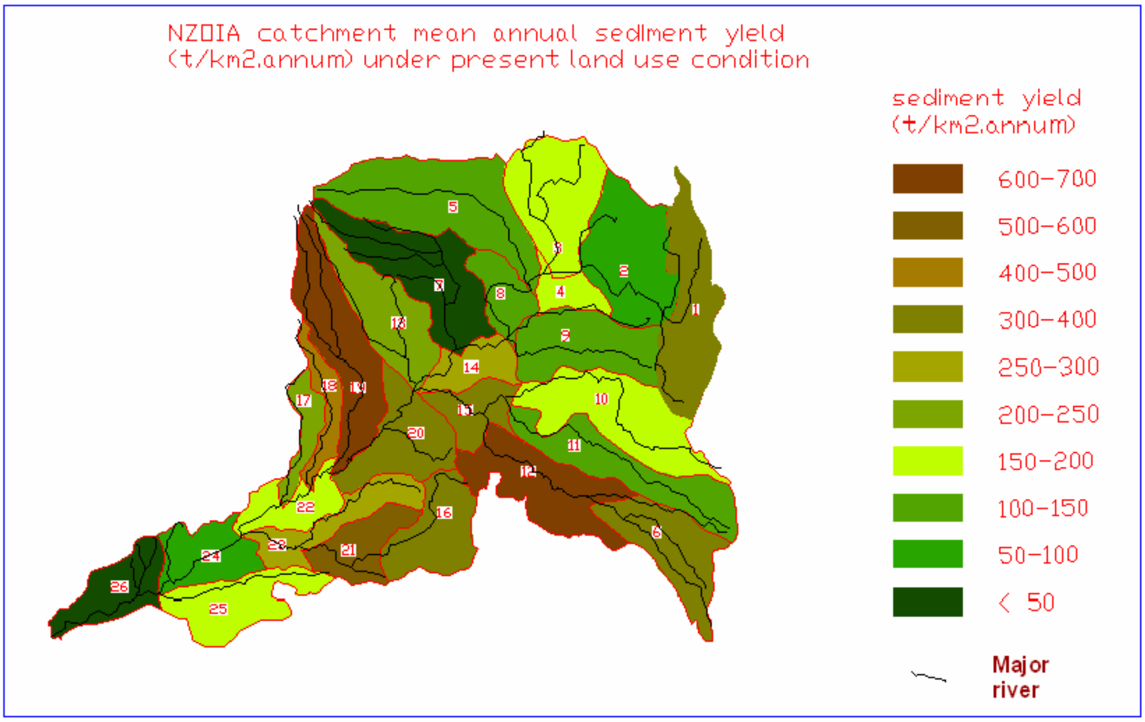

Figure 8-19 Nzoia simulated sub-catchment sediment yield

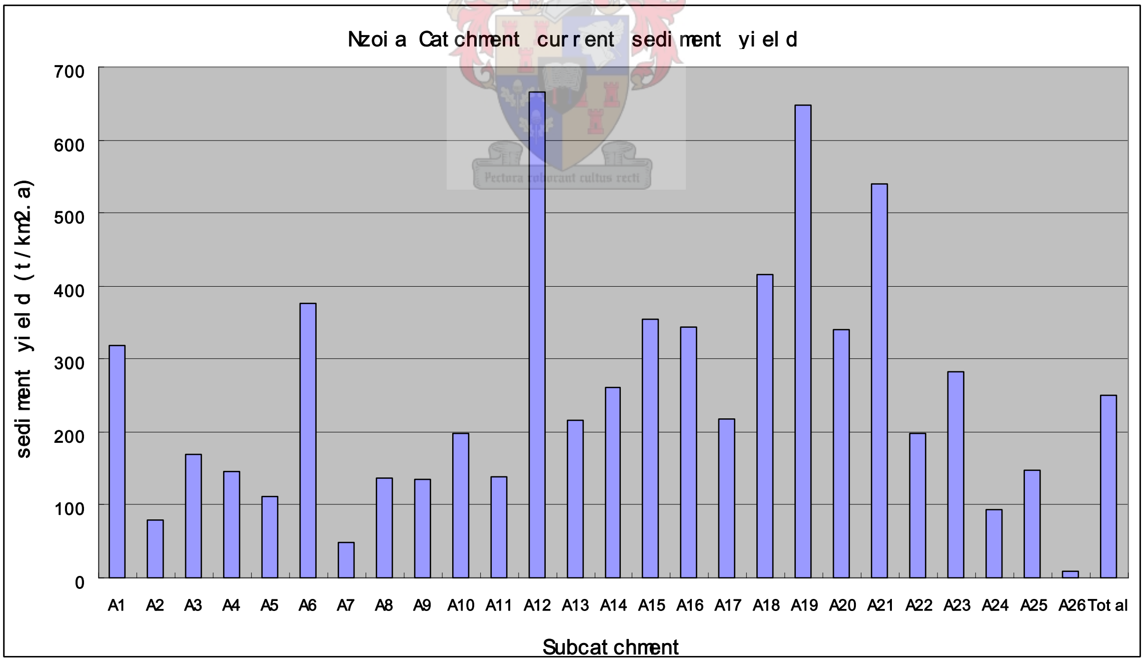

Figure 8-20 Nzoia catchment sediment yield – under current condition land use

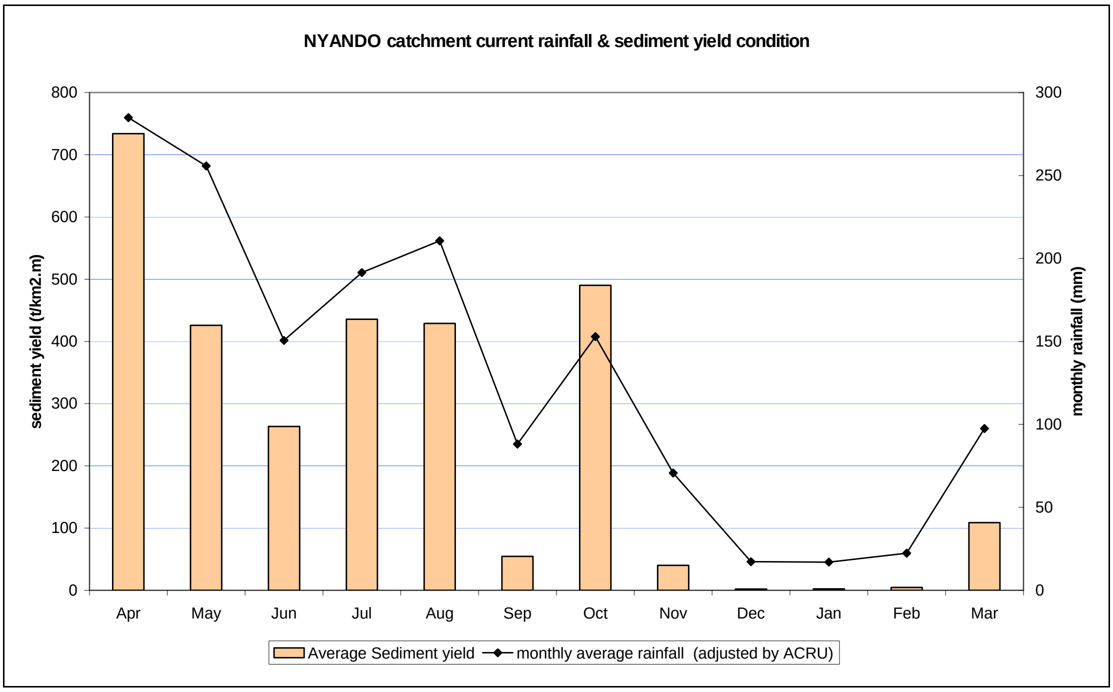

Figure 8-21 Nzoia catchment simulated monthly sediment yield

8.3.2 Rehabilitation/land use change scenarios

Two scenarios were investigated to reduce the catchment sediment yield. In scenario 1 eleven sub-catchments where current sediment yields are greater than the catchment average were replanted with grassland, while in scenario 2 only 50 % of the areas were replanted with grass (Figures 8-23 and 8-24). The simulation results are shown in Figures 8-25 and 8-26.

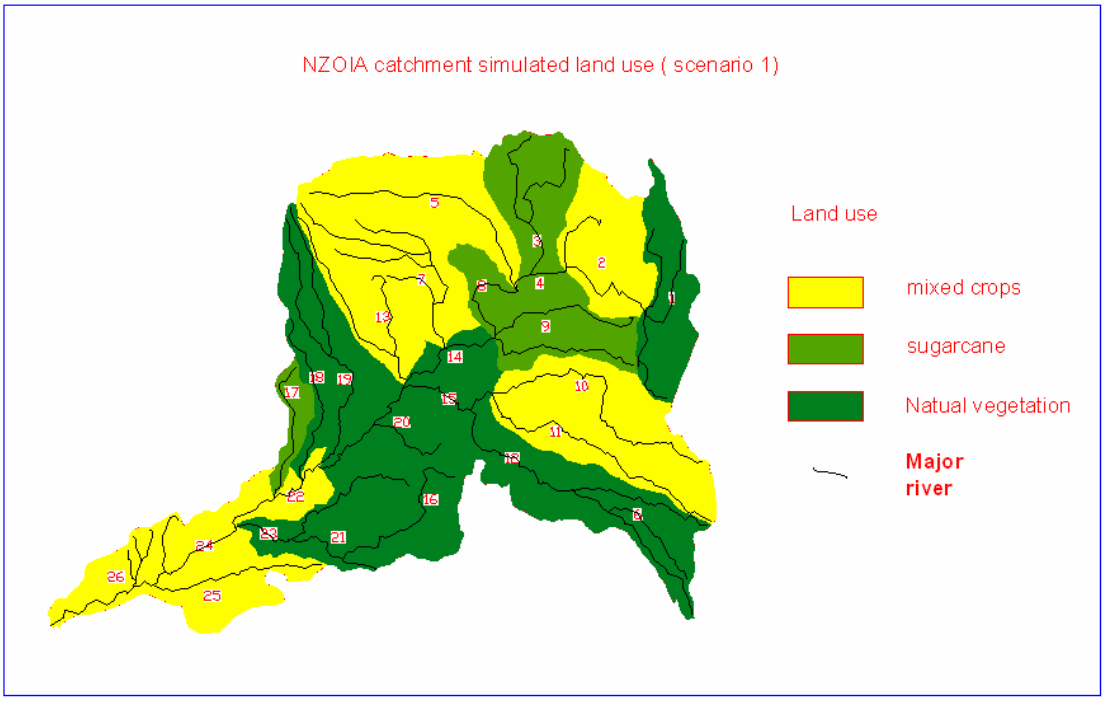

Figure 8-22 Nzoia catchment land use (scenario 1)

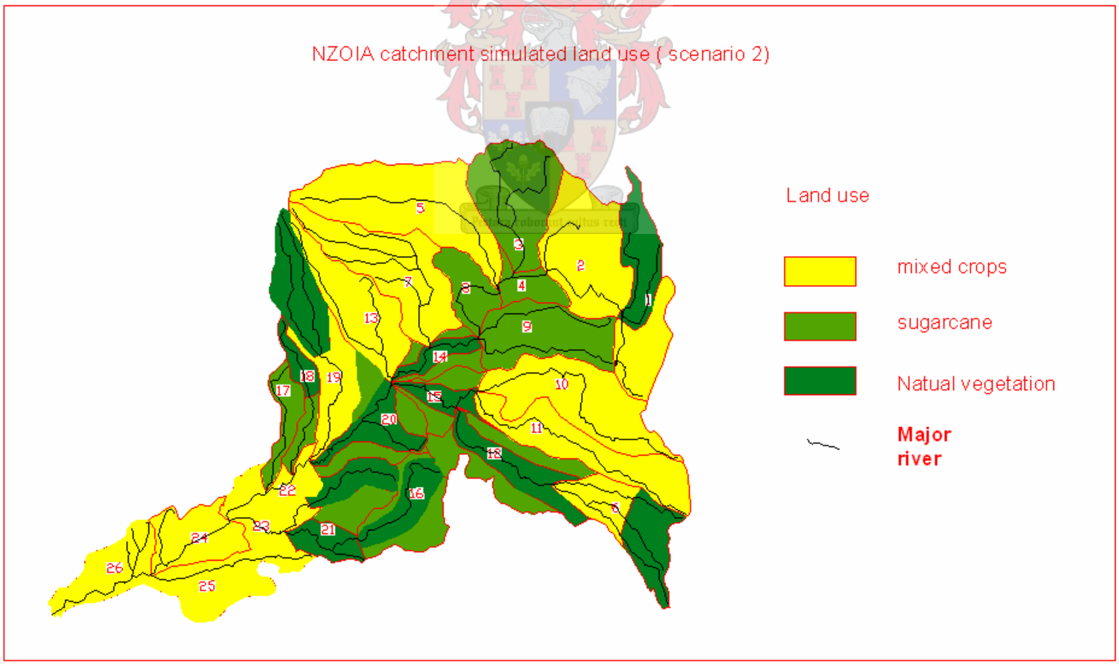

Figure 8-23 Nzoia catchment land use (scenario 2)

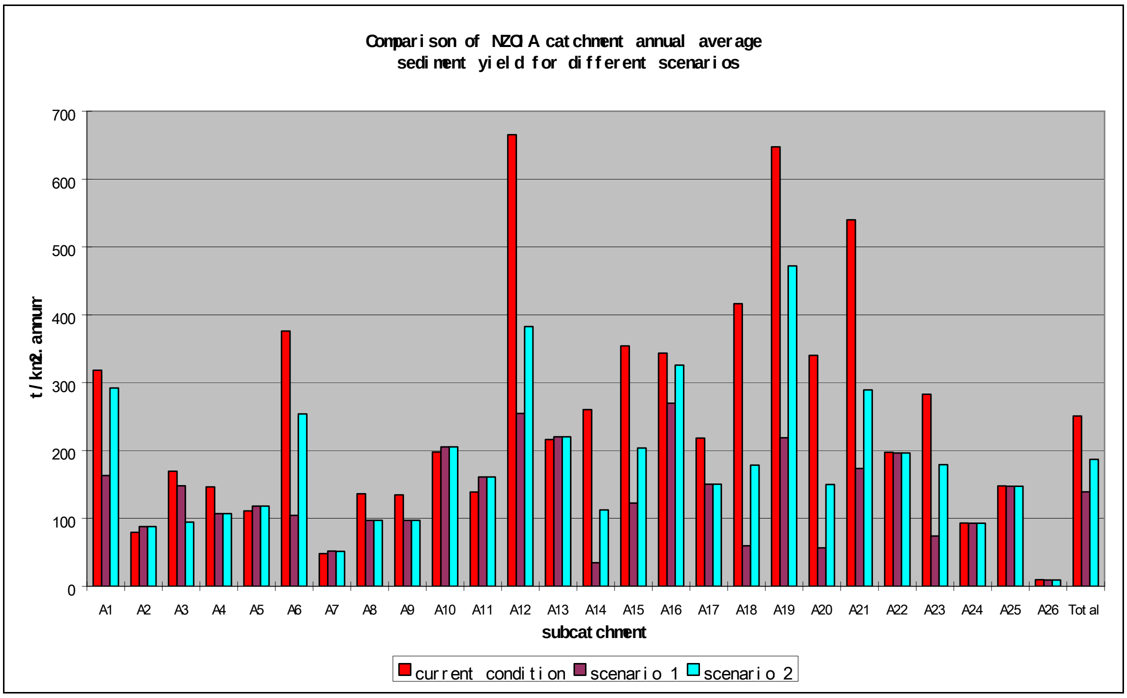

Figure 8-24 Nzoia simulated sediment yields

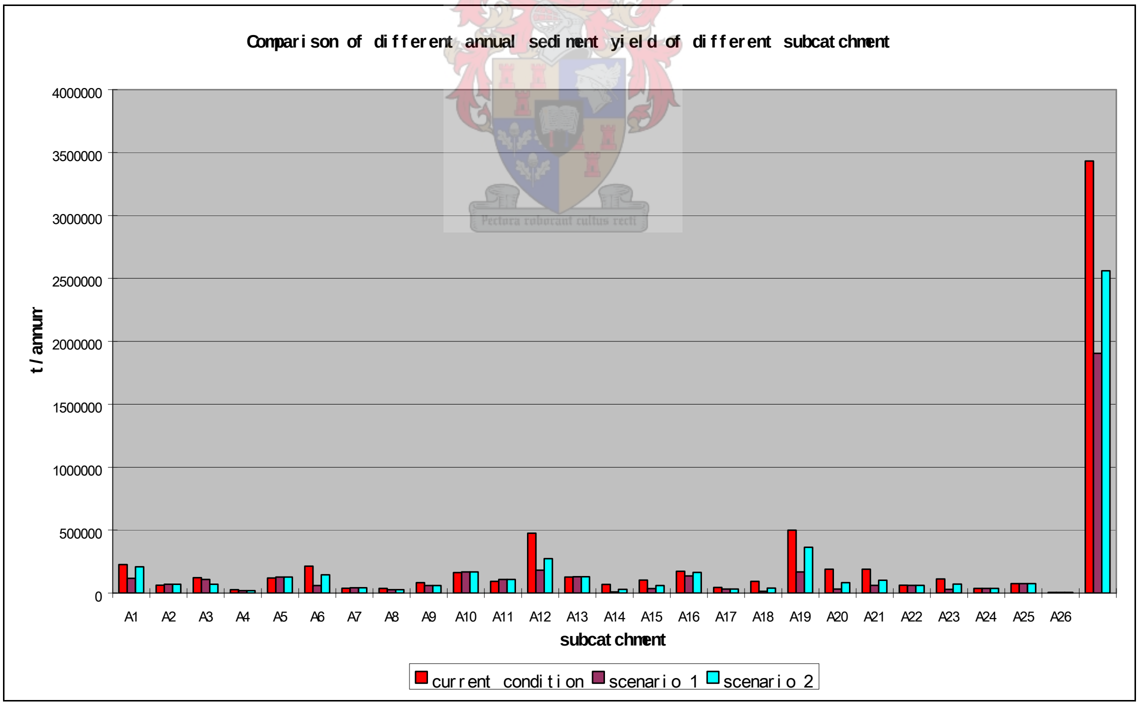

Figure 8-25 Nzoia simulated sub-catchment sediment loads

8.3.3 Discussion of the results of scenarios

The simulated results of the two scenarios are summarized in Table 9-6. The results indicate that rehabilitation with grass could make a major difference to the current sediment yield.

Table 8-6 Simulation result of scenarios of Nzoia catchment

Sediment yield	**current condition**	t/km^2.a	251	**Percentage decrease**
	scenario 1	t/km^2.a	139	44.5 %
	scenario 2	t/km^2.a	187	25.4 %
Sediment load	**current condition**	t/a	3433532	**Percentage decrease**
	scenario 1	t/a	1904131	44.5 %
	scenario 2	t/a	2560588	25.4 %

8.4 DISCUSSION OF SCENARIO RESULTS

Firstly, according to the results of the sediment yield simulations, it is obvious that land use changes in critical sub-catchments could significantly reduce the sediment yield. Grassland is very effective, whereas irrigated sugarcane may also be considered. Maybe too much emphasis is currently placed on agroforestry as the main land use mechanism, as the natural vegetation (grassland) could be much more effective.

Secondly, river bank erosion protection through riparian vegetation is also important, but in certain high stream power zones, dumped rock should also be considered.

CHAPTER 9 CONCLUSIONS AND RECOMMENDATIONS

9.1 CONCLUSIONS

As soil erosion is becoming an increasing and world wide problem, the development of a water soil erosion model is useful for controlling and managing the existing and future water and land resources. Since the early days of developing computer models, they have become necessary tools to simulate solutions to different types of problems in water soil erosion. The key objective of this study was to assess the applicability of the ACRU agrohydrological modelling system for sediment yield prediction in large catchments under conditions of limited data availability.

The Nyando River catchment (3655 km^2) and the Nzoia River catchment (13691 km^2) along the Victoria Lake, Kenya were selected for analysis. These two catchments are major flow sources of Lake Victoria from the Kenya side, and also major sources of sediment flow into Lake Victoria.

9.1.1 Flow calculations

The ACRU model has been designed as a multi-level model with either multiple options or alternative pathways available in many of its routines. The flow calculation largely depends on available input data, such as catchment rainfall, soil types, and climate information. The Nyando catchment contains three rainfall stations with daily rainfall records from 1950 to 2004, and so does the Nzoia catchment. The daily rainfall in ten sub-catchments of Nyando and twenty six sub-catchments of Nzoia had to be calculated by using Equation 5.1. Since soil types were not available for the model, default values which are specified for southern Africa, had to be used. The factors of land use cover were estimated in different ways for the two study catchments: the Nyando catchment was roughly divided into five land use zones varying with altitude, while the Nzoia catchment has more complicated land uses patterns which were derived from large scale (1:250 000) topographic maps. The MAE is only about 750mm per year, which is much less than the MAP. Evaporation adjustment factors were required in ACRU modeling, which were estimated by trial and error methods to achieve acceptable evaporation values.

9.1.2 Sediment yield calculation

Sediment yield calculation is one of the functions of the ACRU modeling system, which is based on the Modified Universal Soil Loss Equation (MUSLE). The MUSLE converts different field situations to different single factors and multiples to forecast sediment yield. According to the available information of the study model, only two factors could be adjusted which were the soil erodibility factor and land cover factor. The accuracy of sediment yield calculations depends mainly on the accuracy of flow calculation, and therefore the cover factor had to use the same land cover as confirmed by the flow calculation. As with the factor estimation in the flow calculation, the calculations of soil erodibility and cover factor also have different estimation methods depending on the availability of the input data. Unfortunately, as both factors only had limited data available, the calculation had to choose the simplest of the methods. However, simulated areas with high sediment yield were successfully verified from previous studies: satellite images and field work, especially in Nyando catchment near the river mouth.

Pectora roborant cultus recti

9.1.3 Simulation Results

The accuracy of the results is mainly determined by the accuracy and availability of input data. Errors in the sediment yield simulation depend on various factors, such as the sub-catchment divide and the accuracy of the flow simulation etc. Comparing the un-calibrated sediment yield result with observed yield and with the calibrated yield (Table 9-1), it can clearly be seen that the soil erosion model is expected to overestimate yield before calibration. This is often the case since the MUSLE is fundamentally a soil erosion model, not a sediment yield model. In reality eroded sediment is deposited again in the catchment, making the sediment yield lower, especially in large catchments.

The sediment yield calibrations were verified against satellite images of degraded areas and observed sediment load data

Table 9-1 Comparison of un-calibrated yield with observed yield and calibrated yield

Sediment yield	Unit	Nyando	Nzoia
Observed	$t/km^2.a$	346	230
Before calibration	$t/km^2.a$	392	752
After calibration	$t/km^2.a$	350	249

The ACRU simulation of the current sediment yield showed that at least three sub-catchments had greater sediment yields than observed annual average levels in the Nyando catchment; sub-catchment 9 is in the worst condition of environmental degradation. Several scenarios have been investigated to reduce serious soil erosion and protect riparian habitats, such as possible land use rehabilitation with grassland and planting tree belts along the rivers. Sugar cane is also a good substitute to replace the current land use.

The Nzoia River has the highest discharge to Lake Victoria along Kenya's border. The soil erosion problem is also increasing on a daily basis, accompanied by increased human activities in the Nzoia catchment. The current condition simulation shows that there are 11 sub-catchments with higher than average sediment yields. Two scenarios were simulated to decrease the current sediment yield. The first was to plant a tree belt along the channel together with rehabilitated grassland in all 11 catchments. The second was merely to replant 50% of the 11 sub-catchments with grassland, preferably indigenous species. Both scenarios indicate that grassland planting is the best scheme to reduce soil erosion.

9.1.4 Limitations

a) Field visits can often give the modeler an idea of the hydrological responses of the various sub-catchments. The modeler can gain a direct impression on land cover, soil types and catchment development aspects which are not reflected in the traditional information source (Pike, 2003).

b) A great number of default values were used in this model study, which undeniably affect the accuracy of simulations. In addition, the topographic maps which were used for geographic information collection were published in the 1970's, while the real field situations have been greatly changed in the last 30 years, with the population of Kenya growing by four times in the last two decades. Many factors (e.g. land use, ground slope, etc) are obviously affected by human activities.

c) The sub-catchment plot also affects the accuracy of the simulation; the ACRU User Manual suggests that sub-catchment plots should be smaller than 50km^2. However, in this study model plotted sub-areas are much greater than this, especially in the Nzoia catchment, which has a 13691 km^2 study area, and is divided into only 26 sub-catchments, with the largest sub-area larger than 1000 km^2. This is due to data limitations, such as topographic map scale (1:250 000) which is not completely suitable and limited rainfall data.

d) Given all the constraints of poor catchment data, limited hydrological data, and large catchments, it is important that the sediment yield model should be calibrated against observed field data. Once this has been done, scenario analysis, to investigate possible land use changes, can be done with reliability.

Pectora roborant cultus recti

9.2 RECOMMENDATIONS

The following recommendations are made:

a) The ACRU model can be used for large catchments (area larger than 2000 km^2). However, good spatial data is required for model configuration. The ACRU model should not be used as a black box, especially under limited data conditions. For sediment simulations, MUSLE must be calibrated against observed data.

b) The mathematical model is a useful 'tool' that can simulate different land use scenarios, however, for a feasible scheme to be put into practice it must be considered with the local socio-economical and environmental situation (viz. population increase, knowledge on land resources potential, socio-economic level, natural resource, and government support, etc.).

c) The model should be applied on large catchments with good spatial data to evaluate the sub-catchment size requirements.

CHAPTER 10 REFERENCES

Basson, G.R. (2004), Review of state-of-the-art research on erosion and sediment dynamics from catchment to coast, University of Stellenbosch.

Basson, G.R. (2005), Pilot study on sedimentation and sediment characteristics on Nyando and Nzoia River mouths and Winam Gulf of Lake Victoria, Lake Victoria Environmental Management Project final report, University of Stellenbosch.

Collins, J. (2001), Soil erosion, University of Western Cape ENVIRO FACTS.

DeRoo, A.P.J. (1996), The LISEM project: An introduction, Hydrological Processes, 10, 1021-1025, http://www.alterra-research.nl/pls/portal30/docs/folder/erochinut/erochinut/Lisem.htm

Elliot.W.J., Foster.G.R., Elliot.A.V (1991), Soil erosion: processes, impacts and prediction. In Lal & Pierce Soil management for sustainability.

European Soil Erosion Model (EUROSEM), www.silsoe.cranfield.ac.uk, 2006

Ewen.J., Parkin.G., O'Connell.P.E. (2000), SHETRAN: Distributed River Basin Flow and Transport Modeling System, Hydrologic Engineering, Vol. 5, No. 3, pp. 250-258.

Field.L. (1997), Best Management Practices of Soil Erosion, Agricultural & Biological Engineering Department, Purdue University, West Lafayette, US.

Anthoni.J.F. (2000), Soil erosion and conservation. www.seafriends.orgnz/enviro/ soil / erosion.htm

Gorgens.A.H.M. (1983), Conceptual Modelling of the Rainfall-Runoff Process in Semi-Arid Catchments, Hydrological Research Unit, Rhodes University, Report No. 1/83, Grahamstown, South Africa

Grijsen.J.G. (1986), River Flow Simulation in Rive Flow Modelling and Forecasting (ed. D.A.Kraijenhoff and J.R.Moll), 241-272

Hansen.T.S., Walsh.M. (2000), Assessment of NSWCP activites in the Nyando Basin, Improved land management in the Lake Victoria basin, Linking land and lake, research and extension, final technical report startup phase, International center for research in agroforestry and Kenya ministry of agriculture and rural development, P69

Heezen, H. (1964) in Turekian, Karl, K. (1968): Oceans. Prentice-Hall, p25

Kienzle.S.W. and Lorentz.S.A. (1993), Production of a soil erodibility map and simulation of sediment yield in the Henley Dam catchment, Natal. - Proc. 6th S. Afr. Nat. Hydrol. Symp., Dept. of Agricultural Engineering., University of Natal, Pietermaritzburg, RSA, 7-8 September 1993, 565-574.

Morgan, R.P.C., Quinton, J.N., Smith, R.E., Govers, G., Poesen, J.W.A., Auerswald, K., Chisci, G., Torri, D. and Styczen, M.E. (1999), The European soil erosion model (EUROSEM): A dynamic approach for predicting sediment transport from fields and small catchments - Reply. Earth Surface Processes and Landforms, http://www.es.lancs.ac.uk/people/johnq/eurosem/EuroSEM%20-%20Home. htm, 2003

Nitsche.N.C. (2000), Assessment of a hydrodynamic water quality model, DUFLOW, for a winter rainfall river. Unpublished master thesis, University of Stellenbosch.

Nzoia River, www.en.wikipedia.org 2006

Olago.D. (2005), Climate and Hydrological and Extremes in Lake Victoria Basin, Department of Geology, University of Nairobi, Nairobi, Kenya.

Onyango, L., Swallow, B. and Meinzen-Dick, R. (2005), Hydronomics and terranomics in the Nyando basin of Western Kenya, Paper presented at the International workshop on 'African Water Laws: Plural Legislative Frameworks for Rural Water Management in Africa', 26-28 January 2005, Gauteng, South Africa

Onyango, L., Swallow, B. and Meinzen-Dick, R. (2005), Hydronomics and terranomics in the Nyando basin of Western Kenya, International workshop on 'African Water Laws: Plural Legislative Frameworks for Rural Water Management in Africa',South Africa. www.nri.org/waterlaw/AWLworkshop/ONYANGO-L.pdf

Piper, B.S., Plinston,D.T. and Sutcliffe.J.V. (1986), The water balance of Lake Victria, Hydro. Sci. J. 31:25-37

Predicting soil erosion from fields and small catchments: The EUROSEM model, www.silsoe.cranfield.ac.uk, 2006

Rademeyer, R. (2004), Catchment characteristics, Flood Hydrology course notes, University of Stellenbosch.

River Basin Modelling Systems, Water Resource Systems Research Laboratory (WRSRL), www.ncl.ac.uk/wrgi/wrsrl/index.html, 2006

Shepherd, K., Walsh, M. (2000), Assessment of soil degradation in the Kavirondo Gulf Basin (Winam Gulf) of Lake Victria, Improved land management in the Lake Victoria basin, Linking land and lake, research and extension, final technical report startup phase, International center for research in agroforestry and Kenya ministry of agriculture and rural development, p34.

Simons, D.B. and Senturk, F. (1992), Sediment Transport Technology, Water Resources Publications, Littleton, Col.

Sjors.A.B. (2001), Erosion history of the Ragen and Nyalunya area, Nyando district, Kenya, Arbetsgruppen för Tropisk Ekologi, Committee of Tropical Ecology, Uppsala University, Sweden. www.env-impact.geo.uu.se/MFS72.pdf.

Smithers.J., Schulze.R. (2002), ACRU Agrohydrological Modelling System User Manual, Version 3.00.

Soil erosion outline, http://www.nju.edu.cn, 2006

Soil erosion, www.botany.uwc.ac.za, 2001

Swallow, B. (2000), The effects of scales, flows and filters on property rights and collective action in catchment management. Paper presented at the Technical Workshop on Watershed management Institutions, System-wide program on Collective Action and Property rights (CAPRi), Managua, March 13-16, 2000.

The LISEM model, www.geog.uu.nl, 2006

Van Der Walt, S.C. (2005), Mathematical modelling of sediment transport dynamics in the Berg River considering current and future water resources development scenarios, Unpublished master thesis, University of Stellenbosch.

Water Erosion Prediction Project (WEPP), The National Soil Erosion Research Laboratory, USA, (1995) Soil Erosion and WEPP Technology, http://topsoil.nserl.purdue.edu, 2006

Water Erosion Prediction Project (WEPP), The National Soil Erosion Research Laboratory, USA,

(1995) WEPP: Spilling the Secrets of Water Erosion, WEPP: Spilling the Secrets of Water Erosion, 2005

Weather, www.bbc.co.uk 2005

WILLAMS, J.R. (1975), Sediment routing for agricultural watersheds. -Water Resources Bulletin, vol.11 no.5, p.965-974.

WILLAMS, J.R. and BERNDT, H.D. (1977), Sediment yield prediction based on watershed hydrology, Transactions of the ASAE, p.1100-1104

Pectora roborant cultus recti

APPENDIX A

ACRU OUTPUT VARIABLE DIRECTORY (ACRU USER MANUAL, 3.00)

VARIABLE	DESCRIPTION	MONTHLY/ ANNUAL PRINTOUT	UNITS
AET	Total evaporation (actual evapotranspiration)	Sum	mm
AET1	Total evaporation (actual evapotranspiration) from A-horizon	Sum	mm
AET2	Total evaporation (actual evapotranspiration) from B-horizon	Sum	mm
AMTPUM	Volume of water pumped from the stream for off-channel storage	Sum	m^3
APAN	A-pan equivalent reference potential evaporation	Sum	mm
ASOEV	Actual evaporation from the soil surface	Sum	mm
ATRAN1	Actual transpiration from the A-horizon	Sum	mm
ATRAN2	Actual transpiration from the B-horizon	Sum	mm
ATRAN3	Evaporation from the intermediate zone	Sum	mm
ATRAN4	Evaporation from the capillary fringe	Sum	mm
CAYD	Crop coefficient	Average	-
CAYIRD	Crop coefficient for irrigated crop	Average	-
CELRUN	Total streamflow from subcatchment, including upstream contributions	Sum	mm
D_POT	Deep percolation from the irrigated area	Sum	mm
DAMPER	Reservoir storage as percentage of full supply capacity	Average	%
DEF1	Soil moisture deficit in A-horizon in relation to drained upper limit	Average	mm
DEF2	Soil moisture deficit in B-horizon in relation to drained upper limit	Average	mm
DPE	Maximum evaporation (potential evapotranspiration)	Sum	mm
EOP	Maximum transpiration of the irrigated crop	Sum	mm
EP	Actual transpiration of the irrigated crop	Sum	mm
ERFL	Effective rainfall (rainfall available for plant growth)	Sum	mm
ERFLIR	Effective rainfall on irrigated field (rainfall available for plant growth)	Sum	mm
ES	Actual evaporation from the soil surface of the irrigated area	Sum	mm
ETLYS	Total evaporation from a lysimeter	Sum	mm

VARIABLE	DESCRIPTION	MONTHLY/ ANNUAL PRINTOUT	UNITS
ETRAN1	Effective transpiration from A-horizon (when mean temperature > input threshold)	Sum	mm
ETRAN2	Effective transpiration from B-horizon (when mean temperature > input threshold)	Sum	mm
F_APIR	Actual amount of irrigation water applied to the field	Sum	mm
GIRRIG	Gross irrigation demand	Sum	mm
GRDCOV	Percentage of ground covered/shaded for the irrigated area	Average	%
OBSTO1	Observed soil moisture content of A-horizon (input)	Average	mm
OBSTO2	Observed soil moisture content of B-horizon (input)	Average	mm
OVERFL	Overflow from dam spillway	Sum	mm
PEIRR	Actual irrigation water applied to field, expressed as a percentage of net irrigation required (i.e. *F_APIR/REQIR*100*)	Minimum	%
PERC	Unsaturated drainage from the B-horizon to intermediate/groundwater zone	Sum	mm
POSOEV	Maximum (potential) evaporation from the soil surface	Sum	mm
POTR1	Maximum transpiration from the A-horizon	Sum	mm
POTR2	Maximum transpiration from the B-horizon	Sum	mm
PP1	Maximum evaporation (potential evapotranspiration) from the A-horizon	Sum	mm
PP2	Maximum evaporation (potential evapotranspiration) from the B-horizon	Sum	mm
QPEAK	Simulated peak discharge	Maximum	$m^3.s^{-1}$
QPKOBS	Observed peak discharge (input)	Maximum	$m^3.s^{-1}$
QUICKF	Stormflow leaving catchment outlet on a given day	Sum	mm
RADINF	Distance to which water table depression is effective	Average	m
RDEPTH	Depth of the zone of maximum rooting activity for the irrigated crop	Average	m
REQIR	Net irrigation required	Sum	mm
RFL	Rainfall (input), adjusted when requested	Sum	mm
RFLIR	Rainfall on irrigated field (input), adjusted when requested	Sum	mm
RUN	Baseflow	Sum	mm
RUNCO	Baseflow store	Average	mm
SEDYLD	Sediment yield from catchment	Sum	t
SIMSQ	Simulated runoff (stormflow + baseflow) from (sub)catchment only (excludes upstream contributions)	Sum	mm

VARIABLE	DESCRIPTION	MONTHLY/ ANNUAL PRINTOUT	UNITS
SIMWTD	Simulated shallow groundwater depth	Average	m
SMIZ	Soil water content in intermediate zone	Average	mm
STO1	Soil water content in A-horizon	Average	mm
STO2	Soil water content in B-horizon	Average	mm
STQIR	Stormflow from irrigated area	Sum	mm
STRMFL	Observed streamflow (input)	Sum	mm
SUMDD	Depression of water table due to land-use change	Average	mm
SUR1	Saturated drainage from A-horizon to B-horizon	Sum	mm
SUR2	Saturated drainage from B-horizon to intermediate/groundwater zone	Sum	mm
SUR3	Saturated drainage from intermediate to groundwater zone	Sum	mm
SURIR	Baseflow from irrigated field	Sum	mm
SW_MAX	Soil water content of the irrigated field	Average	mm
TDELT	Difference between mean and threshold temperature	Average	°C
TMEAN	Mean daily temperature (• C)	Average	°C

APPENDIX B

INTRODUCTION OF GENERAL TRENDS IN STREAMFLOW SIMULATIONS (ACRU USER MANUAL, 3.00)

*** Trend 1**

Characteristics - Intercept acceptable

- Slope too steep
- Qs too high

Inferences - low flows simulated well

- high flows oversimulated systematically
- high stormflows too responsive in model

Possible Causes - outliers of daily rainfall

- total soil depth too shallow (too much stormflow generated)
- critical soil depth *SMDDEP* too shallow (too much stormflow generated)
- saturated top- to subsoil drainage rate *ABRESP* too low (should drain faster)
- saturated subsoil to intermediate zone drainage rate BFRESP too low (should drain faster)
- coefficient of initial abstractions *COIAM* too low in wet season (initial abstractions too low i.e. too much rainfall converted to streamflow)
- adjunct impervious area fraction *ADJIMP* too high (too much saturated overland flow)
- same-day stormflow response fraction *QFRESP* too high (too much same-day response; more of the stormflow could be interflow)
- root mass distribution fraction of topsoil *ROOTA* too low in wet season (not enough plant water extraction from topsoil between storms).

*** Trend 2**

Characteristics - Intercept acceptable

- Slope too flat
- Qs too low

Inferences - low flows simulated well

- high flows undersimulated systematically
- stormflows not responsive enough

Possible Causes - daily rainfalls too low

- inliers of daily rainfall

- total soil depth too deep
- *SMDDEP* too deep
- *QFRESP* too low (too little same-day response)
- *ABRESP* too high
- *BFRESP* too high
- *COIAM* too high in wet season (may be a high rainfall intensity region, or soils may crust; hence reduce *COIAM*).

*** Trend 3**

Characteristics - intercept too high
- slope acceptable
- Qs x too high

Inference - systematic oversimulation of both high and low flows
- likely to be an all-year or winter rainfall region

Possible Causes - observed streamflow is underestimated systematically
- precipitation is overestimated systematically
- total soil depth too shallow (too much stormflow generated)
- subsoil horizon thickness too shallow (i.e. *DEPBHO* too low; too much drainage, hence much baseflow is generated)
- *COFRU* too low (large groundwater store produces baseflow too slowly)
- *ABRESP* and *BFRESP* too high (drainage occurs too rapidly)
- *SMDDEP* too shallow

*** Trend 4**

Characteristics - intercept too low
- slope acceptable
- Qs x too low

Inference - systematic undersimulation of both high and low flows

Possible Causes - Qo is overestimated systematically
- P is underestimated systematically

- *SMDDEP* too deep (not enough stormflow produced)
- total soil depth (*DEPAHO* + *DEPBHO*) too deep (not enough baseflow generated)
- *BFRESP* too low (drainage too slow)
- *COFRU* too small.

*** Trend 5**

Characteristics - intercept too low
- slope too high
- Qs acceptable

Inference - undersimulation of low flows with simultaneous oversimulation of high flows
- highly seasonal rainfall distribution
- should generate less stormflow and more baseflow

Possible Causes - *SMDDEP* too shallow (too much stormflow generation)
- *DEPBHO* too deep (too little drainage for baseflow generation)
- *QFRESP* too high (too much same-day response from stormflows)
- *COIAM* too low in rainy season (too little infiltration created)
- *ABRESP* too low (drainage too slow)
- *BFRESP* too low (potential drainage generated too slowly)
- *Er* too low in rainy season (soil does not dry out rapidly enough between storms)
- *CAY* too low in rainy season (soil does not dry out)
- *ROOTA* too low in rainy season (topsoil does not dry out)
- *COFRU* too high (baseflow recession rate too rapid)

*** Trend 6**

Characteristics - intercept too high
- slope too low
- Qs acceptable

Inferences - oversimulation of baseflows with simultaneous undersimulation of stormflows

- probably a low intensity winter or all year rainfall distribution
- should produce less baseflow, then distribute it more rapidly
- should produce more stormflow

Possible Causes - *SMDDEP* too deep (generates too little stormflow)

- total soil depth (*DEPAHO* + *DEPBHO*) too shallow (creates too much baseflow)
- particularly *DEPBHO* may be too shallow (creates too much baseflow)
- *BFRESP* too high (drainage takes place too rapidly)
- *QFRESP* too low (too little stormflow runs off on same day)
- *COIAM* too high in rainy season (creates too much infiltration)
- Er too high in rainy season (soil dries too rapidly)
- *CAY* too high in rainy season (soil dries too rapidly)
- *ROOTA* too high in rainy season (topsoil dries too rapidly)
- *ABRESP* too high (drainage too rapid and less stormflow generated).

*** Trend 7**

This is what you are striving towards!

APPENDIX C

INITIAL SCS CURVE NUMBERS (CNII) FOR SELECTED LAND COVER AND TREATMENT CLASSES, STORMFLOW POTENTIALS AND HYDROLOGICAL SOIL GROUPS (SCHULZE, SCHMIDT AND SMITHERS, 1993)

Land Cover Class	Land Treatment/ Practice/Description	Stormflow Potential	Hydrological Soil Group						
			A	A/B	B	B/C	C	C/D	D
Fallow	1 = Straight row		77	82	86	89	91	93	94
	2 = Straight row + conservation tillage	High	75	80	84	87	89	91	92
	3 = Straight row + conservation tillage	Low	74	79	83	85	87	89	90
Row Crops	1 = Straight row	High	72	77	81	85	88	90	91
	2 = Straight row	Low	67	73	78	82	85	87	89
	3 = Straight row + conservation tillage	High	71	75	79	83	86	88	89
	4 = Straight row + conservation tillage	Low	64	70	75	79	82	84	85
	5 = Planted on contour	High	70	75	79	82	84	86	88
	6 = Planted on contour	Low	65	69	75	79	82	84	86
	7 = Planted on contour + conservation tillage	High	69	74	78	81	83	85	87
	8 = Planted on contour + conservation tillage	Low	64	70	74	78	80	82	84
	9 = Conservation structures	High	66	70	74	77	80	82	82
	10 = Conservation structures	Low	62	67	71	75	78	80	81
	11 = Conservation structures + conservation tillage	High	65	70	73	76	79	80	81
	12 = Conservation structures + conservation tillage	Low	61	66	70	73	76	78	79
Garden Crops	1 = Straight row	High	68	71	75	79	81	83	84
	2 = Straight row	Low	45	56	66	72	77	80	83
Small Grain	1 = Straight row	High	65	71	76	80	84	86	88
	2 = Straight row	Low	63	69	75	79	83	85	87
	3 = Straight row + conservation tillage	High	64	70	74	78	82	84	86
	4 = Straight row + conservation tillage	Low	60	67	72	76	80	82	84
	5 = Planted on contour	High	63	69	74	79	82	84	85
	6 = Planted on contour	Low	61	67	73	78	81	83	84
	7 = Planted on contour + conservation tillage	High	62	68	73	77	81	83	84
	8 = Planted on contour + conservation tillage	Low	60	66	72	76	79	81	82
	9 = Planted on contour - winter rainfall region	Low	63	66	70	75	78	80	81
	10 = Conservation structures	High	61	67	72	76	79	81	82
	11 = Conservation structures	Low	59	65	70	75	78	80	81
	12 = Conservation structures + conservation tillage	High	60	67	71	75	78	80	81
	13 = Conservation structures + conservation tillage	Low	58	64	69	73	76	78	79
Close Seeded Legumes or Rotational Meadow	1 = Straight Row	High	66	72	77	81	85	87	89
	2 = Straight Row	Low	58	65	72	75	81	84	85
	3 = Planted on contour	High	64	70	75	80	83	84	85
	4 = Planted on contour	Low	55	63	69	74	78	81	83
	5 = Conservation structures	High	63	68	73	77	80	82	83
	6 = Conservation structures	Low	51	60	67	72	76	78	80
Sugarcane	1 = Straight row: trash burnt		43	55	65	72	77	80	82
	2 = Straight row: trash mulch		45	56	66	72	77	80	83
	3 = Straight row: limited cover		67	73	78	82	85	87	89
	4 = Straight row: partial cover		49	60	69	73	79	82	84
	5 = Straight row: complete cover		39	50	61	68	74	78	80
	6 = Conservation structures: limited cover		65	70	75	79	82	84	86
	7 = Conservation structures: partial cover		25	46	59	67	75	80	83
	8 = Conservation structures: complete cover		6	14	35	59	70	75	79

Land Cover Class	Land Treatment/ Practice/Description	Stormflow Potential	Hydrological Soil Group						
			A	A/B	B	B/C	C	C/D	D
Veld (range) and Pasture	1 = Veld/pasture in poor condition	High	68	74	79	83	86	88	89
	2 = Veld/pasture in fair condition	Moderate	49	61	69	75	79	82	84
	3 = Veld/pasture in good condition	Low	39	51	61	68	74	78	80
	4 = Pasture planted on contour	High	47	57	67	75	81	85	88
	5 = Pasture planted on contour	Moderate	25	46	59	67	75	80	83
	6 = Pasture planted on contour	Low	6	14	35	59	70	75	79
Irrigated Pasture		Low	35	41	48	57	65	68	70
Meadow		Low	30	45	58	65	71	75	81
Woods and Scrub	1 = Woods	High	45	56	66	72	77	80	83
	2 = Woods	Moderate	36	49	60	68	73	77	79
	3 = Woods	Low	25	47	55	64	70	74	77
	4 = Brush - Winter rainfall region	Low	28	36	44	53	60	64	66
Orchards	1 = Winter rainfall region, understorey of crop cover		39	44	53	61	66	69	71
Forests and Plantations	1 = Humus depth 25mm; Compactness : compact		52	62	72	77	82	85	87
	2 = " " " moderate		48	58	68	73	78	82	85
	3 = " " " loose/friable		37	49	60	66	71	74	77
	4 = Humus depth 50mm; Compactness : compact		48	58	68	73	78	82	85
	5 = " " " moderate		42	54	65	70	75	78	81
	6 = " " " loose/friable		32	45	57	62	67	71	74
	7 = Humus depth 100mm; Compactness: compact		41	53	64	69	74	77	80
	8 = " " " moderate		34	47	59	64	69	72	75
	9 = " " " loose/friable		23	37	50	56	61	64	67
	10 = Humus depth 150mm; Compactness: compact		37	49	60	66	71	74	77
	11 = " " " moderate		30	43	56	61	66	69	72
	12 = " " " loose/friable		18	33	47	52	57	61	65
Urban/Sub-urban Land Uses	1 = Open spaces, parks, cemeteries 75% grass		39	51	61	68	74	78	80
	cover		49	61	69	75	79	82	84
	2 = Open spaces, parks, cemeteries 75% grass		89	91	92	93	94	95	95
	cover		81	85	88	90	91	92	93
	3 = Commercial/business areas 85% impervious		77	81	85	88	90	91	92
	4 = Industrial districts 72% impervious		61	69	75	80	83	85	87
	5 = Residential: lot size 500m² 65% impervious		57	65	72	77	81	84	86
	6 = " 1000m² 38% impervious		54	63	70	76	80	83	85
	7 = " 1350m² 30% impervious		51	61	68	75	78	82	84
	8 = " 2000m² 25% impervious		98	98	98	98	98	98	98
	9 = " 4000m² 20% impervious		98	98	98	98	98	98	98
	10 = Paved parking lots, roofs, etc.		76	81	85	88	89	90	91
	11 = Streets/roads: tarred, with storm		72	77	82	85	87	88	89
	sewers,curbs		74	79	84	88	90	91	92
	12 = " gravel								
	13 = " dirt								
	14 = " dirt-hard surface								